

## **Distribution Agreement**

In presenting this thesis or dissertation as a partial fulfillment of the requirements for an advanced degree from Emory University, I hereby grant to Emory University and its agents the nonexclusive license to archive, make accessible, and display my thesis or dissertation in whole or in part in all forms of media, now or hereafter known, including display on the world wide web. I understand that I may select some access restrictions as part of the online submission of this thesis or dissertation. I retain all ownership rights to the copyright of the thesis or dissertation. I also retain the right to use in future works (such as articles or books) all or part of this thesis or dissertation.

Signature:

---

Stephanie Lynn Pollitt

---

Date

**LIM and SH3 Protein 1 in Actin-Based Cellular Motility and Axon Guidance**

By

Stephanie Lynn Pollitt  
Doctor of Philosophy

Graduate Division of Biological and Biomedical Science  
Neuroscience

---

James Zheng, PhD.  
Advisor

---

Gary J. Bassell, Ph.D.  
Committee Member

---

Arthur English, Ph.D.  
Committee Member

---

Victor Faundez, M.D., Ph.D.  
Committee Member

---

Kenneth Moberg, Ph.D.  
Committee Member

---

Shoichiro Ono, Ph.D.  
Committee Member

**Accepted:**

---

Lisa A. Tedesco, Ph.D.  
Dean of the James T. Laney School of Graduate Studies

---

Date

# **LIM and SH3 Protein 1 in Actin-Based Cellular Motility and Axon Guidance**

By

Stephanie Lynn Pollitt  
B.S., University of California, Davis, 2014

Advisor: James Q. Zheng, Ph.D.

An abstract of  
a dissertation submitted to the Faculty of the  
James T. Laney School of Graduate Studies of Emory University  
in partial fulfillment of the requirements for the degree of  
Doctor of Philosophy  
in Graduate Division of Biological and Biomedical Sciences  
Neuroscience  
2020

## Abstract

### **LIM and SH3 Protein 1 in Actin-Based Cellular Motility and Axon Guidance**

By Stephanie Lynn Pollitt

The actin cytoskeleton drives cellular motility and is essential for neuronal development and function. LIM and SH3 Protein 1 (LASP1) is a unique actin-binding protein that is expressed in a wide range of cells including neurons, but its roles in cellular motility and neuronal development are not well understood. In this thesis work, I have investigated these outstanding questions in the contexts of lamellipodial actin structures and axonal development. I first show that LASP1 is expressed in rat hippocampus early in development, and this expression is maintained through adulthood, which supports the notion that LASP1 may play a role in early axonal growth. High-resolution imaging reveals that LASP1 is selectively concentrated at the leading edge of lamellipodia in migrating cells and axonal growth cones. This local enrichment of LASP1 is dynamically associated with the protrusive activity of lamellipodia, depends on the barbed ends of actin filaments, and requires both the LIM domain and nebulin repeats of LASP1. To understand the function of LASP1 in actin-based axon motility, I performed loss-of-function experiments. I found that knockdown of LASP1 in cultured rat hippocampal neurons resulted in a substantial reduction in axonal outgrowth and arborization. Furthermore, knockdown of the *Drosophila* homolog Lasp from a subset of commissural neurons in the developing ventral nerve cord produced defasciculated axon bundles that do not reach their targets. These data support a novel role for LASP1 in actin-based lamellipodial protrusion and establish LASP1 as a positive regulator of both *in vitro* and *in vivo* axon development. In the second part of my thesis work, I have developed an innovative approach that will enable immunolabeling of selected cells in multi-cell culture and tissue. This approach takes advantage of lipid oxidation-induced membrane permeability by reactive oxygen species (ROS) for selective labeling of single cells, termed RASCL (ROS-Assisted Single Cell Labeling). I have successfully utilized RASCL to label the actin cytoskeleton in selected cells of a multi-cell culture. Future optimization and use in brain slices will enable this technique to significantly advance our understanding of the subcellular distribution of specific proteins in a selected set of cells of intact tissues.

# **LIM and SH3 Protein 1 in Actin-Based Cellular Motility and Axon Guidance**

By

Stephanie Lynn Pollitt  
B.S., University of California, Davis, 2014

Advisor: James Q. Zheng, Ph.D.

A dissertation submitted to the Faculty of the  
James T. Laney School of Graduate Studies of Emory University  
in partial fulfillment of the requirements for the degree of  
Doctor of Philosophy  
in Graduate Division of Biological and Biomedical Sciences  
Neuroscience  
2020

## Acknowledgements

This work would not have been possible without the support and guidance of several outstanding individuals.

Firstly, thank you to my advisor, Dr. James Zheng, whose guidance was essential to the development and execution of this project. Thank you for your enthusiasm and energy.

Secondly, thank you to my committee, Drs. Ken Moberg, Victor Faundez, Art English, Gary Bassell, and Sho Ono, whose support was invaluable throughout this process. Thank you for your advice and reassurance when I needed it. Special thanks to Dr. Ken Moberg, who trained me in *Drosophila* husbandry, and to Dr. Victor Faundez, who pushed me to be the best scientist I could be.

I am grateful to my labmate and co-author, Dr. Ken Myers, for his training, guidance, and moral support.

Thank you to the members of the Zheng lab, both past and present, who have taught me and assisted me in completing this work. In particular, thank you to Drs. Julia Omotade and Amanda York, whose teaching and patience were essential to my early success in the lab. Thank you to Jinny Yoo, whose assistance with the analysis was important for the timely completion of many experiments.

I am grateful to my classmates in the Neuroscience program, whose support and advice helped make me a better scientist and friend. Thank you for all of the great memories I'll cherish for years to come.

Thank you to my family: my mother, father, and brother, who always made time for me around my busy schedule, and tolerated my lengthy explanations of my research. Your love and support have made me the person I am today.

Finally, to my cat, Marie Curie. Your endless curiosity and silly antics kept me sane. While your attempts to contribute to the text of this work did not make it into the final version, I appreciate your efforts nonetheless.

## Table of Contents

|   |           |
|---|-----------|
| <b>Chapter 1: Introduction</b> .....  | <b>1</b>  |
| 1.1. Mechanisms of Actin-Based Cellular Motility .....  | 3         |
| 1.1.1. Actin and Actin Polymerization.....  | 3         |
| 1.1.2. Actin-Binding Proteins and Higher Order Actin Structures .....   | 5         |
| 1.2. Axon Guidance, Signaling, and Mechanisms .....   | 6         |
| 1.2.1. A Brief History of the Axon Guidance Field.....  | 7         |
| 1.2.2. <i>Drosophila melanogaster</i> as a Model System for Neurodevelopment.....   | 8         |
| 1.2.3. Axon Guidance Cues and their Detection: Navigating the Extracellular Space.....  | 10        |
| 1.2.4. The Development of Axon Collaterals .....  | 13        |
| 1.2.5. Regulation of Actin Remodeling Downstream of Axon Guidance Signaling.....  | 14        |
| 1.2.5.1. Actin Depolymerizing Factor and Cofilin .....  | 14        |
| 1.2.5.2. The Rho GTPases .....  | 17        |
| 1.2.5.3. GEFs and GAPs: Key Regulators of Actin Motility.....   | 18        |
| 1.3. LIM and SH3 Protein 1 (LASP1): a Review of the Literature and Outstanding Questions .....  | 19        |
| 1.3.1. The Nebulin Family of Actin-Binding Proteins.....  | 19        |
| 1.3.2. LASP1: a Review.....   | 21        |
| 1.4. Dissertation Hypothesis and Questions.....   | 23        |
| 1.5. Figures .....  | 24        |
| <b>Chapter 2: LIM and SH3 Protein 1 Localizes to the Leading Edge of Protruding Lamellipodia and Regulates Axon Development</b> ..... | <b>26</b> |
| 2.1. Summary .....  | 27        |
| 2.2. Introduction .....   | 27        |
| 2.3. Methods .....  | 30        |
| 2.4. Results .....  | 36        |
| 2.4.1. LASP1 Expression in Neurons and its Dynamic Localization to the Leading Edge of Actin-Based Membrane Protrusions .....         | 36        |
| 2.4.2. Mechanisms of LASP1 Localization to the Leading Edge .....   | 39        |
| 2.4.3. LASP1 Promotes Axon Elongation and Branching.....  | 42        |
| 2.4.4. Lasp Promotes Axon Commissure Development and Fasciculation <i>in vivo</i> .....   | 44        |
| 2.5. Discussion .....   | 46        |

|  |           |
|--|-----------|
| 2.6. Figures .....   | 53        |
| 2.7. Supplemental Tables .....   | 67        |
| <b>Chapter 3: RASCL: A New Method for Labeling Optically- and Genetically-Selected Intracellular Protein Targets .....</b> | <b>71</b> |
| 3.1. Summary .....   | 72        |
| 3.2. Introduction .....  | 72        |
| 3.3. Methodology .....   | 73        |
| 3.4. Description of Materials.....   | 75        |
| 3.5. Procedure.....  | 76        |
| 3.6. Results .....   | 77        |
| 3.6.1. Efficacy of the RASCL Technique with Small Fluorescent Probes .....   | 78        |
| 3.6.2. RASCL-Induced Antibody Labeling .....   | 79        |
| 3.7. Future Troubleshooting for RASCL .....  | 80        |
| 3.8. Discussion and Future Directions .....  | 81        |
| 3.9. Figures.....  | 83        |
| <b>Chapter 4: Discussion and Concluding Remarks .....</b>  | <b>86</b> |
| 4.1. Summary .....   | 87        |
| 4.1.1. Evidence for LASP1 as a Possible Regulator of Actin Polymerization or Anti-Capping .....                            | 87        |
| 4.1.2. RASCL: A New Method for Labeling Optically- and Genetically-Selected Intracellular Protein Targets.....             | 90        |
| 4.2. Future Directions.....  | 90        |
| <b>References .....</b>  | <b>93</b> |

## Figures and Tables

|  |    |
|--|----|
| Figure 1-1: Diagram of Actin-Based Growth Cone Motility.....   | 24 |
| Figure 1-2: Diagram of LASP1 and LASP2 .....   | 25 |
| Figure 2-1: LASP1 is expressed in the developing brain and localizes to the axon growth cone                             | 53 |
| Figure 2-2: GFP-LASP1 localizes to protruding membranes .....  | 55 |
| Figure 2-3: The LIM domain and nebulin repeats are essential for LASP1 localization to the leading edge .....            | 57 |
| Figure 2-4: LASP1 localizes to actin plus ends at the leading edges of CAD cells .....                                   | 58 |
| Figure 2-5: Free actin plus ends are required for LASP1 localization to the leading edge .....                           | 59 |
| Figure 2-6: Knockdown of LASP1 truncates axon elongation and reduces branching in cultured hippocampal neurons .....     | 61 |
| Figure 2-7: Knockdown of LASP1 reduces growth cone protrusion and branch formation in cultured hippocampal neurons ..... | 63 |
| Figure 2-8: Lasp knockdown leads to defects in axon commissure formation in <i>Drosophila</i> .....                      | 65 |
| Supplemental Table 2-1: Total Axon Outgrowth Statistics: n and p values .....  | 67 |
| Supplemental Table 2-2: Axon Branching Statistics: n and p values .....  | 68 |
| Supplemental Table 2-3: Growth Cone Motility Statistics: n and p values .....  | 69 |
| Supplemental Table 2-4: Branch Dynamics Statistics: n and p values .....   | 70 |
| Figure 3-1: Diagram of RASCL mechanism of labeling.....  | 83 |
| Figure 3-2: RASCL Labeling of F-actin with small probe phalloidin .....  | 84 |
| Figure 3-3: RASCL Antibody Labeling of Microtubules .....  | 85 |

# Chapter 1: Introduction

Portions of this chapter were adapted from the following publication:

Omotade OF\*, **Pollitt SL\***, Zheng JQ. Actin-based growth cone motility and guidance. *Molecular and Cellular Neurosciences*. 2017 Oct;84:4-10. doi: 10.1016/j.mcn.2017.03.001. PMID: 28268126.

**\* contributed equally to this work**

Wiring of the central nervous system requires the precise development and guidance of axonal projections towards their synaptic targets. Defects in wiring result in dysfunctional circuits that cause disorders in a variety of neural systems, such as intellectual disability and motor disorders (Chilton and Guthrie, 2016; Jamuar et al., 2017). Axon growth depends on a highly mobile structure at the tip of the axon called the growth cone, which is comprised of two hallmark actin-based membrane protrusions: filopodia and lamellipodia (Gomez and Letourneau, 2014). Filopodia are composed of bundled, linear actin filaments (F-actin), whereas lamellipodia contain a meshwork of short, branched F-actin. It is the rapid assembly and disassembly of these F-actin structures that drive the protrusion of filopodia and lamellipodia underlying growth cone motility (Gomez and Letourneau, 2014). This actin-based motility engine in the growth cone is targeted by signaling cascades downstream of a variety of extracellular cues to achieve specific growth cone responses, which range from acceleration of growth to directional turning, pausing, and retraction. It is the combination of different guidance cues with specific spatiotemporal patterns driving various growth cone responses that enable to the axon to navigate long distances towards its target region. While significant progress has been made in identifying the guidance molecules, respective receptors, and downstream signaling cascades, the precise mechanisms by which these cues regulate actin dynamics to produce directional axon outgrowth remain to be fully elucidated. This dissertation largely focuses on one unique actin-binding protein, LIM and SH3 Protein 1 (LASP1), and its role in actin-based motility and axon development. In this introduction, I discuss the most significant findings in the fields of actin-based cellular motility and axonal development.

## **1.1. Mechanisms of Actin-Based Cellular Motility**

Cellular motility and migration play important developmental, physiological, and pathological roles in the human body. Key examples include layer formation in the developing brain, motile T cells activated during immune responses, and the abnormal motility found in metastatic cancer, respectively (Luster et al., 2005; Wang et al., 2005; Geschwind and Rakic, 2013). Previous studies in the cell migration field have identified the actin cytoskeleton as essential for migration and motility across cell types, through a combination of rapid structural turnover and coupling to the extracellular matrix (Le Clainche and Carlier, 2008). Therefore, to understand neuronal development and axon growth, it is instructive to examine cellular motility through the lens of the dynamic actin cytoskeleton.

### **1.1.1. Actin and Actin Polymerization**

Actin is a family of 42 kDa globular proteins (G-actin), with three major subfamilies in vertebrates:  $\alpha$ -actin,  $\beta$ -actin, and  $\gamma$ -actin (Perrin and Ervasti, 2010). While these proteins are over 93% identical to one another, there is some distinction in their expression by cell type:  $\alpha$ -actin is predominantly expressed in muscle, while  $\beta$ - and  $\gamma$ -actin are ubiquitously expressed.  $\alpha$ -actin is broken down into three isoforms, which are distinctly expressed in skeletal, cardiac, and smooth muscle.  $\gamma$ -actin also has two isoforms, one expressed in smooth muscle and another that is ubiquitously expressed, along with the single  $\beta$ -actin isoform (Perrin and Ervasti, 2010). Previous studies have found that sequence differences between the muscle isoforms and the ubiquitous isoforms may result in different binding affinities with actin binding proteins such as cofilin and profilin (Larsson and Lindberg, 1988; De La Cruz, 2005). It is therefore likely that actin isoforms contribute to the different behaviors of motile cells versus contractile cells.

Together, these actin families represent the most abundantly expressed protein in eukaryotic cells, comprising between 1-5% of the total protein in non-muscle cells (Lodish et al., 2016).

Globular actin monomers (G-actin) are capable of polymerizing into actin filaments (F-actin, also microfilaments), which present as two sub-filaments twisted together into a microfilament approximately 8nm in diameter (Blanchoin et al., 2014). Each actin subunit is an ATPase, where the G-actin monomer binds to an ATP molecule that gets hydrolyzed after assembly into an actin filament. While ATP hydrolysis is not required for polymerization, it does affect the affinity of certain actin-binding proteins, as well as the stability of the filament overall (Blanchoin and Pollard, 1999; Hao et al., 2008). Actin filaments are polarized, with a plus (or barbed) end and a minus (or pointed) end. *In vitro*, actin polymerization occurs over five times faster at the plus end than the minus end (Lodish et al., 2016). This polarization is due to the critical concentration at each end, which is the term for the equilibrium concentration of G-actin with filaments. At the plus end of the filament, the critical concentration is 0.1 $\mu$ M, but at the minus end it is 0.8 $\mu$ M. This means that at high concentrations of actin, polymerization will occur at both ends, but below 0.8 $\mu$ M, actin polymerizes only at the plus end of the filament. However, living cells must have high concentrations of actin synthesized to allow timely motile responses to their environments. Therefore, the *in vivo* polarization of actin polymerization is manipulated by G-actin-binding proteins. Two prominent examples are thymosin  $\beta$ 4, which acts to sequester G-actin, and profilin, which is believed to promote actin assembly at the plus end and inhibit assembly at the minus end (Pollard and Borisy, 2003). These proteins work in concert to buffer the concentration of actin around the filament ends while maintaining a rapidly releasable pool of actin monomers ready to polymerize. This allows the cell to adjust the critical concentration to achieve polarized actin polymerization even in high concentrations of G-actin.

### 1.1.2. Actin binding proteins and higher order actin structures

Individual actin filaments must be organized into higher-order structures in order to carry out cellular functions. In cells, several actin-binding proteins are responsible for connecting, capping, nucleating or otherwise altering actin filaments to produce these higher-order actin structures. Different actin structures have different physical and physiological properties, which allow them to perform cell type-specific tasks (Blanchoin et al., 2014). In the context of cellular motility, the two most vital actin-based structures are lamellipodia, or sheets of branched F-actin, and filopodia, which are bundled F-actin protrusions (Pollard et al., 2000). These structures can be differentiated by two distinct polymerizing proteins: lamellipodia is characterized by Arp2/3, which produces actin branches, while filopodial tips are primarily polymerized by formins (Le Clainche and Carlier, 2008) (**Figure 1-1**). Both of these structures are found at the leading edge of migrating cells, and provide the mechanical force necessary for cellular protrusion. Actin in lamellipodia and filopodia undergoes near constant retrograde flow, or the movement of a monomer within the filament from the polymerization zone near the membrane towards the cell center. This flow is driven by two forces: the rearward force of G-actin monomers being added to existing filaments, and myosin II contractility pulling F-actin towards the center of the cell (Lin CH, Espreatico EM, Mooseker MS, 1996; Blanchoin et al., 2014). Retrograde flow can be converted into cellular protrusion through the coupling of actin filaments to the extracellular matrix by way of adhesions, which act much like track cleats to redirect the force of retrograde flow towards the plasma membrane and produce forward motion (Le Clainche and Carlier, 2008; Blanchoin et al., 2014) (**Figure 1-1**). To direct this movement, these major components of actin-based motility and all of their supporting processes are subject to intense regulation by a variety

of signaling cascades. One relevant example is neuronal development, where axons must detect biochemical and biophysical cues in the extracellular environment in order to reach their proper synaptic targets. Therefore, to fully understand actin-based motility in these contexts, it is necessary to examine the processes of signal detection and communication to the actin cytoskeleton.

## **1.2. Axon Guidance, Signaling, and Mechanisms**

Early in brain development, newly born neurons migrate to their respective destinations, where they polarize to form an axon and several dendrites. Axons must grow rapidly and precisely to form synaptic connections with their designated targets. An essential aspect of axon development is axon guidance, the process by which axons detect the signals present in their environment to navigate towards their synaptic targets. These complex signals are detected by a highly motile structure at the tip of the axon called the axon growth cone. The growth cone is responsible for navigating the path through the developing tissue to form a synaptic connection in the correct location. The motility of axon growth cones is achieved in large part by the actin cytoskeleton, which dominates the peripheral region, or leading edge, of the growth cone. Within the growth cone, as in migrating cells, two major F-actin structures appear: lamellipodia, and filopodia, which promote rapid axon growth downstream of axon guidance signaling. The motility of these structures is carefully and strictly controlled by numerous actin-binding proteins, which allow the growth cone to react to guidance cues and grow only along the proper path. This pathfinding process is common amongst all animals with a centralized nervous system, from flies and nematodes to mammals. In humans, defective axon pathfinding is associated with numerous neurological disorders, such as Joubert syndrome, corpus callosum

agenesis, and Kallman syndrome (Engle, 2010). To understand how this developmental process occurs, numerous researchers have investigated many aspects of axon guidance, from the guidance cues and their detection to their effects on cytoskeletal dynamics and growth. The following subsections outline the most relevant findings from this body of literature.

### **1.2.1. A Brief History of the Axon Guidance Field**

The grandfather of the modern axon guidance field was a Spanish scientist named Santiago Ramon y Cajal, who studied developing neurons to understand their structure and function. Using a silver chromate (Golgi) staining method, Cajal discovered a structure at the tips of young axons that he termed the axon growth cone (Cajal, 1890). Cajal described the structure as a “cone-shaped thickening” with “edges [that] bristle with spikes or lamellar processes,” which we would now term filopodia and lamellipodia (Cajal et al., 1904). He was able to observe the growth of these axons over development, and, with remarkable insight, postulated that the growth cone was extending and changing shape throughout development. This confirmed the Neuron Doctrine, which said neurons developed and functioned as separated units, with a method that was easily replicated by any scientist of the day, and established Cajal as the founder of modern neuroscience. For his work, Cajal was awarded the Nobel Prize in 1906, along with Camillo Golgi, who had vehemently disagreed with the Neuron Doctrine but had invented the staining method used by Cajal (Sotelo, 2002). Cajal also postulated that the growth of axons may be chemotaxic in nature (Cajal, 1892), but was never able to satisfactorily prove this hypothesis. Thus, the field of chemotaxic axon guidance and Cajal’s hypothesis waned as scientists turned towards mechanical cues as triggers for axon growth (Sotelo, 2002; Smith, 2009).

As technology improved and more sophisticated experiments were possible, more and more scientists began to revisit the chemotaxis hypothesis. In the early 1940's, one such scientist named Roger Sperry published a remarkable paper in which he detailed the results of removing, rotating, and replacing the eyes of newts. In these invertebrates, axons from the rotated retina were able to regrow, but they synapsed in the inverted spatial orientation, such that the newts reached downwards to catch prey lures above them (Sperry, 1943). Sperry followed up these experiments by surgically uncrossing the optic chiasm of frogs, resulting in a left-right reversal of the frogs' prey capture behaviors (Sperry, 1945). These results indicated that axons are not intrinsically "programmed" to seek a particular target, but instead require external cues that lead them towards their synaptic locations. Furthermore, these creatures could not form adaptive behaviors from these disordered connections, indicating that the spatial organization of synapses was essential for functional behavior. These findings formed the basis for Sperry's famous Chemoaffinity Hypothesis, which was the founding basis for modern axon guidance research (Meyer, 1998). Without the pioneering work performed by these outstanding figures in the field, the work presented in this thesis would not be possible.

### **1.2.2. *Drosophila melanogaster* as a Model System for Neurodevelopment**

Advances in the field of axon guidance would not have been possible without the use of the fruit fly model system, *Drosophila melanogaster*. Fruit flies offer several key advantages over other animal species that have allowed them to remain in use for over seventy years of biological research. Firstly, the *Drosophila* lifespan is very short, two months on average, allowing full lifespan studies without the slow pacing of mammalian studies (Linford et al., 2013). Secondly, fruit flies reproduce rapidly, which means that genetic crosses that would take

years of buildup and genetic screening in mammals can be accomplished in a matter of weeks. Thirdly, due to its longevity of use in the field of genetics, the *Drosophila* model system features a wide variety of available genetic tools, such as genetically- and temperature-induced expression of recombinant genes that were available long before the advent of Crispr. Fourthly, and of key importance for developmental studies, fruit flies have three major stages of life: embryos, which last 24 hours; larvae, which develop over three instar stages lasting approximately 6 days; pupa, where larvae crawl up the sides of their containers and form a hard casing to allow for metamorphosis; and adulthood, where after about four days they emerge from their pupa cases in their final adult forms (Linford et al., 2013). Interestingly, from a neurodevelopment point of view, the 24 hours of embryonic growth encompass several key stages of axon guidance and development, allowing the rapid visualization of axons as they grow. The *Drosophila* ventral nerve cord can be considered the equivalent of the mammalian spinal cord, and contains similar axon bundles, or commissures, that must navigate key decision points to cross the midline appropriately and reach their synaptic targets.

The *Drosophila* model system has enabled a number of advances in the axon guidance field due to its fast-developing, relatively simplistic nervous system. For example, the work of Corey Goodman in discovering several axon guidance molecules and their receptors was accomplished using the *Drosophila* model system, whose simple genome of four chromosomes allowed Goodman to pioneer the use of genetic screens in axon guidance research. By exposing flies to mutagens and examining the resultant disruptions to left-right motor coordination, Goodman and his colleagues were able to discover one of the key axon guidance receptor families, called Roundabout (Robo), and its associated transmembrane protein commissureless (comm) (Seeger et al., 1993; Kidd et al., 1998). This was accomplished by staining for the axons

of the embryonic ventral nerve cord to observe how genetic mutations disrupted midline crossing (Seeger et al., 1993; Kolodziej et al., 1996). To this day, many researchers still choose to study axon guidance signaling mechanisms in *Drosophila*, due to its extensive library of genetic mutations and available tools (Garbe et al., 2007; Evans and Bashaw, 2012; O'Donnell and Bashaw, 2013a; Zarin et al., 2013; Neuhaus-Follini and Bashaw, 2015).

### **1.2.3. Axon Guidance Cues and their Detection: Navigating the Extracellular Space**

Axon growth cones navigate their environments with assistance from a variety of molecules in the extracellular space known as axon guidance cues. These cues can take many forms, and are far more extensive than Cajal could have ever imagined. In general, these cues can be classified on a spectrum from chemoattractive, where the growth cone will move towards the cue, to chemorepulsive, which repels the growth cone away from it. While initial studies of axon guidance defined cues as diffusible molecules secreted from key locations in the developing tissue, further studies have widened that view to include many types of proteins and molecules that take a variety of forms. Below is an outline of the most widely recognized axon guidance cues and their effects on the axon growth cone.

The canonical axon guidance cues fall under four families: the Netrins, Semaphorins, Slits, and Ephrins (Kolodkin and Tessier-Lavigne, 2011). These cues can be diffusible or membrane-bound, and are detected by receptors expressed in the plasma membrane of the axon growth cone. These receptors then trigger spatiotemporally-localized signaling cascades that direct cytoskeletal rearrangement to promote growth cone attraction or repulsion, depending on the particular combination of cue and receptor expressed by the growth cone (Vitriol and Zheng, 2012). Of these classic families, the first to be discovered was the Netrin family, which was

identified through parallel studies in *C. elegans* and mammals (Hedgecock et al., 1990; Kennedy et al., 1994; Serafini et al., 1994). Netrin, called uncoordinated-6 (UNC-6) in *C. elegans*, was first discovered as a secreted molecule that attracts commissural growth cones towards the midline (though more recent studies suggest that it may also be membrane-bound to act locally via mechanotransduction) (Kennedy et al., 1994, 2006; Deiner et al., 1997; Brankatschk and Dickson, 2006). However, purified protein experiments with chick Netrin-1 and Netrin-2 found a more nuanced response: increasing levels of Netrin applied to chick explants resulted in less growth cone attraction (Serafini et al., 1994). After many years of experiments from multiple groups, it was discovered that Netrin can be attractive or repulsive depending on the receptors expressed on the surface of the growth cone. When Netrin binds to DCC homodimers, it acts as a chemoattractant (Chan et al., 1996; Keino-masu et al., 1996; Kolodziej et al., 1996). However, if Netrin is bound to a heterodimer between DCC and UNC-5, or UNC-5 and its co-receptor down syndrome cell adhesion molecule (DSCAM), it causes growth cone repulsion (Hamelin et al., 1993; Colavita and Culotti, 1998; Keleman and Dickson, 2001; Purohit et al., 2012; Finci et al., 2014). In this way, Netrin can attract growth cones towards the midline, and once they've reached it, repel them towards the contralateral side (Boyer and Gupton, 2018). The key to this intricate process lies in the growth cone, and its ability to rapidly and precisely swap out the guidance receptors expressed on its surface. This switch depends on four major factors: the expression level of netrin receptors on the membrane surface, secondary messengers such as cyclic AMP (cAMP) or calcium, the concentration of Netrin-1, and the presence of other cues in the extracellular environment (Boyer and Gupton, 2018). The Netrin family of axon guidance cues provides an extreme example of the complex and tightly regulated processes that the growth cone must undergo in order to detect and properly translate the signposts present in its

environment. Of the three remaining families of classic guidance cues, the Slit family members are repulsive cues that drive axon branching; Semaphorins are also largely repellent through their receptors in the Plexin family; and the Ephrins are mixed attractive or repulsive, though largely at short range due to their transmembrane domains (Kolodkin and Tessier-Lavigne, 2011).

Of the non-canonical axon guidance cues, four families of morphogens or growth factors have been characterized that also dictate growth cone motility: Sonic Hedgehog (Shh), Wnts, Transforming Growth Factor  $\beta$  (TGF $\beta$ ), and Bone Morphogenic Protein (BMP). These cues are diffusible, with the exception of Shh, which is sometimes membrane bound (Yang and Terman, 2012). Of the morphogens, Wnt is the best studied, particularly because of species-based differences in its function. In *Drosophila*, Wnt5 acts through the Derailed receptor to drive repulsion of axons away from the posterior commissure (Yoshikawa et al., 2003). However, in mammals, Wnt4 mediates anterior attraction of commissural spinal axons expressing Frizzled 3 after midline crossing (Lyuksytova et al., 2003; Killeen and Sybingco, 2008). Similarly, Shh can mediate attraction or repulsion, depending on the cell type (Trousse et al., 2001). These cell type-specific roles for Wnt and Shh demonstrate how the combination of the cue, its receptor, and cell type determine how a particular guidance cue will affect growth cone behavior.

Finally, there are the cell-adhesion molecules (CAMs), which had been studied long before the canonical axon guidance molecules were ever discovered. The CAM family largely consists of immunoglobulins (Igs) and cadherins, transmembrane proteins that allow cell to cell contact and recognition across cell types (Kolodkin and Tessier-Lavigne, 2011). One example of how this directs axon guidance is the Ig family member Fasciclin II (FasII), which allows homophilic adhesion between axons so they can recognize other axons headed in the same direction and form tight bundles with them (Harrelson and Goodman, 1988; Snow et al., 1988;

Lin and Goodman, 1994; Lin et al., 1994). Together, these families of axon guidance cues are responsible for the direction of billions of axons towards their synaptic targets.

#### **1.2.4. The Development of Axon Collaterals**

The axon growth cone must traverse long distances to reach its target. In many cases, particularly in the central nervous system, these axons must innervate multiple targets to achieve the final circuitry necessary for adult brain function. Thus, axons can form numerous collaterals, or branches, at designated stages during development, as well as later during adulthood in response to learning (DeBello et al., 2001; Kalil et al., 2011). Previous evidence has indicated that axon branches can form in response to neurotrophins and classical guidance cues, which demonstrates that axon branching can in some cases be regulated by similar signaling mechanisms as growth cone motility (Gallo and Letourneau, 1998; Dent et al., 2004). A closer examination of axon branch formation in response to cues demonstrates that many of the downstream signaling pathways that promote axon outgrowth in response to the classically attractive cue, Netrin-1, also promote branch development (Tang and Kalil, 2005). Furthermore, the formation, elongation, and elimination of axon branches require the reorganization of the cytoskeleton, with actin accumulation playing an essential role (Gallo and Letourneau, 1998; Kalil et al., 2000). Regions along the axon where the growth cone had paused its forward motion have been shown to leave behind active actin lamellipodial and filopodial structures, which can develop into interstitial branches days after the growth cone has moved beyond the target location (Szebenyi et al., 1998). In regions where actin filaments have formed these protrusions in the axonal membrane, microtubules can invade and promote branch elongation and stabilization (Kalil et al., 2000). These cytoskeletal elements are regulated by a variety of

signaling pathways, which in the case of actin converge on actin-binding proteins to promote, stabilize, or degrade axon branches (Sainath and Gallo, 2014; Spillane and Gallo, 2014). From there, elongation of axon branches can often follow similar mechanisms of guidance and cytoskeletal regulation as the primary growth cone (Tang and Kalil, 2005; Kalil and Dent, 2014).

### **1.2.5. Regulation of Actin Remodeling Downstream of Guidance Signaling**

The remodeling of the actin cytoskeleton by actin regulatory proteins is highly conserved across cell types and species. This evolutionary choice allows essential processes such as axon guidance to occur rapidly and precisely across organisms, without significant genetic overhauls to the system of cytoskeletal regulation that may result in embryonic lethal wiring errors (Menzies et al., 2004). To illustrate this phenomenon more clearly, below are several examples of important actin regulatory proteins and their specific roles in axon guidance-related cytoskeletal regulation.

#### **1.2.5.1. Controlled Cytoskeletal Breakdown: Actin Depolymerizing Factor and Cofilin**

Guidance of developing axons involves directional steering of the growth cone towards or away from the attractive or repulsive cues. This is largely achieved by rapid remodeling of the actin cytoskeleton and its dynamics. Among many actin regulatory molecules, ADF/cofilin (AC) plays an essential role in regulating actin dynamics during growth cone elongation and guidance. The activity of AC is primarily regulated by phosphorylation on a highly conserved serine residue, Ser3 (Agnew et al., 1995; Moriyama et al., 1996). Ser3 phosphorylation inactivates AC's ability to bind F-actin to depolymerize and sever the filaments. The LIM (Lin- 11/Isl-1/Mec-3)

kinases and the TES (testicular protein) kinases are the two kinase families that phosphorylate and inactivate ACs (Agnew et al., 1995; Yang et al., 1998; Toshima et al., 2001). Two distinct families of phosphatases, named Slingshot (SSH) and chronophin (CIN), dephosphorylate AC for re-activation (Niwa et al., 2002; Ohta et al., 2003; Meng et al., 2004; Gohla et al., 2005). Both LIM kinases and SSH phosphatases are regulated by a wide range of signaling pathways including Rho GTPases and  $Ca^{2+}$ , thus placing AC at the converging point of intricate signaling pathways to regulate actin dynamics (Bernstein and Bamburg, 2010).

While AC primarily functions to sever and depolymerize F-actin, the effects of AC activity on growth cone motility are complex. On one hand, AC activity is essential for the actin dynamics underlying growth cone motility, and overexpression of AC in neurons leads to increased neurite outgrowth (Meberg et al., 1998). This is consistent with the observation that high actin turnover is associated with increased growth cone motility (Bradke and Dotti, 1999). In this case, AC is likely responsible for turning over the F-actin at the rear of the lamellipodia to support the rapid forward protrusion in part by supplying G-actin to the leading edge for polymerization. On the other hand, AC activation has been associated with growth cone collapse in response to repulsive cues (Hsieh et al., 2006; Piper et al., 2006). In this case, overall depolymerization of F-actin in growth cones was observed, suggesting that AC was activated globally throughout the growth cone to cause the destruction of F-actin structures. Therefore, different spatiotemporal patterns of AC activities may be responsible for generating distinct effects on growth cone motility. Our lab reported previously that attractive and repulsive turning of nerve growth cones is mediated by asymmetric AC inhibition and activation, respectively (Wen et al., 2007). These findings are consistent with the depolymerizing/severing functions of AC on the actin cytoskeleton, but appear to differ from that observed in fibroblasts and

carcinoma cells in which local AC activation promotes actin-based protrusion (Ghosh et al., 2004; Desmarais et al., 2005). Moreover, activation of AC in growth cone attraction was also observed in cultured dorsal root ganglion neurons (Marsick et al., 2010). It is plausible that different types of cells and their unique cytosolic environments, together with the spatiotemporal patterns of AC activation, may determine the final outcome on the actin structure and dynamics in the growth cone. As discussed previously, the final effects of AC on actin structures and dynamics likely depend on a number of factors such as the spatiotemporal pattern, degree of the activation, and the local G- to F-actin ratio.

Adding to the complexity of AC regulation and effects on the actin cytoskeleton, recent studies show that AC-mediated F-actin disassembly is enhanced by actin oxidation through the redox enzyme Mical. Specifically, the synergistic actions of AC and Mical mediate growth cone collapse in response to the repulsive cue Semaphorin in invertebrates (Hung et al., 2010; Grintsevich et al., 2016). Mical associates with PlexA, a receptor for Semaphorins in *Drosophila* (Hung and Terman, 2011). Activated Mical can cause F-actin disassembly via oxidation of the bound actin subunits at their M44 residues, and the oxidized G-actin also exhibits disrupted polymerization (Hung et al., 2011). Interestingly, Mical-mediated oxidation of F-actin improves cofilin binding to augment cofilin's filament severing and disassembly properties (Grintsevich et al., 2016). The coordinated efforts between the oxidation of actin by Mical and the severing of actin filaments by AC lead to growth cone collapse, which is an example of how AC recruitment can contribute to repulsive signaling. While these findings are interesting, whether Mical functions in vertebrate semaphorin signaling remains to be determined.

### **1.2.5.2. The Rho GTPases**

The Rho family of small GTPases consists of three members, RhoA, Rac, and Cdc42, and they play a crucial role in mediating complex signaling and the remodeling of the actin cytoskeleton. In nerve cells, RhoA is associated with inhibitory signaling that impairs growth cone motility, whereas Rac1 and Cdc42 are primarily downstream effectors of growth-promoting and attractive cues (Hall and Lalli, 2010). Activation of the RhoA GTPase has been associated with growth cone inhibition by a number of inhibitory/repulsive cues such as myelin associated glycoprotein, NOGO, and Semaphorins (Fujita and Yamashita, 2014). RhoA acts through Rho kinase ROCK, which can in turn regulate several distinct downstream targets to regulate the actin cytoskeleton in growth cones. ROCK can phosphorylate and activate LIMK1, leading to the inactivation of cofilin. Such a pathway has been indicated in growth cone inhibition by several repulsive cues (Aizawa et al., 2001; Marsick et al., 2012). In this case, however, inhibition of growth cone motility is likely achieved through the activation of actomyosin contractility through ROCK phosphorylation of myosin light chain kinase (Amano et al., 1998; Kubo et al., 2008). Indeed, inhibition of myosin II has been shown to promote growth cone extension over inhibitory molecules (Hur et al., 2011). The finding that pharmacological disruption of F-actin abolished actomyosin-mediated growth cone retraction (Wang and Zheng, 1998) suggests its requirement for intact F-actin structure. Therefore, ROCK inhibition of cofilin may be important for actomyosin contractility and growth cone inhibition. Given that different guidance receptors could be coupled to distinct downstream targets, the above described multiple pathways involving AC exemplifies the complexity, flexibility, and adaptability of the guidance mechanisms underlying precise wiring of the nervous system.

### 1.2.5.3. GEFs and GAPs: Key Regulators of Growth Cone Motility

The Rho GTPases are activated by the guanine exchange factors (GEFs) and inactivated by the GTPase-activating proteins (GAPs) (Hall, 1998). In neurons, it has been shown that both RhoA and Rac1 can be activated by a GEF named TRIO, or Triple Functional Domain Protein. TRIO has been the subject of significant interest recently due to its unusual structure and key role in axon guidance. First discovered in 1996, TRIO is named for its three functional domains: a RhoG/Rac1 GEF domain, a RhoA GEF domain, and a serine/threonine kinase domain (Debant et al., 1996; van Rijssel and van Buul, 2012). Through these domains, TRIO can lead to LIM kinase activation to inhibit AC activity (Ng and Luo, 2004). The presence of GEF domains for two Rho GTPases in opposing guidance responses makes TRIO unique and suggests its involvement in multiple signaling pathways. For example, the Rac1 GEF domain of TRIO was found to function in non-canonical Notch signaling in *Drosophila* motor neurons, in which Notch activates TRIO and Rac1 to reduce fasciculation of the motor axons (Song and Giniger, 2011). TRIO is phosphorylated by Fyn Src Kinase at Y2622 in response to Netrin signaling in rat cortical neurons to activate Rac1 and produce axon outgrowth (DeGeer et al., 2013). Phosphorylated TRIO in turn increases surface expression of the Netrin receptor DCC. Thus, the growth cone behaviors produced by TRIO-based activation of Rac1 seem to depend on the cellular and signaling contexts. Rac1 can also be activated by a second GEF found in the growth cone, known as Tiam-1. Similar to TRIO, Tiam-1 is a common GEF for both ced-10 (Rac1 in *C. elegans*) and mig2 (RhoG in *C. elegans*). Tiam-1 activation of ced-10/Rac1 was found to activate lamellipodial and filopodial protrusion downstream of Netrin/DCC signaling, in a mechanism distinct from TRIO activity (Demarco et al., 2012). This indicates that though TRIO activates the same Rho GTPases as Tiam-1, it acts downstream of different receptor pathways independently

of Tiam-1, and may therefore elicit different growth cone behaviors from Rac1 activation. Further research is required to elucidate how these differing contexts of Rac1 activation can produce such distinct effects on the actin cytoskeleton and overall growth cone behavior.

### **1.3. LIM and SH3 Protein 1 (LASP1): a Review of the Literature and Outstanding Questions**

Careful examination of the actin regulators that drive growth cone motility and guidance reveals a few universal truths. Firstly, that these actin regulators are typically highly conserved across species and are widely expressed in a variety of motile cell types. Secondly, they are often dysregulated in diseases of cellular motility, such as cancer. And finally, these proteins are able to connect with a variety of binding partners to promote key cellular functions. One unusual actin-binding protein LIM and SH3 Protein 1 (LASP1) fits all of these standards, and has been shown to be expressed in axon growth cones. However, neither its role in actin regulation, nor its function in the growth cone have yet been established. Below I describe the background literature on LASP1's fellow Nebulin family members, its sister protein LASP2, and the evidence linking LASP1 to mental disorders, cancer, and immune cell chemotaxis.

#### **1.3.1. The Nebulin Family of Actin-Binding Proteins**

LASP1 is a member of the Nebulin family of proteins, which are characterized by their ability to bind to actin filaments. This is accomplished through a series of nebulin repeats, which are found in the structures of each of the five family members, Nebulin, Nebulette, N-RAP, LASP1, and LASP2. The members of the Nebulin family of proteins vary widely in size, with

the largest, Nebulin, containing 185 nebulin repeats and the two smallest, LASP1 and LASP2, containing only two and three, respectively (Pappas et al., 2011). Of all the proteins that make up the family, Nebulin is the best-studied member. In humans, mutations in the *Nebulin* gene cause nemaline myopathy, a human muscle disorder with varying degrees of severity from muscle weakness to neonatal lethality (Pelin et al., 1999; Sanoudou and Beggs, 2001; Lehtokari et al., 2006). Initial studies of Nebulin have hypothesized that it could act as a molecular ruler, regulating the length of the thin actin filaments in skeletal muscle by providing a structural template (Trinick, 1994; Horowitz, 2006). However, with recent technical advances, more refined studies have found that while Nebulin is able to determine the length of thin filaments, it does so by stabilizing actin filaments to a minimum length only, and it does not meet the “necessary and sufficient” criteria for a molecular ruler (Pappas et al., 2010). However, this technicality does not diminish the importance of Nebulin for sarcomere regulation.

Of the other Nebulin family members, Nebulette is the only one expressed exclusively in cardiac cells. In this context, Nebulette seems to function similarly to Nebulin, in that it maintains a minimum length for the actin filaments. However, it also seems to interact with troponin and tropomyosin and promote their localization to thin filaments (Moncman and Wang, 2002; Bonzo et al., 2008). This helps to regulate the beating of cardiomyocytes in culture, and stabilizing thin filaments in cardiac muscle. Mutations in Nebulette are implicated in dilated cardiomyopathies, which in some cases can cause upregulation of N-RAP (Sussman et al., 1998; Purevjav et al., 2010). N-RAP is expressed in striated muscle, where it regulates myofibril differentiation and assembly. It is the only member of the Nebulin family without an SH3 domain, and the only member outside the LASP subfamily to contain a LIM domain.

The LASP subfamily consists of two, highly similar proteins: LASP1 and LASP2 (**Figure 1-2**). Their sequences and structures are highly similar, however they do not share a gene. LASP2 is a splice variant of Nebulette, with four unique exons that add an N-terminal LIM domain, among other variations (Pappas et al., 2011). LASP2 is also only expressed in mammals, whereas LASP1 is expressed in a variety of organism types (Bliss et al., 2013). While LASP1 is expressed in virtually every cell type, LASP2 is expressed largely in the brain and lungs. Furthermore, LASP2 is implicated in a variety of actin structures and cellular functions, including cell spreading and adhesion (Terasaki et al., 2004; Grunewald and Butt, 2008). Despite their similar structures, LASP1 and LASP2 share only a few confirmed binding partners: zyxin and F-actin (Grunewald and Butt, 2008; Bliss et al., 2013). Due to the lack of a reliable antibody against LASP2, it is difficult to say whether future studies will be able to find more LASP2 binding partners that overlap with LASP1. Within the brain, LASP2 has recently been shown to promote dendrite growth and the development of dendritic spines (Myers et al., 2020). However, as it was only discovered recently, not much more is known about its functions.

### **1.3.2. LASP1: a Review**

LIM and SH3 Protein 1 (LASP1) is a unique F-actin binding protein with many of the characteristics of a signaling molecule. LASP1 contains three protein binding domains: an N-terminal LIM domain, two nebulin repeats that bind F-actin, and a C-terminal Src Homology 3 (SH3) domain (Schreiber et al., 1998) (**Figure 1-2**). Through these domains, LASP1 is able to interact with several key binding partners, including VASP, an actin anti-capping protein, and zyxin, a protein associated with connecting actin to adhesions (Orth et al., 2015) (**Figure 1-2**). LASP1 is also highly expressed in the nervous system during development, and the LASP1 gene

has been linked to both autism and schizophrenia. Previous studies have found that LASP1 is highly expressed in both humans and nonhuman primates from as early as 8 weeks post conception, which is confirmed by one study showing its expression in dissociated hippocampal growth cones (Allen Developing Transcriptome) (Phillips et al., 2004). In a study of the genetic causes of autism, Stone et al. (2007) found a significant transmission bias of autistic disorders through a Single Nucleotide Polymorphism (SNP) in the LASP1 gene. In mouse models of schizophrenia, LASP1 was found to be significantly down-regulated, and in humans a SNP (T allele) in the LASP1 promoter was found to be more prevalent in patients with schizophrenia than in demographically-matched controls (Joo et al., 2013). LASP1 is clearly vital for nervous system function, yet the cellular role of LASP1 that accounts for its associated diseases is unknown. LASP1 was first discovered in a cDNA analysis of metastatic breast cancer and has since been implicated in the aggressiveness and invasiveness of numerous cancer cell types, including ovarian, renal, colorectal, and prostate cancers (Tomasetto et al., 1995b; Grunewald et al., 2007; Zhao et al., 2010; Hailer et al., 2014; Yang et al., 2014). On the cellular level, LASP1 appears to promote cell motility: knock-down or overexpression result in decreased or increased actin-based cellular protrusion, respectively (Grunewald et al., 2006). However, the mechanism by which LASP1 promotes actin-based motility is currently unclear. Furthermore, while LASP1 has been found to play a role in the CXCR2-based chemotaxis of cultured immune cells, suggesting that LASP1 functions in signal transduction and directional cell motility, its role in growth cone chemotaxis and motility is unknown (Raman et al., 2010). Answering these questions is critical to understanding the full function of this fascinating protein.

#### 1.4. Dissertation Hypothesis and Questions

Actin-binding proteins are critical to the motility of cells and the guidance of axons towards their synaptic targets. Furthermore, actin-binding proteins are highly conserved in their regulatory roles across cell types. The goal of this thesis research is to provide more insight into the function and mechanisms of actin-binding proteins in axon development. Previous studies have shown that actin-binding protein LASP1 promotes the migration of cells and the invasiveness of tumor cells (Butt et al., 2003; Orth et al., 2015). Furthermore, LASP1 plays a key signaling role in immune cells downstream of chemokine receptor CXCR2 (Raman et al., 2010). While LASP1 has been found in axon growth cones, its role in this structure has not been studied (Phillips et al., 2004). These studies provide the basis for the main hypothesis explored in this thesis: that LASP1 acts as a positive regulator of axon development by promoting the motility of axon growth cones. In Chapter 2, I will show that LASP1 interacts with F-actin plus ends at the leading edge of lamellipodial actin structures; that it promotes the elongation and branching of axons *in vitro*; and that *Drosophila* Lasp promotes commissure development and fasciculation *in vivo*. In Chapter 3, I describe a method for labeling endogenous proteins in genetically- and optically-selected cells, which has future implications for studying actin and actin-binding proteins in intact tissue. Finally, Chapter 4 summarizes my findings and presents additional future directions of study that will help elucidate the mechanisms of LASP1 function and the role of actin-binding proteins in axonal development.

## 1.5. Figures

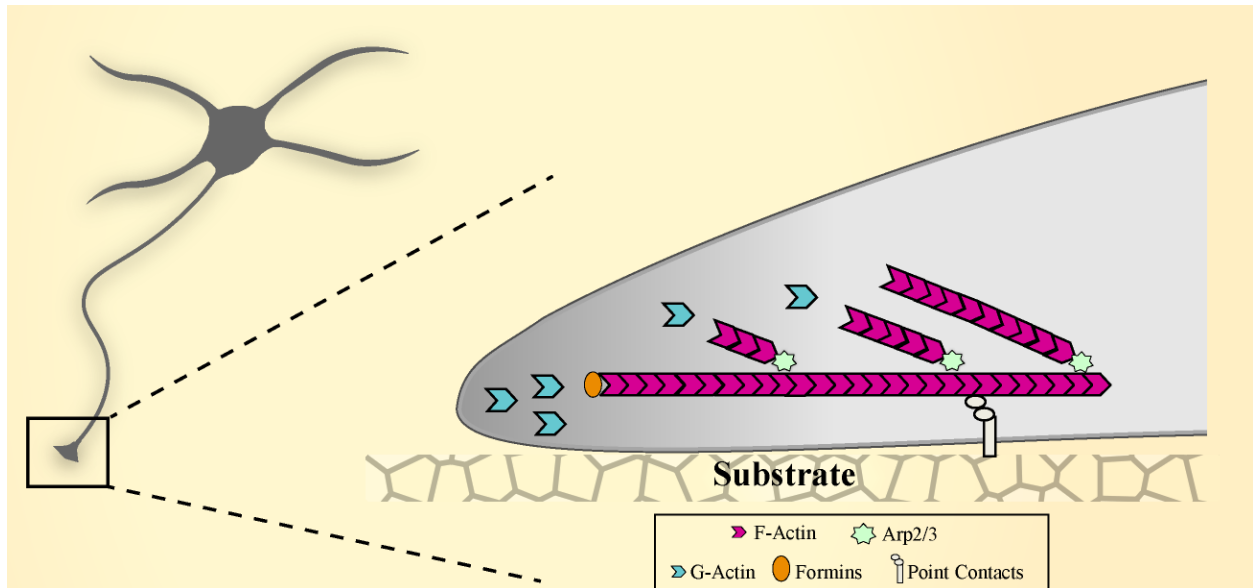


**Figure 1-1:** Diagram of Actin-Based Growth Cone Motility. The axon growth cone is a structure at the tip of the axon, whose peripheral region contains complex actin-based structures. The side view (right) shows actin filaments (F-actin, pink) as they are polymerized from the G-actin (blue). This occurs with the help of two proteins: formins (orange), which add monomers at the tips of actin bundles, and the Arp2/3 complex (light green), which nucleates new filament branches in lamellipodia. Forward motion is accomplished with the assistance of point contact adhesions (white), which connect actin structures to the extracellular substrate and provide traction.

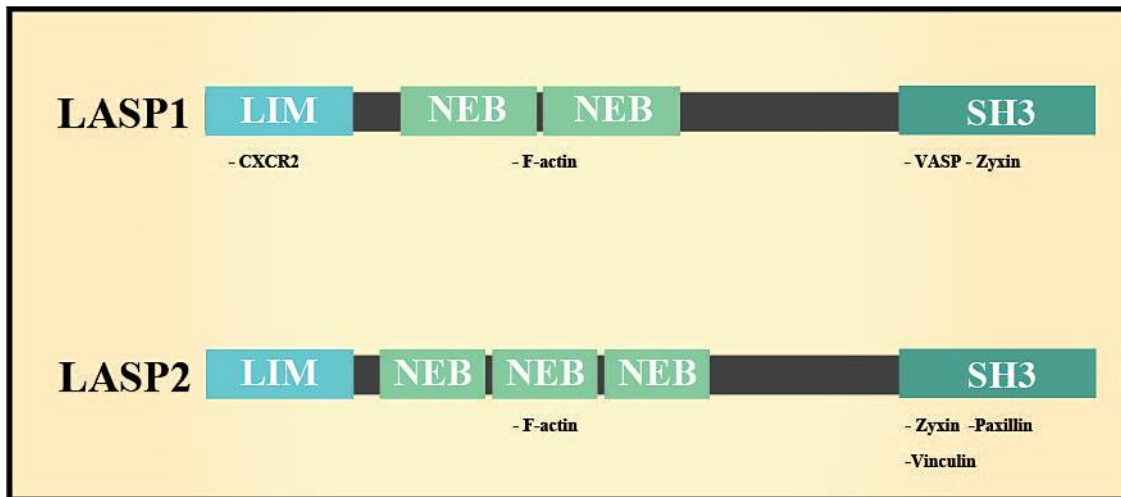


**Figure 1-2:** The structures of LASP1 and LASP2. These two LASP proteins have highly similar structural domains: both proteins have an N-terminal LIM domain and a C-terminal SH3 domain, as well as internal nebulin repeats. However, while LASP1 has two nebulin repeats, LASP2 contains three. There is surprisingly little overlap in their binding partners; while both proteins bind to F-actin through their nebulin repeats and to zyxin, LASP2 favors more adhesion proteins vinculin and paxillin through its SH3 domain, whereas LASP1 binds to VASP, an anti-actin capping protein. Furthermore, LASP1 binds to CXCR2, a chemokine receptor, through its LIM domain, whereas LASP2 currently has no known LIM binding partners (Grunewald and Butt, 2008; Bliss et al., 2013).

## **Chapter 2:**

# **LIM and SH3 Protein 1 Localizes to the Leading Edge of Protruding Lamellipodia and Regulates Axon Development**

Portions of this chapter were adapted from the following publication:

**Pollitt SL, Myers KR, Yoo J, Zheng JQ.** LIM and SH3 Protein 1 Localizes to the Leading Edge of Protruding Lamellipodia and Regulates Axon Development. *Molecular Biology of the Cell. In Revision*

## 2.1. Summary

The actin cytoskeleton drives cell motility and is essential for neuronal development and function. LIM and SH3 Protein 1 (LASP1) is a unique actin-binding protein that is expressed in a wide range of cells including neurons, but its roles in cellular motility and neuronal development are not well understood. Here I report that LASP1 is highly expressed in rat hippocampus early in development, and this expression is maintained through adulthood. High-resolution imaging reveals that LASP1 is selectively concentrated at the leading edge of lamellipodia in migrating cells and axonal growth cones. This local enrichment of LASP1 is dynamically associated with the protrusive activity of lamellipodia, depends on the barbed ends of actin filaments, and requires both the LIM domain and nebulin repeats of LASP1. Knockdown of LASP1 in cultured rat hippocampal neurons results in a substantial reduction in axonal outgrowth and arborization. Finally, loss of the *Drosophila* homolog Lasp from a subset of commissural neurons in the developing ventral nerve cord produces defasciculated axon bundles that do not reach their targets. Together, these data support a novel role for LASP1 in actin-based lamellipodial protrusion and establish LASP1 as a positive regulator of both *in vitro* and *in vivo* axon development.

## 2.2. Introduction:

The development of complex circuits in the central nervous system requires the precise wiring of axons with their synaptic targets. Axon growth and guidance depend upon the axon growth cone, a fan-shaped motile structure at the distal end of the growing axon. To reach its final destination, the growth cone must navigate vast distances in response to a multitude of biochemical and biophysical signals (Kolodkin and Tessier-Lavigne, 2011). The growth cone is

highlighted by two actin-rich protrusions: filopodia, finger-like protrusions containing long linear filamentous actin (F-actin), and lamellipodia, sheet-like thin protrusions powered by a network of branched short F-actin (Dent et al., 2011). Growth cone filopodia are believed to function in sampling the extracellular environment, whereas lamellipodia drive growth cone extension (Vitriol and Zheng, 2012; Omotade et al., 2017). Extracellular guidance cues are translated into spatially-organized intracellular signaling cascades that lead to distinct growth cone responses by targeting the structure and dynamics of the actin cytoskeleton in the growth cone (Kalil and Dent, 2005; Lowery and Van Vactor, 2009; Vitriol and Zheng, 2012). The dynamics of F-actin polymerization, depolymerization, and reorganization are tightly regulated by a large number of actin-binding proteins (Pollard and Borisy, 2003; Vitriol and Zheng, 2012; Gomez and Letourneau, 2014; Omotade et al., 2017). Actin assembly at the leading edge of the lamellipodia is a driving force behind growth cone motility (Pollard and Borisy, 2003; Dent et al., 2011; Yang et al., 2012). During growth cone protrusion, a small subset of actin-binding proteins are specifically recruited to the leading edge to facilitate the addition of actin monomers to the plus ends of actin filaments, which are concentrated at the membrane-actin cytoskeleton interface (Lowery and Van Vactor, 2009; Pollard and Cooper, 2009; Dent et al., 2011). Forward movement of the growth cone requires the action of these actin-binding proteins for new polymerization at the leading edge, together with the engagement of the “molecular clutch” to produce the traction force (Lowery & Van Vactor 2009).

LIM and SH3 Protein 1 (LASP1) is the smallest member of the Nebulin family of actin-binding proteins, of which the founding member Nebulin is well known for its structural role in skeletal muscles (Tomasetto et al., 1995b; Terasaki et al., 2004; Pappas et al., 2011; Orth et al., 2015). LASP1 is highly expressed in a number of tissues including the brain, and its

dysregulation has been implicated in several neurological disorders, including autism spectrum disorder and schizophrenia (Stone et al., 2007; Joo et al., 2013), suggesting a role for LASP1 in nervous system development and function. One study of LASP1 localization provided evidence that LASP1 accumulates in the growth cones of developing neurons, and the dendritic spines of mature neurons (Phillips et al., 2004). In mature neurons, LASP1 localization to spines has been shown to regulate dendritic spine development and synaptic function (Myers et al., 2020). However, no study has examined the function of LASP1 in young neurons, especially in axonal development.

LASP1 contains an N-terminal LIM domain, two internal actin-binding nebulin repeats, and a C-terminal SH3 protein-interaction domain (Tomasetto et al., 1995b; Schreiber et al., 1998). LASP1 was found to be upregulated in numerous cancer types, including ovarian, breast, renal, colorectal, and prostate cancers (Tomasetto et al., 1995a; Grunewald et al., 2006, 2007). This increased LASP1 expression has been shown to positively correlate with cell motility and cancer metastasis (Grunewald et al., 2006, 2007). Therefore, LASP1 appears to regulate actin-based cell motility, but the mechanism by which LASP1 regulates actin-based protrusion and cellular motility is currently unclear. Moreover, if and how LASP1 functions in neurons during early development remains unknown. In this study, I investigated the expression profile, subcellular distribution, and function of LASP1 in developing neurons. I present evidence that LASP1 regulates the actin-based protrusive activities that underlie the axon growth and branching in culture, as well as plays a role in axon development *in vivo*.

### **2.3. Materials and Methods:**

#### *Cell Culture:*

Primary culture of rat hippocampal neurons was performed as previously described (Omotade et al., 2017; Myers et al., 2020). Briefly, E18 rat embryos of both sexes were obtained from time-pregnant Sprague-Dawley rats (Charles River Laboratories, Wilmington, MA). Brains were removed from the embryos and the hippocampi were isolated for dissociation, which consisted of treatment with trypsin for 15 min at 37 °C, followed by pipette trituration in neuronal culture media (Neurobasal<sup>®</sup> medium containing GlutaMAX (Invitrogen), penicillin/streptomycin, and B27 supplement (Thermo Fisher Scientific)). Dissociated hippocampal neurons were plated at a density of 50,000 cells/35 mm dish on acid-washed glass coverslips (for immunohistochemistry) or 250k in 4-well 35 mm glass bottom dishes (Greiner) (for live cell imaging). All coverslips for hippocampal neuron cultures were coated with 0.1 mg/ml poly-D-lysine (Sigma) 24 hours before dissection. Neurons were kept in a 37 °C, 5% CO<sub>2</sub> incubator thereafter in neuronal culture media, with one complete media change 24 hours after plating. All animal use was carried out in compliance with National Institutes of Health guidelines, and protocols were approved by the Emory University's Institutional Animal Care and Use Committee.

Cath.a Differentiable (CAD) cells (Qi et al., 1997) were cultured and maintained in DMEM/F12 (Invitrogen) media supplemented with 8% Fetal Bovine Serum (Atlanta Biologicals) and 1% Penicillin/Streptomycin (Invitrogen). For imaging experiments, CAD cells reaching 90% confluence were resuspended and plated on detergent- and HCl-washed No. 1 glass coverslips coated with 20 µg/ml laminin (CAS#: 114956-81-9, MilliporeSigma, St. Louis, MO). 10,000 cells were plated on 25 mm round coverslips, and allowed to spread for 1-3 hours.

### *Transfection and Constructs:*

CAD cells were transfected 18-24 hours prior to imaging at approximately 70% confluence using Xtreme Gene transfection reagent (Millipore Sigma) and Opti-MEM (Invitrogen) according to manufacturer instructions. The GFP-LASP1 construct has been described previously and was generously provided by Dr. Joachim Kremerskothen (Stölting et al., 2012). To reduce LASP1 expression levels, GFP-LASP1 was subcloned into crippled CMV constructs provided by Dr. Richard Kahn at Emory University, courtesy of Dr. Wesley Sundquist (University of Utah) (Morita et al., 2012; Newman et al., 2016), and GFP-LASP1 was inserted via PCR. The GFP-LASP1 $\Delta$ LIM, GFP-LASP1 $\Delta$ Neb, and GFP-LASP1 $\Delta$ SH3 constructs have been previously described (Stölting et al., 2012; Myers et al., 2020). Lifeact-mRuby (pN1-Lifeact-mRuby) was provided by Roland Wedlich-Soldner, Max-Planck Institute of Biochemistry.

To knockdown LASP1 in hippocampal neurons, two shRNA constructs were inserted in the pSuper-mCherry backbone, shLASP1a and shLASP1b, respectively. The following oligos were annealed and ligated into pSuper.neo+mCherry (Myers et al., 2020) digested with BglIII and XhoI: shLASP1a - 5'

GATCCCAAGGTGAACTGTCTGGATAAGTTCAAGAGACTTATCCAGACAGTTCACCT  
TTTTTTC (Forward)/ 5'

TCGAGAAAAAAGGTGAACTGTCTGGATAAGTCTCTTGAAGTTATCCAGACAGTTCA  
CCTTGGG (Reverse) (previously published) (Myers et al., 2020) and shLASP1b -

5'GATCCCCCATTAAGGAGATCGGTTATTCAAGAGATAACCGATCTCCTTAATGGTT  
TTTC (Forward)/

5'TCGAGAAAAACCATTAAGGAGATCGGTTATCTCTTGAATAACCGATCTCCTTAATG

GGGG (Reverse). The empty pSuper vector, shLASP1a, and shLASP1b were transfected into DIV2 rat hippocampal neurons using the OZBiosciences Neuron Magnetofection kit (OZBiosciences) per manufacturer instructions.

*Immunohistochemistry:*

Neurons were fixed on DIV2 with 4% PFA/4% sucrose in PBS without magnesium or calcium for thirty minutes. CAD cells were fixed one hour after plating on coverslips, using 4% PFA in PBS without magnesium or calcium for fifteen minutes. Cells were permeabilized with 0.2% TritonX 100 in PBS for ten minutes, then left at room temperature in blocking solution (4% BSA, 1% goat serum, 0.1% TritonX 100) for one hour. The cells were then incubated with primary antibodies at 4°C overnight, followed by three washes in PBS, and labeled with fluorescent secondary antibodies at room temperature for 1 hr. The following antibodies were used: LASP1 (1:500 rabbit anti-LASP1, Proteintech 10515-1-AP),  $\alpha$ -tubulin (1:1000 mouse anti- $\alpha$ -tubulin DM1A clone, Sigma T6199) and/or capping protein (1:500 rabbit anti-capping protein  $\beta$ 2, generously provided by Dr. John Hammer of the National Heart Lung and Blood Institute, National Institutes of Health, Bethesda, MD) (Schafer et al., 1994). Alexa Fluor-conjugated secondary antibodies (Invitrogen) were diluted at a concentration of 1:750 in PBS-containing 2% goat serum. Alexa Fluor 568-Phalloidin (Invitrogen) was applied at a 1:100 dilution in PBS for 20 minutes. All labeled coverslips were mounted on glass slides using Fluoromount-G (SouthernBiotech) for imaging.

*Western Blots:*

Rat hippocampi were isolated at the indicated time points, and homogenized through a syringe tip in lysis buffer containing 20 mM TRIS (pH 8.0) 137 mM NaCl, 1% Triton X-100,

10% glycerol, 2 mM EDTA, and cOmplete protease inhibitor cocktail (Sigma) (Omotade et al., 2018). Cultured neurons and CAD cells were lysed directly in 1x Laemmli sample buffer, then boiled for 5 minutes, followed by vortexing for 5 minutes. Equal volumes of cell lysates or equal amounts of protein from tissue homogenates, as assessed by a Bradford assay, were loaded on mini-Protean 12% Tris-glycine acrylamide gels (BioRad) and then transferred to nitrocellulose. Membranes were blocked with 5% milk in PBS-Tween for 1 hour, then incubated overnight at 4°C with primary antibodies. The following antibodies were used for blotting: rabbit anti-LASPI (1:1000, Proteintech), mouse anti- $\alpha$ -tubulin DM1A clone (1:5000, Sigma), rabbit anti-GFP (1:5000, Invitrogen), goat anti-mouse 647 (1:10,000, Invitrogen), or goat anti rabbit HRP (1:10,000, Invitrogen). Membranes were then incubated in Alexa Fluor 647-conjugated secondary antibody (Invitrogen) for 1 hour and visualized by immunofluorescence.

#### *Live Imaging and Drug Treatments:*

CAD cells were plated on laminin-coated coverslips for 1 hour in Krebs-Ringers solution (150mM NaCl, 5mM KCl, 2mM CaCl<sub>2</sub>, 1mM MgCl<sub>2</sub>, 10mM glucose, 10mM HEPES, pH 7.4) supplemented with 20% fetal bovine serum, then mounted in live-cell chambers. To inhibit actin polymerization, the following drugs were used at the indicated final concentrations: 25nM Cytochalasin D (Sigma), 100nM LatrunculinA (EMD Millipore), 10 $\mu$ M SMIFH2 (EMD Millipore), and 100 $\mu$ M CK-666 (EMD Millipore). Cells were imaged for five minutes prior to drug addition, then for 10 minutes immediately following drug addition to monitor changes in localization. Primary hippocampal neurons were cultured and imaged in phenol red-free neuronal culture medium. For multi-day imaging, cells were imaged every 24 hours using software xyz location markers to locate the same neurons each time. For growth cone and branch tracking,

cells were imaged every 10 minutes for 18 hours in a stage top incubator (Tokai-hit) at 37°C in 5% CO<sub>2</sub>.

#### *Actin Barbed End Labeling:*

CAD cells transfected with either CMVΔ4 GFP-LASP1 or GFP were plated on coverslips as described above. Actin barbed ends were labeled as described previously (Gu et al., 2010; Marsick and Letourneau, 2011). Briefly, cells were lightly fixed in permeabilization buffer (138mM KCl, 4mM MgCl<sub>2</sub>, 3mM EGTA, 1% BSA, 20mM HEPES pH 7.5, 1mM ATP, 0.2mg/mL saponin) with 0.05% PFA and 0.05% glutaraldehyde for 1 minute. Next, plus ends were labeled with permeabilization buffer containing 0.45μM rhodamine-non-muscle actin (Cytoskeleton, APHR-A) for 2 minutes. Coverslips were then immediately fixed with 4% PFA and 0.05% glutaraldehyde in PHEM cytoskeletal stabilization buffer (60mM PIPES, 25mM HEPES, 10mM EGTA, 2mM MgCl<sub>2</sub>, 0.12M sucrose, pH 7.0) for 30 minutes and immunostained for GFP (Alexa-488 rabbit anti-GFP, Invitrogen A-21311).

#### *Microscopy:*

CAD cells were imaged on a Nikon Ti microscope (Nikon Instruments Inc) with a Plan Apo 60x objective (NA 1.4) and a Hamamatsu CCD camera (Hamamatsu Photonics). Hippocampal neurons were imaged using a Nikon Eclipse Ti2 microscope with a Plan Apo 20x objective (NA 0.8) and Hamamatsu CCD. *Drosophila* embryos were imaged as z-stacks comprised of at least 42 optical sections (0.75 μm step-size) using a Nikon C2 laser-scanning confocal system with a Nikon Eclipse Ti2 microscope and a Plan Apo 20x objective (NA 0.8). Maximum intensity projections. All microscopes were equipped with Nikon Elements software.

#### *Analysis and Statistics:*

Images were analyzed using the Imaris Neuroscience and Filament tracking modules (growth cone and axon branch tracking), Nikon Elements (kymograph analysis), and FIJI (axon length measurements using Simple Neurite Tracer) (ImageJ, National Institutes of Health). Statistics were calculated using R. Line profiles were made in FIJI, and normalized to the peak maximum intensity with the exception of the soluble GFP channel in **Figure 2-5A**, which was normalized to the cell center. *Drosophila* embryo image stacks were made into maximum intensity projections and analyzed using Nikon Elements. Data were analyzed using a one-way ANOVA with a Tukey HSD post-hoc test, unless otherwise specified. *Drosophila* experiments were analyzed using a Student's t test, or a Welch's t test when variances were unequal. All graphs represent mean  $\pm$  SEM unless otherwise specified.

#### *Drosophila:*

Two crosses from three fly lines were used to produce the embryos measured in this paper. They are as follows: 1) ;[UAS<sub>tau</sub>:myc:GFP]/cytubGAL80; egl GAL4 (gift from Dr. Greg Bashaw, University of Pennsylvania, Philadelphia, PA) 2) ;UAS<sub>dicr</sub>;UAS P(TRiP) LASP RNAi (Bloomington *Drosophila* Stock Center, Bloomington, IN, USA) 3) UAS <sub>dicr</sub> on 2 (gift from Dr. Ken Moberg, Emory University, Atlanta, GA). Embryos were collected and stained for BP102 (1:100 mouse anti-BP102, DSHB) and GFP (1:500 rabbit anti-GFP, Thermofisher A-11122) using a previously published immunocytochemistry protocol (Bashaw, 2010). Briefly, embryos were collected for four hours on apple cider vinegar agar plates, then aged for 14 hours overnight. Embryos were washed briefly in deionized water, then incubated in a 50% bleach solution for five minutes to remove the chorion. The embryos were then rinsed and fixed in 3.7% formaldehyde under a layer of heptane for 15 minutes. The fixative layer was then removed and replaced with pure methanol. The embryos were vortexed for 1 minute, then rinsed three times

with methanol and transferred to PBS. Permeabilization of the embryos was achieved by adding 1% TritonX in PBS (PBSTx) and incubating for 5 minutes on an orbital shaker. Embryos were then blocked using 2% normal goat serum diluted in PBSTx for 10 minutes. Primary antibody was diluted in blocking buffer and applied overnight at 4°C on an orbital shaker. After rinsing the embryos three times in PBSTx, secondary antibodies (goat anti-rabbit 488 and goat anti-mouse 546, Invitrogen) were applied to the embryos at 1:500 in blocking buffer for two hours at room temperature. Embryos were rinsed three times in PBSTx, then sorted for fluorescence on an epifluorescence microscope (approximately 50% of the embryos do not inherit the UAS<sub>tau</sub>:myc:GFP gene). Embryos were mounted on slides in Fluoromount-G mounting media (SouthernBiotech) and sealed with nail polish prior to imaging.

## **2.4. Results:**

### **2.4.1. LASP1 expression in neurons and its dynamic localization to the leading edge of actin-based membrane protrusions**

The presence of LASP1 in brain tissue has been reported previously (Orth et al., 2015), but its developmental expression profile and functions in neurons remain unknown. To address these questions, I first examined LASP1 expression in the hippocampus, a complex brain structure that has previously been found to be critical for learning and memory (Jarrard, 1993; Gonçalves et al., 2016). Immunoblotting for LASP1 was performed with hippocampal lysates harvested at embryonic day 18 (E18), postnatal day 8 (P8), P12, P23, and adulthood. These key stages capture the progression of neuronal development, from axon elongation to synapse

formation and maturation (Crain et al., 1973; Harris et al., 1992; Fiala et al., 1998; Tyzio et al., 1999). These data show that LASP1 is expressed at a relatively high level in the E18 hippocampus, and that this high expression persists through each stage to adulthood (**Figure 2-1A**). The high levels of LASP1 expression at E18 suggests a possible function for LASP1 in early neuronal development. To investigate this possibility, I examined the subcellular distribution of LASP1 in dissociated rat hippocampal neurons after two days *in vitro* (DIV2) using immunofluorescence. By DIV2, hippocampal neurons have an established polarity with one long axon and multiple short dendrites (Dotti et al., 1988; Kaech and Banker, 2006). I found that LASP1 is highly enriched in the axonal growth cone (**Figure 2-1B**). The growth cone is consisted of two distinct compartments: the peripheral and central regions (P- and C-region), of which the P-region is a broad and flat area highlighted by actin-rich lamellipodia and filopodia whereas the C-region, located behind the P-region and connected to the axonal shaft, is enriched in microtubules and cellular organelles (Vitriol and Zheng, 2012). LASP1 signals appear to be mostly concentrated in the P-region of the growth cone (**Figure 2-1B**). A close examination supports the notion that LASP1 is largely found in the P-region, particularly at the leading edge of the growth cone lamellipodia (**Figure 2-1C** top row, orange arrowheads), as well as along filopodial actin bundles (**Figure 2-1C** bottom row, white arrowheads). A similar spatial pattern was found in cultured Cath.a Differentiable (CAD) cells, a mouse neuroblastoma cell line (**Figure 2-1D**). Within 2 hours of plating on laminin-coated coverslips, CAD cells attach and spread large, broad lamella with motile lamellipodia around the cell's periphery. Immunostaining for LASP1 in these cells shows bright, concentrated signals at the edges of the lamellipodia, as well as on some filopodia with thick F-actin bundles. Given that lamellipodia and filopodia are known to be significant drivers of actin-based membrane protrusion and cellular motility, this

raises the possibility that LASP1 could regulate the actin-based projections that underlie growth cone motility and axon development.

To understand the spatiotemporal dynamics behind LASP1 localization and its potential functions in actin-based motility, I took advantage of the large, motile lamellipodia seen in spreading CAD cells to perform live cell imaging. Here, GFP-tagged LASP1 is co-expressed with the F-actin marker, Lifeact-mRuby, in CAD cells (**Figure 2-2A**). To ensure that exogenous GFP-LASP1 can faithfully represent the spatiotemporal pattern of endogenous LASP1, I experimented with various levels of GFP-LASP1 expression using constructs with reduced CMV promoter strengths (Morita et al., 2012). I found that high expression under a full strength CMV promoter (CMV $\Delta$ 0 GFP-LASP1) resulted in overexpressed GFP-LASP1 that not only highlighted the leading edges of lamellipodia (**Figure 2-2A** top row, orange arrowheads), but also labeled F-actin bundles in the lamella and other structures (**Figure 2-2A** top row, white arrowheads). While this localization is similar to what has been previously reported (Nakagawa et al., 2006), it is clearly different from the endogenous LASP1 localization detected by immunofluorescence (**Figure 2-1D**). I therefore experimented with the more severely crippled CMV constructs to obtain lower levels of expression. The results showed that expression of GFP-LASP1 from the CMV $\Delta$ 4 construct (CMV $\Delta$ 4 GFP-LASP1) most closely approximated the endogenous localization of LASP1 seen in **Figure 2-1** (**Figure 2-2A**, bottom row). Western blotting confirmed that GFP-LASP1 expressed using CMV $\Delta$ 4 is similar to the endogenous LASP1 level, whereas CMV $\Delta$ 0 resulted in more than 10 times the level of GFP-LASP1 overexpression compared to the endogenous LASP1. Therefore, CMV $\Delta$ 4 GFP-LASP1 was used for all live cell imaging.

To observe the spatiotemporal dynamics of LASP1, I performed live imaging on motile CAD cells expressing GFP-LASP1 and Lifeact-mRuby (**Figure 2-2C**). To highlight the pool of LASP1 at the leading edge of the lamellipodia, I generated ratiometric images of LASP1:F-actin signals, which are color coded such that the yellow/red hot colors represent high ratio values whereas blue/purple cool colors indicate low ratio values. It is clear that a narrow yellow band outlining the lamellipodia around the cells can be seen, suggesting high LASP1:F-actin ratio values at the leading edge of lamellipodia (**Figure 2-2C**, bottom row). It should be noted that the high LASP1:F-actin ratio values are not observed evenly along the leading edge, and there are locations that the LASP1:F-actin ratio appears to be low (**Figure 2-2C**, orange arrowheads). To further understand the dynamics of LASP1 localization to the leading edge, I produced several kymographs using the time-lapse sequence. It is clear that LASP1 becomes enriched at the leading edge during forward membrane protrusion, and disappears when the protrusion is paused or retracting (**Figure 2-2C**, right, orange arrowheads). Therefore, LASP1 localization to the leading edge of lamellipodia is tightly associated with membrane protrusion.

#### **2.4.2. Mechanisms of LASP1 localization to the leading edge**

I first investigated which domains of LASP1 are required for its localization to the leading edge of protruding lamellipodia. Here, GFP-tagged LASP1 deletion mutants, in which the LIM, nebulin, or SH3 domain was removed (Stölting et al., 2012; Myers et al., 2020), were co-expressed with Lifeact-mRuby in CAD cells for live imaging. Deletion of the SH3 domain (GFP-LASP1 $\Delta$ SH3) did not alter its localization to the leading edge of lamellipodia (**Figure 2-3A**). However, removal of either the LIM domain (GFP-LASP1 $\Delta$ LIM) or nebulin repeats (GFP-LASP1 $\Delta$ Neb) resulted in a loss of LASP1 localization to the leading edge (**Figure 2-3A**). Line

profiles of LASP1 fluorescence show that both the full length GFP-LASP1 and GFP-LASP1 $\Delta$ SH3 proteins exhibited a fluorescence peak at the leading edge of the lamellipodia, which was not observed for GFP-LASP1 $\Delta$ LIM and GFP-LASP1 $\Delta$ Neb (**Figure 2-3B**). Although the SH3 domain has been implicated in most of LASP1's known protein interactions (Orth et al., 2015), these data indicate that the LIM domain and nebulin repeats are required for LASP1 localization to the leading edge. While the nebulin repeats are well known for F-actin binding (Pappas et al., 2011), the involvement of the LIM domain for LASP1 localization to the leading edge is of interest. Given that the leading edge of lamellipodia is the site of actin polymerization underlying membrane protrusion, it is plausible that the LIM domain and nebulin repeats may work cooperatively to target LASP1 to the site of active actin polymerization and potentially regulate protrusive activity.

The leading edge of lamellipodia is known for its high concentration of the barbed ends of actin filaments, which are required for the rapid actin polymerization underlying membrane protrusion (Pollard and Borisy, 2003). I thus examined if LASP1 at the leading edge is co-localized with actin barbed ends. I adopted a barbed end assay (Gu et al., 2010; Marsick et al., 2010; Marsick and Letourneau, 2011) together with immunofluorescent staining of LASP1. Due to an incompatibility between the barbed end labeling and LASP1 immunolabeling protocols, I was unable to perform immunostaining on the endogenous LASP1 using our antibody after the cells have undergone barbed end labeling. To get around this issue, I expressed LASP1 at a low level using CMV $\Delta$ 4 GFP-LASP1 and performed immunolabeling using an anti-GFP antibody. Consistently, the rhodamine-actin-labeled barbed ends of actin filaments were found to be concentrated in a narrow band at the leading edge of the lamellipodia. Soluble GFP signals exhibited no localization in CAD cells and were distributed throughout the cell, with the highest

concentration at the cell center due to its larger volume (**Figure 2-4A**, top row). Fluorescence line profiles confirmed that there is no overlap between the normalized GFP signal and the barbed ends. Strikingly, GFP-LASP1 signals were seen to be largely overlapping with the barbed end signals, both highlighting the leading edge of the lamellipodia (**Figure 2-4A**, bottom row). Line profile quantification shows that the peak of LASP1 signal intensity overlaps with the narrow band of actin barbed ends. While LASP1 signals were seen further into the lamellipodia without barbed end signals, this may be explained by the short labeling window when only a small amount of rhodamine-actin can be incorporated into the F-actin network, or the light fixation prior to barbed end labeling that may have cross-linked LASP1 to the actin filaments. Nonetheless, the overlap between the peak of LASP1 and actin barbed ends supports the notion that LASP1 is likely targeted to sites of actin polymerization in the lamellipodia. Finally, immunostaining for GFP-LASP1 and actin capping protein (CP) also showed that these two proteins are highly co-localized in the lamellipodia (**Figure 2-4B**). Given that CP is enriched at the barbed ends of actin filaments, and it works cooperatively with the Arp2/3 family of nucleation factors for lamellipodial protrusion (Pollard et al., 2000), these data suggest that LASP1 may associate with actin barbed ends in lamellipodia to potentially regulate actin-based motility.

To further examine the association between LASP1 and the barbed ends of actin filaments, I applied a low concentration of Cytochalasin D (CytoD), a pharmacological inhibitor that caps the barbed ends of actin filaments to block further polymerization. I performed live imaging on CAD cells co-expressing CMV $\Delta$ 4 GFP-LASP1 and Lifeact-mRuby, and applied 25nM CytoD after a five minute baseline period (**Figure 2-5A**). Within three minutes of drug application, GFP-LASP1 disappeared from the leading edge of lamellipodia in CAD cells, as

depicted by ratiometric images and kymographs (**Figure 2-5A**). It should be noted that at this low concentration, CytoD did not cause drastic changes in the actin cytoskeleton and no obvious retraction of lamellipodia was observed. Since CytoD inhibits actin polymerization, I tested whether the loss of LASP1 signals at the leading edge is a result of reduced polymerization. I performed the same experimental paradigm using three different inhibitors of actin polymerization whose mechanisms of action differ significantly from CytoD: Latrunculin A, which sequesters actin monomers (100nM LatA, **Figure 2-5B**), SMIFH2, which inhibits formin-based polymerization (10 $\mu$ M, **Figure 2-5C**), and CK-666, which prevents Arp2/3-based actin nucleation (100 $\mu$ M, **Figure 2-5D**). None of these drugs abolished the LASP1 localization to the leading edge of lamellipodia. These data support the notion that LASP1 is associated with barbed ends at the leading edge of protruding lamellipodia.

### **2.4.3. LASP1 promotes axon elongation and branching**

The striking dynamic pattern of LASP1 localization to the leading edge of protruding lamellipodia suggest that LASP1 may regulate actin-based motility. While CAD cells offer an advantage for high-resolution image-based analysis of LASP1 localization and dynamics, they are not the best system to reliably assess actin-based motility. Because LASP1 is localized to the leading edge of growth cone lamellipodia and filopodia (see **Figure 2-1**), I used primary hippocampal neurons in culture to examine the effects of LASP1 knockdown on growth cone motility. Our lab has developed two distinct shRNA hairpins that target non-overlapping regions of LASP1 mRNA to knock down LASP1 in hippocampal neurons and to control for off-target effects. Here, shLASP1a and shLASP1b were designed to target the coding sequence and the 3'UTR, respectively, and were inserted into a multicistronic vector that expresses mCherry

(Myers et al., 2020). shLASP1a and shLASP1b can effectively knockdown endogenous LASP1 in hippocampal neurons to  $30.7\% \pm 7.0\%$  and  $44.1\% \pm 15.9\%$  (mean  $\pm$  SEM), respectively after 72 hours, as assessed by Western blot (**Figure 2-6A**). To measure the effect of LASP1 depletion on axon outgrowth, I plated dissociated rat hippocampal neurons in multi-chamber glass bottom dishes, then transfected them on DIV2 with shLASP1a, shLASP1b, or the empty vector as a control. Images of transfected neurons were captured every 24 hours starting at DIV3 through DIV7. Axon outgrowth over each 24 hour period was measured by tracing only the new axon growth using the FIJI simple neurite tracer program (Longair et al., 2011). Representative traces were color coded for each 24 hour period and collapsed across all time points (**Figure 2-6B**). While control neurons grew long, complex axonal arbors, neurons depleted of LASP1 produced shorter and more simplified axons. Quantitatively, the total axon outgrowth in LASP1 knockdown neurons was significantly lower than controls across all time points (n = approximately 30 cells per condition across three culture replicates, see Supplemental Table 2-1 for exact n and p values; \*  $p < 0.05$ ; \*\*  $p < 0.005$ ; \*\*\*  $p < 0.001$  by one-way ANOVA Tukey HSD post-hoc test) (**Figure 2-6C**). Counting the number of newly formed branch points for each condition showed a significant reduction in the axonal complexity of knockdown neurons compared to controls across all time points (see Supplemental Table 2-2 for exact n and p values; \*  $p < 0.05$ ; \*\*  $p < 0.005$ ; \*\*\*  $p < 0.001$  by one-way ANOVA Tukey HSD post-hoc test) (**Figure 2-6D**). These results suggest that LASP1 plays a significant role in promoting axon outgrowth and arborization.

While it is clear that loss of LASP1 causes a reduction in axon length, whether this is due to increased growth cone retraction or reduced growth cone protrusion is uncertain. Furthermore, it is unclear whether LASP1 supports branch development by promoting branch formation or by

preventing branch termination. To understand the role of LASP1 in growth cone motility and branching dynamics, I plated and transfected neurons to knockdown LASP1 as described above, then captured images at DIV5 every 10 minutes for 18 hours. When I examined the growth cones from control neurons, I found that they protruded in stair-like bursts over the 18 hour imaging period, while growth cones from LASP1 knockdown cells were nearly static over the same timeframe (**Figure 2-7A**). To quantify this, the Imaris tracking software was used to semi-automatically detect and track individual growth cones (Imaris v.9.5.1, Bitplane Inc.). Analysis of growth cone motility showed that LASP1 knockdown growth cones were slower and had reduced persistence (ratio of displacement to total distance traveled) compared to controls (\*  $p < 0.05$ ; \*\*  $p < 0.005$ ; \*\*\*  $p < 0.001$  as calculated using a one-way ANOVA Tukey HSD post-hoc test (see Supplemental Table 2-3 for exact n and p-values); from 3 independent culture replicates)(**Figure 2-7B**). Careful examination of axon branch dynamics showed that knockdown of LASP1 significantly reduced the production and termination of new axonal branches with no significant effect on their total lifetime (n = 3 neurons per condition, 3 independent culture replicates; \*  $p < 0.05$ ; \*\*  $p < 0.005$ , see Supplemental Table 2-4 for exact p-values; calculated using a one-way ANOVA Tukey HSD post-hoc test)(**Figure 2-7C**). Together with the imaging data in CAD cells, these results support the notion that LASP1 functions to regulate the actin-based protrusions that underlie the growth and branching of developing axons in culture.

#### **2.4.4. Lasp promotes axon commissure development and fasciculation *in vivo***

To examine the role of LASP1 in axon development *in vivo*, I selected the *Drosophila* model system, both for its well-developed toolbox to study axon development and for its expression of only one LASP1 homologue, called Lasp (Suyama et al., 2009; Orth et al., 2015).

Specifically, I chose to focus on the ventral nerve cord of *Drosophila*, which at early stages of development contains stereotypic railroad-like bundles of commissural axons (**Figure 2-8A**, center images) that show clear phenotypes when axon guidance-related proteins are disrupted (Evans and Bashaw, 2010). To facilitate the identification of axonal defects, I targeted a specific subset of neurons in the ventral nerve cord using the UAS-Gal4 inducible system. For this set of experiments, Gal4 is expressed under a cell type-specific promoter, binds to the UAS element, and drives expression of the gene downstream of UAS. Here, I utilize the *eagle*-Gal4 element (*egl*-Gal4), which drives UAS-gene expression in two pairs of neuron clusters per abdominal segment of the ventral nerve cord, and has been used extensively in previous studies of axon guidance receptors and signaling pathways (Garbe et al., 2007; O'Donnell and Bashaw, 2013b, 2013a). Gal4 drives expression of GFP to visualize these neurons, Lasp RNAi to knockdown Lasp protein, and dicer to enhance RNAi efficiency. As a control, the *egl*-GAL4 element was used to drive expression of the GFP and dicer genes only, without the LASP RNAi. Both the Lasp-knockdown and control crosses produced viable embryos, which were fixed at stage 16 and immunostained for both GFP and central nervous system axons (BP102) as described previously (Bashaw, 2010). Z-stacks of the embryonic ventral nerve cords were analyzed for abnormalities in midline crossing. In the control embryos, I observed tight bundles of commissural axons that cross over to the contralateral neuron cluster, which is consistent with previous studies using this driver (**Figure 2-8A** top, B left) (Garbe et al., 2007). However, I observed several aberrant phenotypes in the Lasp knockdown embryos (**Figure 2-8A** bottom row; **Figure 2-8B**). First, several segments displayed axons that did not reach their contralateral target. In some cases, this was due to incomplete midline crossing, while in other cases the axons crossed the midline but turned away from their destination or did not extend fully along their typical path (**Figure 2-8A**,

yellow arrowheads). In total this phenotype occurred in 30% of the measured knockdown segments on average, compared to approximately 1% of the control embryo segments (**Figure 2-8C**) (n = 10 wild-type and 18 knockdown embryos,  $p = 0.0008398$  via Welch two-sample t-test). Second, I observed two forms of defasciculation (**Figure 2-8A**, blue arrowheads). The first was an unravelling of the normally tight axon bundles, to the point that spaces were visible between the axons, which was observed in over 70% of all knockdown segments measured, indicating that Lasp promotes the tight bundling of commissural axons ( $p = 6.88e-06$  via two-sample t test). The second form of commissure defasciculation I observed was individual axons leaving the main axon bundle as well as the typical commissural path, and terminating far away from the synaptic target. This phenotype was documented in approximately 30% of the control embryo segments but over 75% of the knockdown segments, indicating that Lasp promotes axons continuing to grow along the path of their commissure bundles ( $p = 0.000298$  via two-sample t-test). While the incomplete commissure formation phenotype is highly consistent with the *in vitro* data, where axons do not extend far without LASP1, the defasciculation phenotypes indicate a possible role for LASP1 in *in vivo* axon guidance.

## 2.5. Discussion:

Actin-based cellular motility is essential for many developmental events, such as neuronal development, as well as for many pathological events, including cancer cell metastasis (Kalil and Dent, 2005; Lowery and Van Vactor, 2009). During brain development, neurons send axonal projections through the developing tissue to their respective synaptic targets. Essential for this process is the axon growth cone, an actin-rich structure at the tip of the axon that responds rapidly to extracellular cues in order to navigate towards its goal in a process known as axon

guidance (Kolodkin and Tessier-Lavigne, 2011). Growth cones contain two actin-based membrane protrusions: lamellipodia and filopodia, which undergo dynamic protrusive activities as a part of the process of axon growth. The actin dynamics underlying growth cone motility is targeted by a plethora of spatially- and temporally- restricted signaling cascades and actin regulatory proteins to achieve directional outgrowth during axon guidance (Lowery and Van Vactor, 2009; Pollard and Cooper, 2009; Dent et al., 2011). In this study, I present evidence that LASP1, a unique member of the Nebulin family of actin binding proteins, localizes to the actin polymerization zone during membrane protrusion and plays an important role in axon development. Previous studies in non-neuronal cells have implicated LASP1 in cell migration and focal adhesion, with no clear mechanism of action in actin-based cellular motility (Orth et al., 2015). LASP1 is expressed in the brain and has been implicated in a number of neurological and neurodevelopmental disorders (Phillips et al., 2004; Stone et al., 2007; Joo et al., 2013), but a role for LASP1 in early brain development has not yet been established. In this study, I present evidence that LASP1 is highly expressed during brain development prior to synapse formation. Further analyses show that LASP1 is dynamically enriched at the leading edge of protruding lamellipodia in motile neuronal cells. Importantly, LASP1 localization appears to depend on the free barbed ends in lamellipodial actin networks, suggesting that LASP1 plays a role in the actin polymerization underlying membrane protrusion, growth cone motility, and cellular migration. Consistently, LASP1 knockdown resulted in impaired axon growth cone protrusion speed and branch formation in cultured primary hippocampal neurons. Finally, knockdown of the *Drosophila* LASP1 orthologue, *Lasp*, resulted in a significant disruption of axon midline projections and defasciculation of commissural axon bundles *in vivo*. These findings support

LASP1 as a novel actin regulatory protein that promotes the actin-based motility underlying axon elongation and guidance during early brain development.

Filopodia and lamellipodia are two established actin-based membrane protrusions found in motile growth cones. It is commonly believed that growth cone filopodia play a sensory role as they sample the environment to a greater extent than the growth cone itself. Filopodia contain bundles of actin filaments, and their growth depends largely on the formin family of actin nucleating factors and regulators. Lamellipodia are thin, sheet-like membrane protrusions that are believed to primarily function in growth cone movement. Lamellipodia contain a branched network of short actin filaments with their barbed (plus) ends pushing against the plasma membrane. Forward protrusion of lamellipodia is believed to be driven by Arp2/3-based nucleation and polymerization at the leading edge where addition of actin monomers to the barbed ends push the membrane forward, followed by the engagement of the molecular clutch for interaction with the extracellular matrix (Suter and Forscher, 2000; Case and Waterman, 2015). The immunofluorescence imaging in **Figure 2-1** showed that LASP1 is selectively enriched in the peripheral region of the growth cone where filopodia and lamellipodia exist. Importantly, LASP1 signals were associated with the leading edge of lamellipodia as well as some filopodia. These observations suggest that LASP1 may function in the actin-based protrusive activities underlying growth cone movement. This hypothesis is supported by my imaging work on LASP1 localization and dynamics in motile CAD cells. Here, CAD cells were used for their large and dynamic lamellipodia that enable high-resolution image-based analyses. Importantly, the spatial pattern of LASP1 in CAD cells is very similar to that of the growth cones: local enrichment at the leading edge of the lamellipodia as well as association with some filopodia. The role of LASP1 in actin-based membrane protrusive activities was supported by my live cell imaging

data, as GFP-LASP1 was only found at the leading edges of active protrusions, but disappeared when the protrusion retracted. Furthermore, this leading edge enrichment pattern was found to require both the LIM and nebulin regions of LASP1. Interestingly, Nakagawa et al. reported that the LIM domain and the 1<sup>st</sup> nebulin motif of LASP1's sister protein, LASP2, work cooperatively to bind to actin filaments (Nakagawa et al., 2009). Therefore these results are consistent with previous findings, and indicates the importance of these two domains for spatiotemporal targeting of LASP1 to specific F-actin sites.

What is the mechanism that enables LASP1 localization to the leading edge? The observation that LASP1 accumulates at the leading edge of protruding lamellipodia suggests that LASP1 might be targeted to the region where actin polymerization is most abundant. The finding that cytochalasin D (CytoD) was able to displace LASP1 from the leading edge further supports this notion. CytoD binds and caps the barbed ends of actin filaments to prevent actin polymerization (Goddette and Frieden, 1986). When applied at low concentrations, CytoD is known to be effective in capping the barbed ends of actin filaments without grossly disrupting F-actin structures (Lee et al., 2013). In this work, I found that a low concentration of CytoD (25 nM) did not disrupt the F-actin network of the lamellipodia, but effectively dislodged LASP1 from the leading edge. Importantly, none of the other reagents that inhibit actin assembly through other mechanisms, such as LatA, affected the LASP1 localization pattern. These results suggest that LASP1 is likely associated with barbed ends at the F-actin-membrane interface of lamellipodia. This notion is further supported by direct imaging of actin barbed ends, in which the band of barbed ends at the leading edge of lamellipodia overlaps with LASP1. Furthermore, the data show that LASP1 localization overlaps with capping protein (CP), which is found at the leading edge of lamellipodia and has been shown to cap barbed ends (Akin and Mullins, 2008).

The high degree of colocalization between LASP1 and CP further supports that LASP1 localizes to the leading edge where F-actin barbed ends are in high abundance, and therefore may regulate actin-based membrane protrusion.

Currently, the mechanism by which LASP1 localizes to the leading edge and how it regulates the actin dynamics underlying lamellipodia protrusion remains unknown. It should be noted that my colocalization data of LASP1 and barbed ends of actin filaments do not have the resolution to precisely determine if LASP1 is localized to the barbed ends or immediately adjacent. Since there is no previously published evidence for LASP1 to directly interact with the actin barbed ends, I hypothesize that LASP1 may function via these two non-exclusive mechanisms. First, LASP1 may localize immediately behind the barbed ends to stabilize the segment of newly polymerized actin filaments. Newly polymerized actin is well-known to be less stable than aged filaments, due to rearrangement of the filaments' internal structures (Hao et al., 2008). Therefore, LASP1 may be selectively targeted to the leading edge to stabilize newly generated segments of actin filaments immediately after the barbed ends. This would be a dynamic process, so when the segments of F-actin mature, LASP1 would lose its binding affinity. This would fit with my data suggesting that LASP1 binds to actin filaments at the leading edge, as well as partially supported by the fact that gross overexpression of GFP-LASP1 causes it to bind to most F-actin in the cell. However, it remains unclear how CytoD removes LASP1 from the leading edge. It is possible that CytoD capping of barbed ends, and the subsequent blockade of new assembly, leads to the elimination of unstable "newly generated segments" for LASP1 binding. Although presumably this would also be true for the other polymerization inhibitors I utilized, none of which affected LASP1 localization. The second possibility is that LASP1 may function in actin uncapping or anti-capping to promote filament

polymerization in collaboration with Ena/VASP. Previous studies have shown that VASP can interact with LASP1 via the LASP1 SH3 domain (Keicher et al., 2004). Given that VASP exhibits an extremely similar leading edge localization, that is also membrane protrusion- and free barbed end-dependent (Bear et al., 2002), it is plausible that the function of LASP1 at the edge of lamellipodia involves VASP in some fashion. However, because my data show that LASP1 leading edge enrichment does not require its SH3 domain, it is unlikely that VASP is the mechanism by which LASP1 is recruited to the leading edge. Future experiments employing advanced multi-channel super-resolution imaging, together with selective molecular manipulations, will enable us to delineate the precise mechanisms underlying LASP1 localization and functions.

Given that axonal growth and guidance depend on actin-based growth cone motility, LASP1 may play a role in actin-driven membrane protrusive activities to regulate axon development. In support of this hypothesis, LASP1 knockdown substantially impaired the axon outgrowth and branch formation of cultured hippocampal neurons over several days. Axonal outgrowth is achieved by rapid forward movement of the growth cone interspersed with pauses and retractions (Smirnov et al., 2014). Consistent with the notion that LASP1 may function in growth cone forward movement, I found that both the speed and persistence of growth cone advance was drastically reduced in LASP1-knockdown neurons compared to control cells. Furthermore, I found that loss of LASP1 reduced the production of new branches, with no effect on their lifetime. This indicates that LASP1 is likely promoting the formation of new axon branches, as opposed to stabilizing existing branches. Together, these findings suggest that LASP1 is performing a similar function in neuronal development by promoting the protrusive growth of both new axon branches and growth cones.

To understand how the axonal outgrowth phenotype translates to an *in vivo* model system, I studied commissural neurons in the embryonic ventral nerve cords of *Drosophila*, which expresses only one LASP1 orthologue, Lasp. Knockdown of Lasp in *Drosophila* embryos led to several defects in the axon pathfinding of *egl+* commissural axons. The high number of knockdown commissural axons that failed to reach their contralateral targets is consistent with the notion that LASP1 regulates actin-based motility. The observed defasciculation of axon bundles might be related to the role of LASPs in cell adhesion (Lin et al., 2004; Bliss et al., 2013). In vertebrates, two LASPs, LASP1 and LASP2, are expressed and have been shown to be present and function in cell adhesion complexes. It is also possible that the observed defects may be a result of Lasp functioning downstream of axon guidance signaling pathways, some of which have been shown to drive the fasciculation of growing axon bundles (Wolman et al., 2007). Future studies will be necessary to examine how Lasp is regulated by these pathways, if at all.

In summary, this study shows a novel role for LASP1 in lamellipodial protrusion and axon development through a combination of microscopic, *in vitro*, *in vivo*, and molecular approaches. Together with recent work on LASP1 in synaptic development (Myers et al., 2020), my work indicates that this unique Nebulin family member plays a key role in neuronal development. Importantly, the presence of multiple phosphorylation sites in the linker region of LASP1 and its multiple protein-protein modules also highlight the potential for LASP1 to connect intricate signaling cascades to the actin dynamics underlying axon growth, guidance, and synapse formation. Future studies are needed to better understand the functions of LASP1 in neurons and the precise mechanisms underlying the regulation of actin-based motility.

## 2.6. Figures:

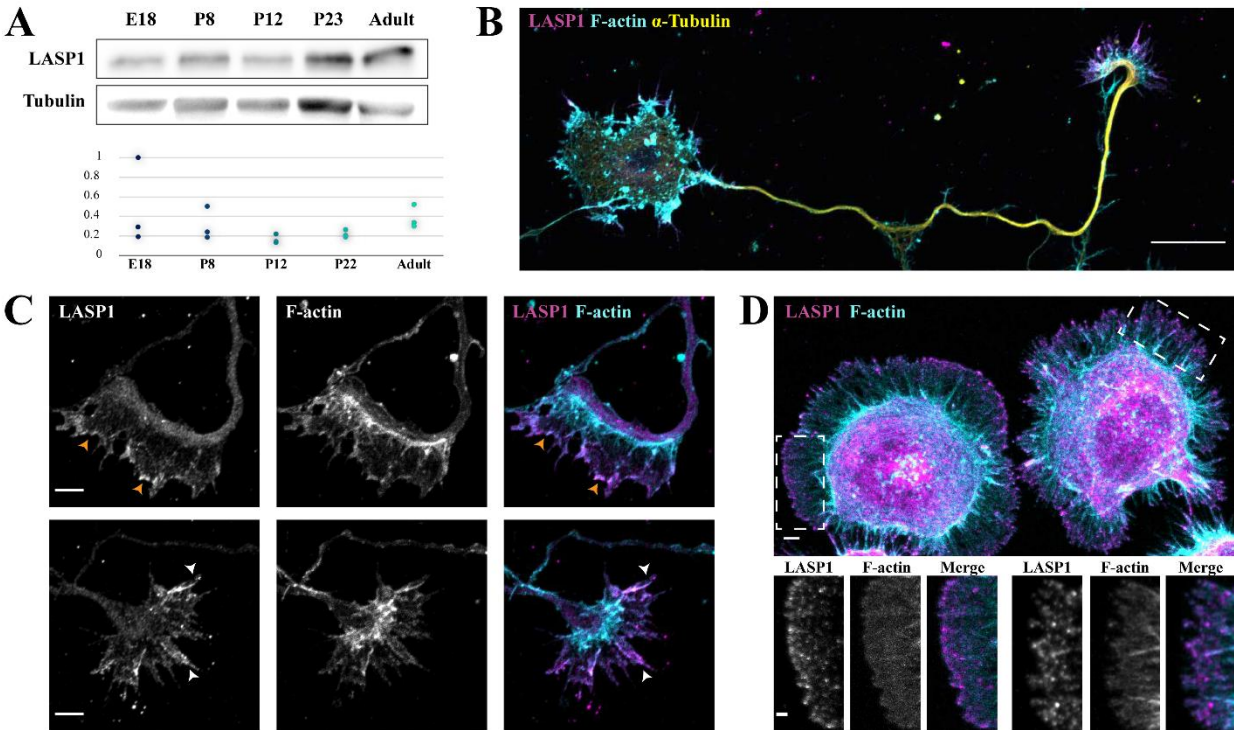


**Figure 2-1.** LASP1 is expressed in the developing brain and localizes to the axon growth cone.

(A) Top, Western blot showing developmental profile of LASP1 in rat hippocampi at the indicated stages. Bottom, graph shows normalized LASP1 levels relative to tubulin loading control. Error bars represent standard error. (B) Representative confocal image of a fixed rat hippocampal neuron in culture at two days in vitro (DIV2), stained for endogenous LASP1 (magenta), F-actin (phalloidin, cyan), and  $\alpha$ -tubulin (yellow). LASP1 largely localizes to the periphery of the axon growth cone. Scale bar equals 20 microns. (C) Representative confocal images of growth cones from fixed DIV2 cultured rat hippocampal neurons, stained for endogenous LASP1 (magenta) and F-actin (phalloidin, cyan). LASP1 localizes to the leading edge of lamellipodia (orange arrowheads), and actin bundles in filopodia (white arrowheads). Scale bar is 5 microns. (D) Representative confocal image of two CAD cells labeled for LASP1

(magenta) and F-actin (phalloidin, cyan). LASP1 localizes to lamellipodia and filopodia in a similar pattern to growth cones. Main scale bar is 5 microns, inset is 2 microns.

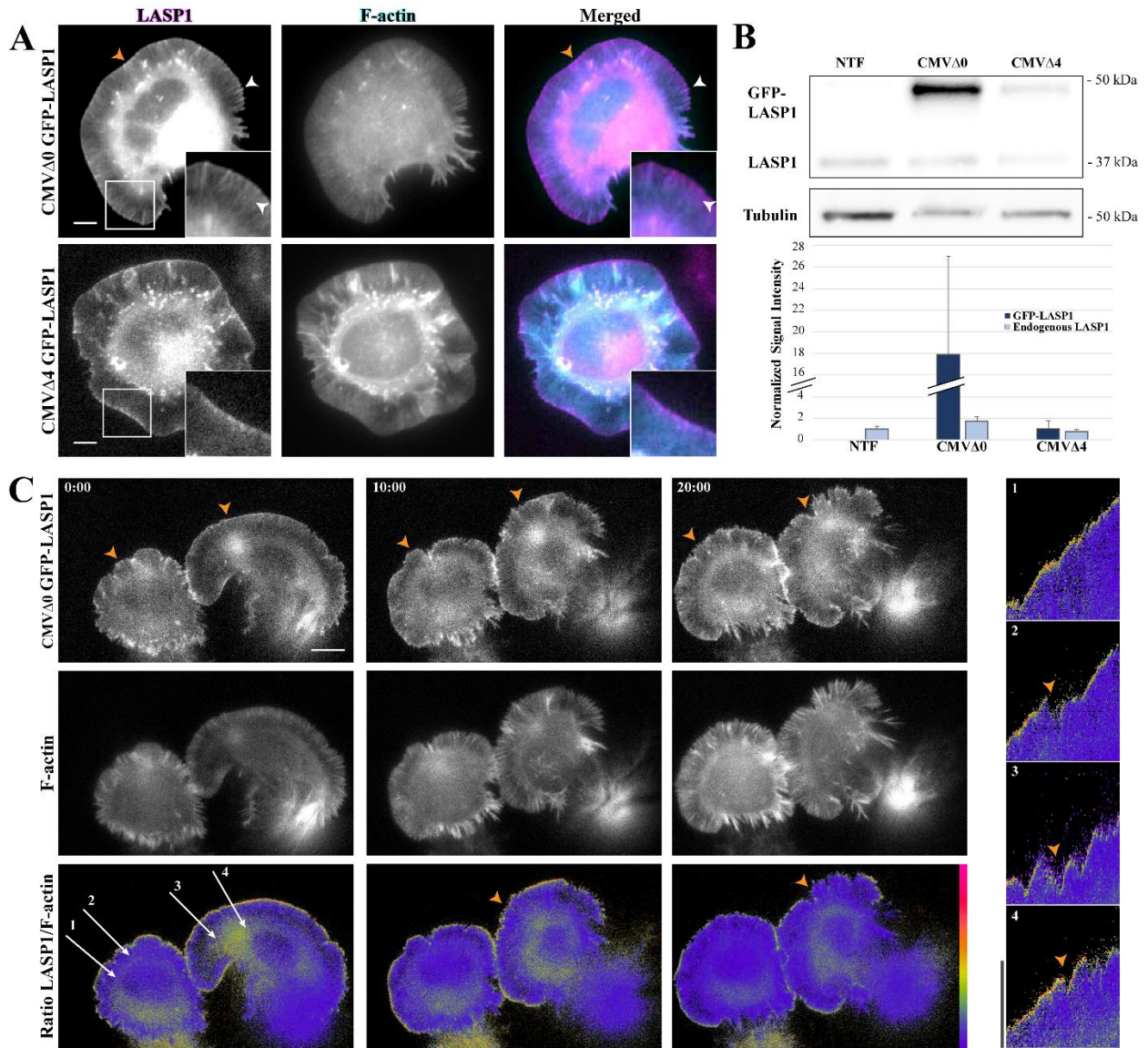


**Figure 2-2.** GFP-LASP1 localizes to protruding membranes. (A) Representative images of live CAD cells co-expressing intact (CMV $\Delta$ 0 GFP-LASP1, top) or crippled (CMV $\Delta$ 4 GFP-LASP1, bottom) CMV promoter-driven GFP-LASP1 (left, magenta), along with Lifeact-mRuby (F-actin, middle, cyan). GFP-LASP1 overexpressed by an intact CMV promoter localizes to the leading edge (orange arrowheads) and actin bundles (white arrowheads), whereas CMV $\Delta$ 4 GFP-LASP1 localizes only to the leading edge, similar to endogenous LASP1. Scale bars equal 5 microns. (B) Top, representative anti-LASP1 and anti-tubulin Western blots from CAD cells transfected with

CMV $\Delta$ 0 GFP-LASP1 or CMV $\Delta$ 4 GFP-LASP1, along with nontransfected controls (NTF).

Bottom, graph shows quantification of GFP-LASP1 expression, normalized to tubulin loading control, with endogenous LASP1 from the non-transfected condition set to 1. Error bars

represent standard error. (C) Time-lapse images of CAD cells co-expressing CMV $\Delta$ 4 GFP-

LASP1 and Lifeact-mRuby. Bottom row, images show GFP to mRuby ratio, color coded with a rainbow heat map (scale to right). Images were captured every five seconds for 20 minutes. Scale

bar equals 10 microns. Right, representative kymographs (correspond to labeled arrows on left

merged image). High levels of GFP-LASP1 can be found at the leading edge during cell

protrusion, but GFP-LASP1 largely disappears from the edge upon cell retraction (orange

arrowheads). Images are representative of ten cells across three independent culture replicates.

Kymograph scale bars: vertical is 10 microns, horizontal is 10 minutes.

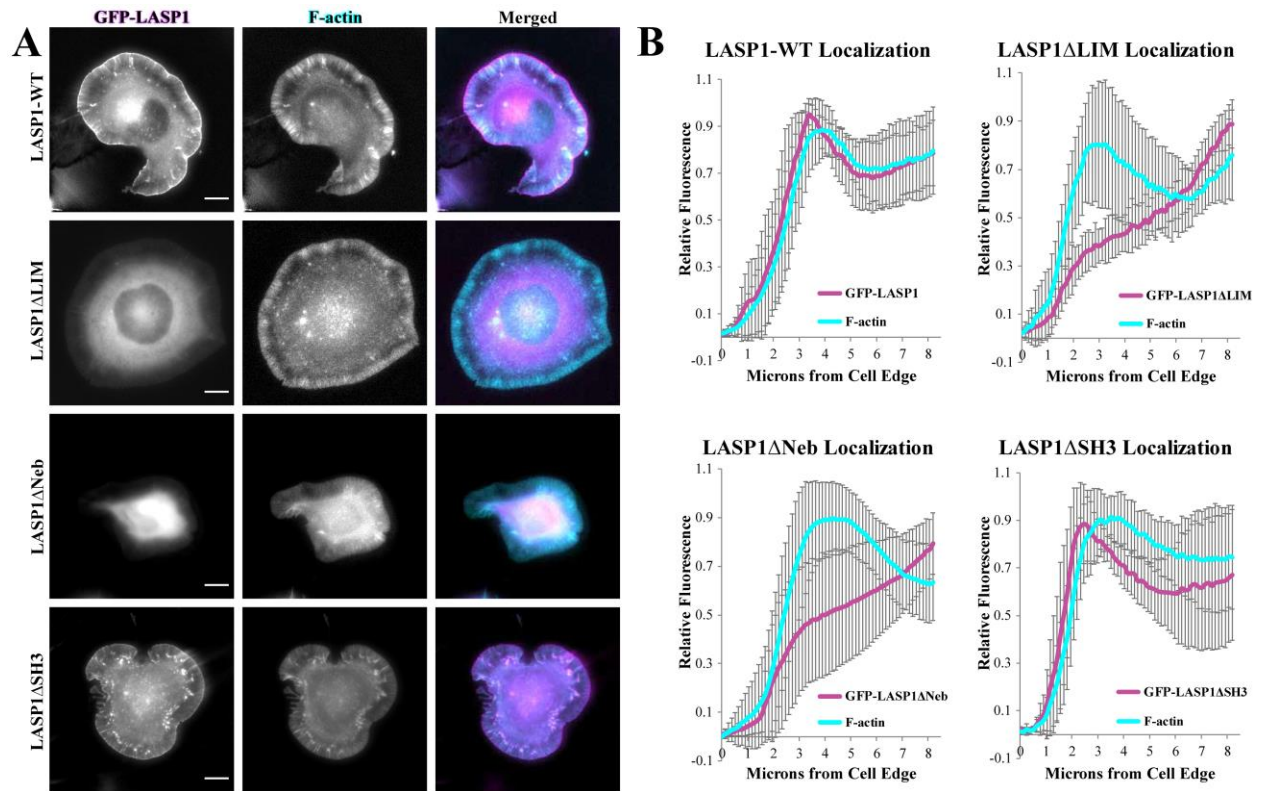


**Figure 2-3.** The LIM domain and nebulin repeats are essential for LASP1 localization to the leading edge. (A) Live CAD cells co-expressing Lifeact-mRuby (F-actin, cyan) and either wild-type GFP-LASP1, GFP-LASP1 $\Delta$ LIM, GFP-LASP1 $\Delta$ Nebulin (GFP-LASP1 $\Delta$ Neb), or GFP-LASP1 $\Delta$ SH3 (magenta). Wild-type GFP-LASP1 and GFP-LASP1 $\Delta$ SH3 localize to the leading edge. However, GFP-LASP1 $\Delta$ LIM and GFP-LASP1 $\Delta$ Neb do not localize to the leading edge, and instead appear mostly soluble. Scale bars equal 10 microns. (B) Line scan analysis of GFP-LASP1 localization at the leading edge (120 line scans from 30 cells across three independent culture replicates). Error bars represent standard error.

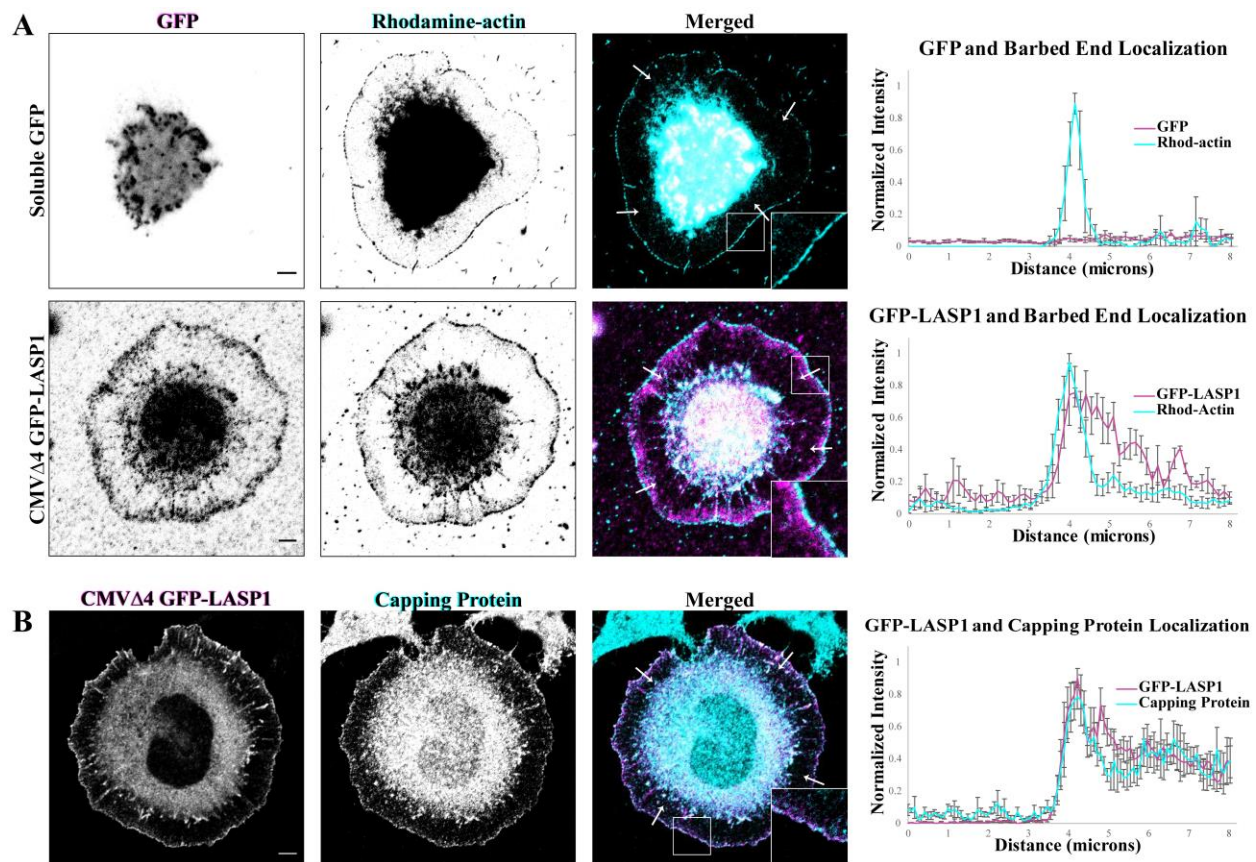


**Figure 2-4.** LASP1 localizes to actin plus ends at the leading edges of CAD cells. (A) Representative images of CAD cells expressing soluble GFP or CMV $\Delta$ 4 GFP-LASP1 (magenta), with actin plus ends labeled with rhodamine-conjugated actin (cyan). Scale bars equal 5 microns. Graphs (right) depict the average of four normalized line profiles from cells on left (arrows in merged images show location of line scans). Error bars represent standard error. LASP1 localization at the leading edge overlaps with the labeled plus ends. Representative of ten cells from three independent culture replicates. (B) Representative images showing colocalization of CMV $\Delta$ 4 GFP-LASP1 (magenta) and endogenous capping protein in CAD cells (cyan). Scale bar equals 5 microns. Graph (right) shows the average of four normalized line profiles from arrows in merged image. Error bars represent standard error.

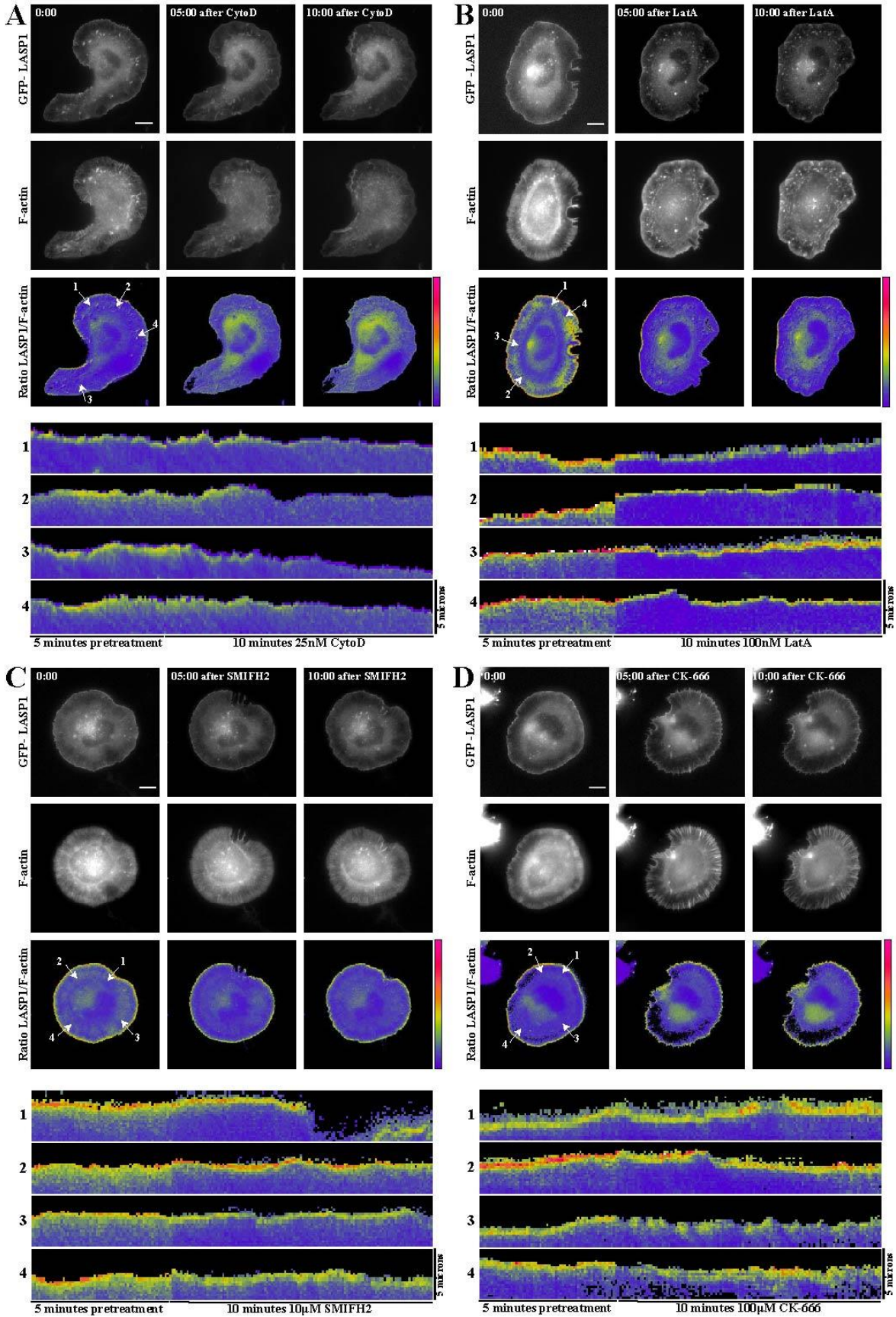


**Figure 2-5.** Free actin plus ends are required for LASP1 localization to the leading edge. Time-lapse images of CAD cells expressing CMV $\Delta$ 4 GFP-LASP1 (top rows) and Lifeact-mRuby (middle rows) at time 0 (left column of each section), 5 minutes after drug treatment (middle column), and 10 minutes after drug treatment (right column). Bottom rows show ratiometric images of GFP-LASP1 to Lifeact-mRuby, rainbow color coded (scale to right). Numbered images below show representative ratio kymographs (corresponding to numbered lines on time 0 ratio image). Images were captured every five seconds. (A) Cells were imaged for 5 minutes prior to the addition of 25 nM CytochalasinD (CytoD) to cap the plus ends of actin filaments. Cells were imaged every 5 seconds for 10 minutes after drug addition. Shortly after addition of CytoD, LASP1 signal is largely absent from the leading edge. (B) Latrunculin A treatment (LatA, 100 nM), which sequesters actin monomers, has no effect on LASP1 localization after 10 minutes. (C) Treatment with formin inhibitor SMIFH2 (10  $\mu$ M) has no effect on LASP1 enrichment at the cell edge. (D) Arp2/3 inhibition (CK-666, 100  $\mu$ M) does not dislodge LASP1 from the edges of the cell. Scale bars equal 10 microns. Images are representative of ten cells per condition across three independent culture replicates.

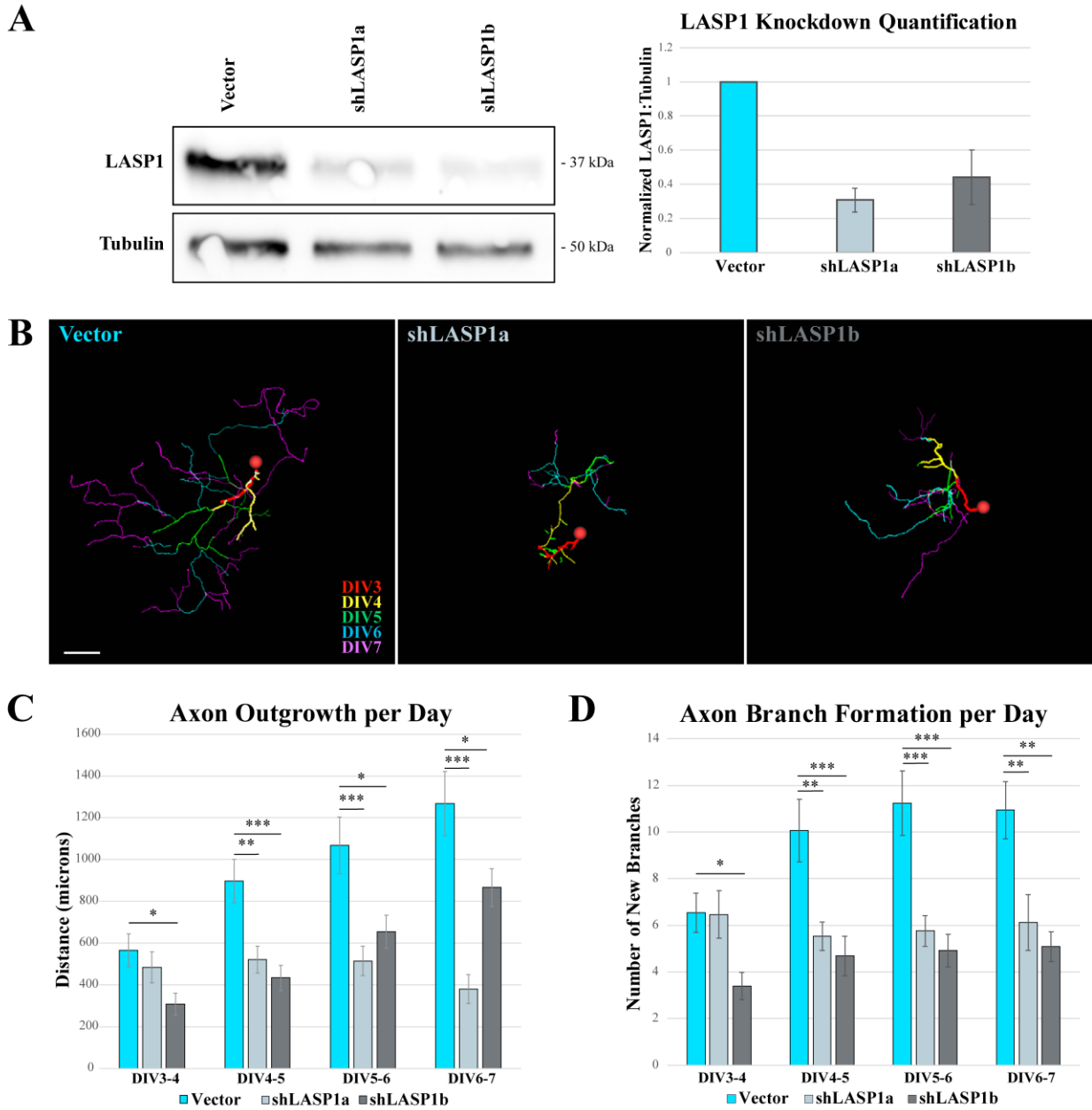


**Figure 2-6.** Knockdown of LASP1 truncates axon elongation and reduces branching in cultured hippocampal neurons. (A) Representative anti-LASP1 and anti-tubulin Western blots of lysates from hippocampal neurons transfected with empty plasmid (vector), shLASP1a, or shLASP1b for 72 hours. Graph shows ~60-70% reduction in LASP1 expression in cultures expressing shRNAs across three independent culture replicates. LASP1 levels are normalized to tubulin loading controls. Error bars represent standard error. (B) Axon tracings of representative rat

hippocampal neurons transfected at DIV2 with empty backbone control (Vector), shLASP1a, or shLASP1b. Neurons were imaged every 24 hours from DIV3 until DIV7, and each day's growth is temporally color-coded (scale lower right, Vector image). Knockdown of LASP1 reduces axon outgrowth over each 24 hour period. Scale bar equals 150 microns. (C) Graph depicting axon outgrowth (in microns) every 24 hours. (D) Graph depicting the number of newly formed branches at each time point. Error bars represent standard error. \*  $p < 0.05$ ; \*\*  $p < 0.005$ ; \*\*\*  $p < 0.001$ . P-values calculated using a one-way ANOVA Tukey's HSD post-hoc test. Data collected from approximately 30 neurons from three independent cultures (see Supplemental Tables 1 and 2 for exact n- and p-values).

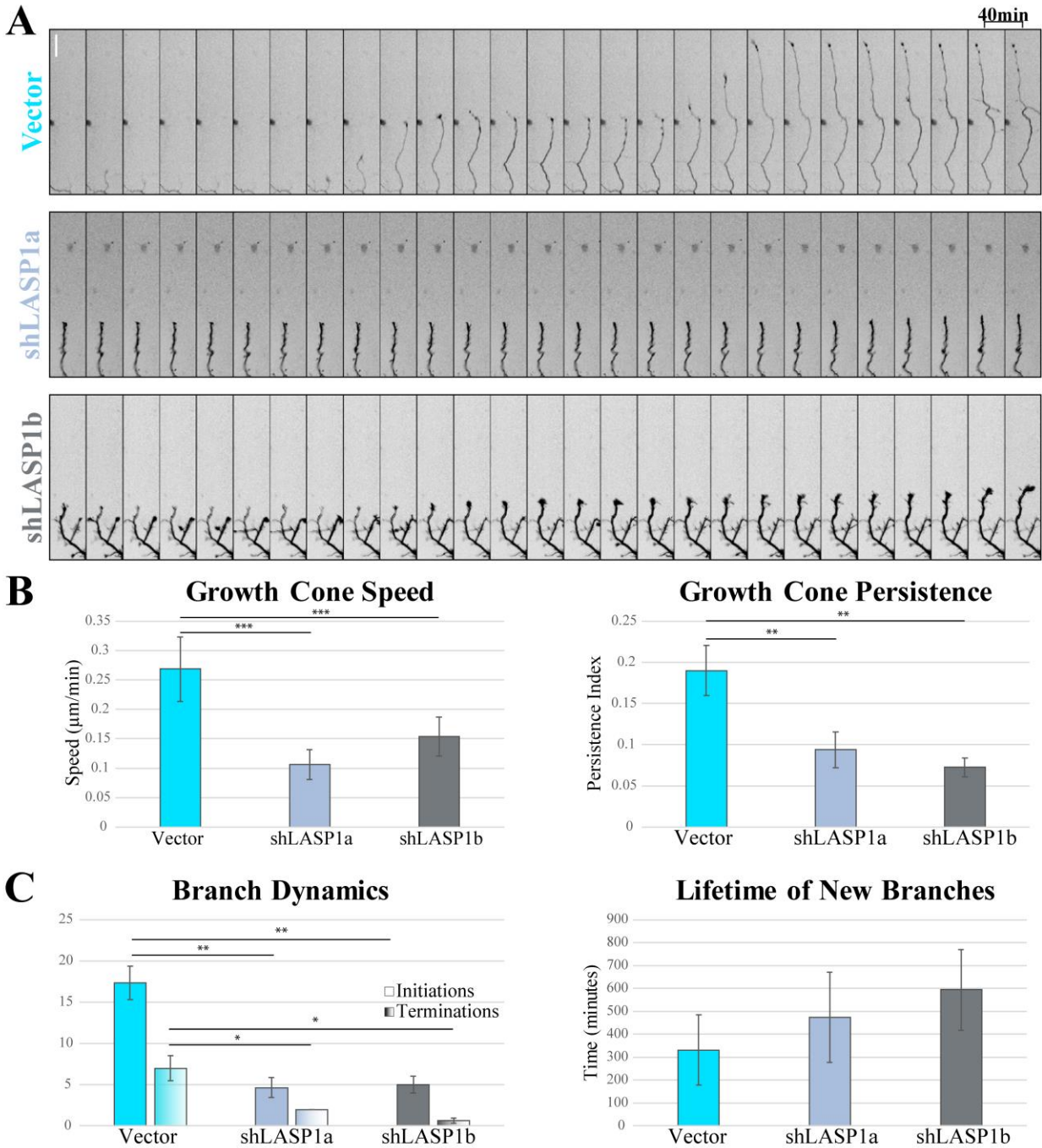


**Figure 2-7.** Knockdown of LASP1 reduces growth cone protrusion and branch formation in cultured hippocampal neurons. (A) Montages of representative growth cones from DIV5 rat hippocampal neurons expressing either Vector control, shLASP1a, or shLASP1b. Montage slices represent 40 minute intervals. Scale bar equals 40 microns. (B) Graph of growth cone speed (left) and persistence (right). Persistence index represents a ratio of growth cone displacement to

total distance travelled. Growth cone speed and persistence are reduced in the absence of LASP1.

(C) Graphs of dynamic axon branch formation, termination (left), and lifetime (right) across all three conditions. Loss of LASP1 causes reduced branch formation and termination, with no significant effect on the lifetime of new branches. Error bars represent standard error. \*  $p < 0.05$ ; \*\*  $p < 0.005$ ; \*\*\*  $p < 0.001$  by one way ANOVA Tukey HSD post hoc test. Experiments represent three independent culture replicates. (See Supplemental Tables 3 and 4 for exact n- and p- values).

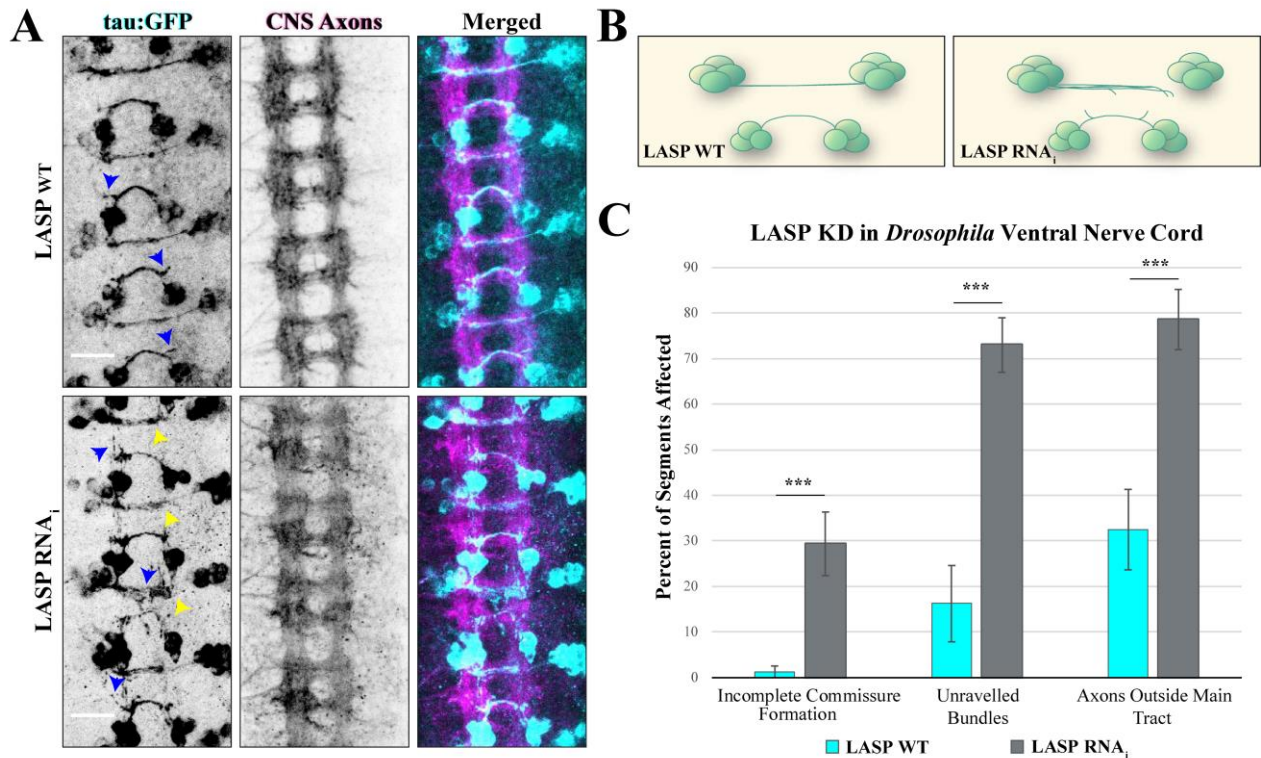


**Figure 2-8.** Lasp knockdown leads to defects in axon commissure formation in *Drosophila*. (A) Representative images of stage 16 *Drosophila* embryos labeled with tau:GFP in *egl*-expressing ventral nerve cord axons. Top row shows dicer-only control embryo (WT-LASP), bottom row shows embryo expressing dicer plus LASP RNA<sub>i</sub> (LASP KD). Left column shows GFP-expressing *egl* neurons (green), middle column shows CNS axon (BP102, magenta), right column shows merged images. Arrowheads indicate defects in commissural axon development, including defasciculation (blue) and axon tracts that do not reach their targets (yellow). Scale bars equal 15 microns. (B) Schematic of one segment from wildtype (left) or LASP knockdown (right) *egl* neurons in the *Drosophila* ventral nerve cord. Lasp knockdown results in numerous guidance defects, including defasciculation of axon bundles and truncated commissures. (C) Graph shows axon guidance defects from 10 control and 18 knockdown embryos collected across three independent experiments. \*\*\* indicate p-values below 0.001, both defasciculation

measures were analyzed using a Student's t test. Incomplete commissure formation calculated using a Welch's t test. Error bars represent standard error.

## 2.7. Supplemental Tables

| Transfection Condition | Time Point | N-values (total number of neurons measured in 3 culture replicates) | P-values (difference from vector control at same time point) |
|------------------------|------------|---|--|
| Vector                 | DIV3-4     | 26  | N/A  |
|                        | DIV4-5     | 30  | N/A  |
|                        | DIV5-6     | 34  | N/A  |
|                        | DIV6-7     | 33  | N/A  |
| shLASP1a               | DIV3-4     | 28  | Not Significant<br>(0.6824)                                  |
|                        | DIV4-5     | 34  | 0.0025   |
|                        | DIV5-6     | 33  | 0.0006   |
|                        | DIV6-7     | 26  | <0.0001  |
| shLASP1b               | DIV3-4     | 25  | 0.0340   |
|                        | DIV4-5     | 32  | 0.0002   |
|                        | DIV5-6     | 37  | 0.0103   |
|                        | DIV6-7     | 36  | 0.0306   |

**Supplemental Table 2-1.** Axon Outgrowth Statistics: n and p-values. Statistical values for **Figure 2-6C** axon outgrowth ANOVA analysis. N values represent the total number of neurons measured across 3 culture replicates. P-values indicate difference from Vector control.

| Transfection Condition | Time Point | N-values (total number of neurons measured in 3 culture replicates) | P-values (difference from vector control at same time point) |
|------------------------|------------|---|--|
| Vector                 | DIV3-4     | 26  | N/A  |
|                        | DIV4-5     | 30  | N/A  |
|                        | DIV5-6     | 34  | N/A  |
|                        | DIV6-7     | 33  | N/A  |
| shLASP1a               | DIV3-4     | 28  | Not Significant (0.9978)                                     |
|                        | DIV4-5     | 34  | 0.0032   |
|                        | DIV5-6     | 33  | 0.0004   |
|                        | DIV6-7     | 26  | 0.0027   |
| shLASP1b               | DIV3-4     | 25  | 0.0316   |
|                        | DIV4-5     | 32  | 0.0005   |
|                        | DIV5-6     | 37  | <0.0001  |
|                        | DIV6-7     | 36  | 0.0001   |

**Supplemental Table 2-2.** Axon Branch Formation Statistics: n and p-values. Statistical values for **Figure 2-6D** branch number ANOVA analysis. N values represent the total number of neurons measured across 3 culture replicates. P-values indicate difference from Vector control.

| Transfection Condition | N-values (total number of growth cones measured) | Growth Cone Speed P-values (difference from vector control) | Growth Cone Persistence P-value (difference from vector control) |
|------------------------|--|---|--|
| Vector                 | 36   | N/A   | N/A  |
| shLASP1a               | 26   | <0.0001   | 0.0188   |
| shLASP1b               | 27   | <0.0001   | 0.0027   |

**Supplemental Table 2-3.** Growth Cone Dynamics Statistics: n and p-values. Statistical values for **Figure 2-7B** growth cone speed and persistence ANOVA analyses. N values represent the total number of growth cones measured across 3 neurons per condition from 3 independent culture replicates. P-values indicate difference from Vector control.

| Transfection Condition | N-values (total number of neurons measured) | Branch Initiation P-values (difference from vector control) | Branch Termination P-values (difference from vector control) | Branch Lifetime P-values (difference from vector control) |
|------------------------|---|---|--|---|
| Vector                 | 3   | N/A   | N/A  | N/A   |
| shLASP1a               | 3   | 0.0022  | 0.0184   | 0.6311  |
| shLASP1b               | 3   | 0.0017  | 0.0061   | 0.2165  |

**Supplemental Table 2-4.** Axon Branch Dynamics Statistics: n and p-values, Statistical values for **Figure 2-7C** axon branch formation, termination, and lifetime ANOVA analyses. N values represent the total number of neurons measured across 3 culture replicates. P-values indicate difference from Vector control.

**Chapter 3:**  
**RASCL: A New Method for Labeling  
Optically- and Genetically-Selected  
Intracellular Protein Targets**

### **3.1. Summary**

One of the first steps towards understanding the function of a given protein is to examine its localization within the cell. While it would be ideal to perform these experiments in intact tissue, standard immunolabeling techniques produce a high level of background that makes it difficult to distinguish individual cells, particularly if the protein of interest is highly expressed. Therefore, the two most commonly used methods for examining subcellular localization of proteins are immunolabeling in dissociated cultured cells and overexpressing fluorescently-tagged exogenous protein in intact tissue. Neither of these options is ideal, as dissociation of cells from their natural environment can change the course of cellular development, and overexpression of tagged proteins can create localization artifacts. To overcome these issues, I have established a method that allows immunolabeling of endogenous proteins in optically- and genetically-targeted cells, using reactive oxygen species (ROS) to permeabilize the membrane. This method, called RASCL (ROS-Assisted Single Cell Labeling), allows us to use a small fluorescent probe to successfully label the actin cytoskeleton with high levels of specificity. Future research will allow us to apply this method with larger probes such as antibodies, and probe intact tissue. Using this method, cell biologists will be able to examine protein localization and function in a wide variety of contexts with fewer methodology-related artifacts.

### **3.2. Introduction**

In the previous chapter, I described how knowing LASP1's localization is critical to understanding its function. This is true of the majority of non-soluble proteins, whose positions in the cell dictate how they perform their roles in cellular processes. Currently, the preferred

method for observing protein localization is immunolabeling for the protein of interest in fixed samples. While it would be preferable to use intact tissue, the intermingling of cells makes subcellular observations nearly impossible, driving many researchers to use cultured cells instead. While cell culture can replicate many aspects of cell morphology *in vivo*, it introduces many variables that can obfuscate experimental results. One alternative method that allows for subcellular localization *in vivo* is expressing fluorescent protein-tagged exogenous proteins of interest into cells via viral transduction. This method allows for sparse labeling of genetically-selected cells, but requires conjugation to bulky fluorescent proteins and high levels of overexpression that can alter localization, particularly for proteins like LASP1 whose localizations grow less specific with overexpression. This can be mitigated somewhat by knocking down the endogenous protein or reducing expression levels, but this can require multiple transductions per sample or make fluorescent signals too dim to image at high resolution. In short, there is at present no single technique that can label endogenous protein in sparse, genetically-selected cells *in vivo*. This chapter describes a highly novel approach to this problem, by combining laser-induced ROS (reactive oxygen species) production with genetic approaches to allow labeling of endogenous proteins in optically- and genetically-labeled cells, a technique called RASCL (ROS-Assisted Single Cell Labeling).

### **3.3. Methodology**

To solve the issue of labeling only the genetically-selected cells in a dense tissue environment, a controlled method was necessary to permeabilize selected cells. One obvious choice was reactive oxygen species, which have been shown to be capable of oxidizing lipids and by doing so, forms holes in the plasma membrane (Wojtovich and Foster, 2014). Better still,

reactive oxygen species can be produced by fluorescent proteins when exposed to intense light of the correct excitation wavelength (Ito et al., 2012). Over the years, these proteins have been refined and engineered to produce stronger reactive oxygen species at a higher efficiency. One such protein is called mini Singlet Oxygen Generator (miniSOG), derived from the fluorescent LOV2 (light, oxygen, and voltage) domain of the *Arabidopsis thaliana* protein phototropin 2, a blue light photoreceptor (Shu et al., 2011; Wingen et al., 2014; Torra et al., 2015). Originally designed to provide contrast for electron microscopy studies, miniSOG has a peak excitation wavelength of ~448nm, and emits light at 500nm and 528nm. Like other LOV-containing proteins, miniSOG binds to flavin mononucleotide (FMN) to produce ROS (Westberg et al., 2015). However, while other ROS-generating proteins typically produce the more stable superoxide ( $\text{O}_2^-$ ), miniSOG can produce oxygen singlets ( $^1\text{O}_2$ ), which is highly destructive and particularly effective on organic molecules with double bonds (Torra et al., 2015; Trewin et al., 2018). These oxygen singlets are free radicals, reacting rapidly with nearby targets (Laloi and Havaux, 2015; Trewin et al., 2018). Given that oxygen singlets do not travel far before being extinguished, researchers have developed a membrane-bound form of the protein, which has been shown to be extremely effective at ablating cells in *C. elegans* (Xu and Chisholm, 2016). Based on these findings, I generated a protocol that would take advantage of this miniSOG tool to label endogenous proteins in genetically- and optically-selected cells (**Figure 3-1**). I performed extensive troubleshooting to maximize ROS production, by supplementing the miniSOG co-factor flavin mononucleotide with Vitamin B<sub>3</sub> (riboflavin), and photobleaching in the presence of dissolved oxygen. Furthermore, to avoid impairing miniSOG activity, I used light (2-4% formaldehyde) fixation where possible. For testing purposes, I labeled cytoskeletal

elements F-actin and microtubules, as they are easily recognizable and present throughout the cell.

### **3.4. Description of Materials**

The following materials were used in this study:

- Transfection:
  - miniSOG membrane7 plasmid (Addgene # 62783)
  - Xtreme Gene transfection Reagent (Sigma)
- Media supplement:
  - Riboflavin B<sub>2</sub> (Sigma R9504): while riboflavin aka Vitamin B<sub>2</sub> is typically already present in the cell media, supplementation makes the miniSOG brighter and enhances labeling success.
- Preparation of Oxygenated Imaging Solution
  - Phosphate Buffered Saline (PBS, no calcium or magnesium): chilled, to enhance oxygen solubility in the solution.
  - Fish Tank Air Stone Bubbler: This is connected to the oxygen tank by tubing, and is suspended in the PBS solution for 1 hour.
  - Tubing
  - Tank of 95% O<sub>2</sub>
- Fixation
  - 16% Formaldehyde, EM grade (Electron Microscopy Services)

- Cacodylate Sucrose Buffer (0.1M sodium cacodylate, 0.1M sucrose pH 7.4)(Han et al., 2011): This buffer stabilizes cytoskeletal elements for labeling purposes.
- Labeling Probes and Antibodies:
  - Phalloidin-568 (Invitrogen)
  - Mouse anti-alpha-Tubulin (DM1a Clone, Sigma)
  - Goat anti-mouse Alexa Fluor 546 (Invitrogen)

### **3.5. RASCL Procedure**

F-actin Labeling in MCF7 cells:

MCF7 cells were cultured using high glucose DMEM with 10% FBS. Cells were transfected with the miniSOG Membrane 7 plasmid using Xtreme Gene transfection reagent. Culture media was supplemented with 150 $\mu$ M riboflavin (precursor to the miniSOG cofactor, flavin mononucleotide) for 36 hours. Cells were plated on PLL-coated glass coverslips, and fixed for 12 minutes with warm 2% formaldehyde diluted in 0.1M cacodylate-0.1M sucrose buffer. Coverslips were carefully mounted in custom imaging chambers while maintaining a bubble of PBS over the cells. The chamber was filled with PBS that had been bubbled with 95% O<sub>2</sub> for 1 hour on ice, then sealed tightly to prevent oxygen escape. Regions with transfected and nontransfected cells were imaged via epifluorescence on an inverted microscope, then bleached using a TIRF 488nm laser (perpendicular angle) at 100% power for 1 minute. A 1:200 concentration of phalloidin-568 (phall-568) was applied to the cells for 1 hour. Cells were then imaged to visualize actin staining. As a control, a 0.2% TritonX-100 solution (TritonX) was

applied to permeabilize all cells, and phall-568 was applied again to label both transfected and nontransfected cells.

Microtubule labeling in CAD cells:

As above, CAD cells were transfected with miniSOG, incubated with riboflavin, and plated on coverslips coated in 20mg/mL laminin instead of PLL (cell type-specific coating preference). CAD cells were fixed with 4% PFA for 15 minutes to preserve the microtubule structures. As above, fixed coverslips were carefully placed in imaging chambers and loaded with oxygenated PBS for imaging. Regions with transfected cells were identified and imaged using epifluorescence, then irradiated with the same TIRF laser settings and duration as above. Mouse anti-tubulin antibody was applied at a concentration of 1:1000 for one hour, followed by a single rinse in PBS. Goat anti-rabbit antibody conjugated to AlexaFluor 546 was applied at a concentration of 1:750 for 30 minutes at room temperature. Cells were rinsed again and imaged, followed by the same TritonX treatment as above. Cells were relabeled with the same primary and secondary antibodies, then reimaged as a positive control.

### **3.6. Results:**

As I set out to perform these experiments, I had three criteria by which to measure the success of RASCL: 1) that the pattern of fluorescent signals resembled the cytoskeletal elements I was probing for; 2) specificity of labeling, where fluorescent signals were only detected in photobleached cells expressing miniSOG, and 3) nontransfected cells could still be labeled after

the application of a universal permeabilizing agent (TritonX 100). These criteria were used to develop this protocol and produce the results below.

### **3.6.1. Efficacy of the RASCL Technique with Small Fluorescent Probes**

Our first test of the RASCL system was to use phalloidin, a small 788 dalton probe conjugated to a fluorescent AlexaFluor dye (phall-568), to label actin filaments. Here, I utilized MCF7 breast cancer cells with striking stress fiber actin structures. In **Figure 3-2A**, images show a region containing a single miniSOG- expressing cell and multiple nontransfected cells. After photobleaching using a 488 laser for 1 minute, phalloidin-568 (phall-568) was added to the imaging solution at a concentration of 1:500 for 20minutes, then rinsed and reimaged (**Figure 3-2B**, left). To ensure that the surrounding cells were still intact, the coverslip was incubated in 0.2% TritonX 100 for 10minutes and restained with phall-568 (**Figure 3-2B**, right). The RASCL-induced staining shows specific labeling of the actin cytoskeleton only in the miniSOG- expressing cell, while neighboring nontransfected cells show no fluorescent signals. Based on this image, it is clear that the oxygen singlets produced in the RASCL reaction do not permeabilize neighboring cells. After TritonX treatment and the second round of labeling, all cells show fluorescent signals consistent with actin structures, indicating that initial labeling was specific to miniSOG-expressing cells and not due to any defects in the surrounding cells. Furthermore, the labeling is consistent between the initial staining and in the staining after TritonX 100 treatment, as demonstrated via colocalization analysis of the two images. Of interest is the difference in fluorescence intensity between the first and second rounds of labeling (indicated by the lookup table scale, **Figure 3-2B** middle), which indicates that ROS-induced

permeabilization is less effective than TritonX treatment. However, future improvements may allow brighter staining of RASCL-permeabilized cells.

### 3.6.2. RASCL-Induced Antibody Labeling

While labeling actin filaments could be a very useful application of the RASCL technique, my goal was to develop a versatile labeling method that could be used on any protein detectible by conventional antibodies. Therefore, the next test of the RASCL system was to use antibodies (~150kDa) against microtubules in place of the smaller phalloidin (0.7kDa) dye. I chose to use Cath.a Differentiable (CAD) neuroblastoma cells for this experiment, both to demonstrate the versatility in cell type of this technique and because CADs are round, flat cells with remarkable tendril-like microtubules radiating out around the cell. Here, a region of CAD cells was selected with one bright miniSOG-expressing cell and another cell with little to no green fluorescence (**Figure 3-3A**). After photobleaching with the same protocol as above, primary mouse anti- $\alpha$  tubulin antibody was applied to the coverslips at a concentration of 1:1000 for 1 hour at room temperature, followed by secondary goat anti-mouse antibody conjugated to AlexaFluor 546 at a concentration of 1:750 for 30 minutes at room temperature (**Figure 3-3B**, left). After imaging, the cells were permeabilized with TritonX as above and restained with the same concentration of primary and secondary antibody for the same duration (**Figure 3-3B**, right). Unlike with the small phalloidin probe above and in CAD cells (not shown), the RASCL-induced antibody labeling only targets a small portion of the bright miniSOG-expressing cell. While this region does appear to show patterns of fluorescent signals consistent with microtubules, this does not permeate the entire cell. Relabeling after TritonX treatment illuminates the whole microtubule network across the miniSOG-expressing cell and the

neighboring cell, making it clear that the “patch” issue is likely due to the lower degree of permeabilization offered by the RASCL technique.

### **3.7. Future Troubleshooting of RASCL**

While this initial study shows that it is possible to achieve specific, targeted labeling of intracellular endogenous proteins using the RASCL method, the issue of patchy antibody labeling across the cell must be addressed. While it is unclear why exactly certain regions of the membrane are permeabilized more than others, the fact that this was not observed with the smaller phalloidin probe suggests that increasing the pore size induced by RASCL treatment could be effective. One possible impediment to pore size could be the uneven distribution of lipid types between the interior and exterior layers of the plasma membrane bilayer (Murayama et al., 2017). This could mean that the exterior lipid layer requires additional exposure to oxygen singlets in order to be destabilized enough to become porous. In future studies, our lab will design a dual-wield miniSOG construct with two proteins linked by a transmembrane domain, such that there will be one miniSOG protein on either side of the membrane. This will double the amount of miniSOG and should effectively saturate both sides of the bilayer with oxygen singlets. While there is some possibility that some of these singlets might oxidize the membranes of nearby cells, this concern is mitigated by the fact that oxygen singlets do not travel far from their origin in organic samples (Trewin et al., 2018).

Should this particular method prove ineffective, it is also possible that the addition of extremely mild detergents or enzymes may prime the membrane for permeabilization by oxygen singlets. For example, saponin is a mild detergent used on live cells for protein extraction, and

could be used effectively at small doses to prime membranes for RASCL treatment (Marsick and Letourneau, 2011). Another possibility is applying Proteinase K, an enzyme that is sometimes used to mildly digest membrane proteins in flow cytometry, prior to photobleaching (Amidzadeh et al., 2014). These are just two examples of the many possible candidate “sensitizers” that could potentially improve RASCL antibody labeling.

### **3.8. Discussion of Applications and Future Directions**

Once perfected, the RASCL technique could be a gateway for cell biologists to study the roles of proteins in intact tissue. While my original goal was to study protein localization *in vivo* without the negative effects of target protein overexpression, there are many creative uses for this technique that could advance our understanding of system and cellular function. One example is cellular morphology and the cytoskeleton. In the brain, there are a wide variety of cell types, each with different morphologies and synapse types. There are still many questions as to how the underlying cytoskeleton is regulated to produce each of these structures, because many of these unique morphologies can develop differently in dissociated embryonic cultures, and labeling the endogenous cytoskeleton *in vivo* is incredibly difficult (Palacios-Prü et al., 1976). Using the RASCL technique combined with 2-photon imaging, future investigators would be able to visualize entire cells and their cytoskeletal elements without the artifacts introduced by overexpression or bulky fluorescent protein tags.

This could also be extended to connective studies, which often use a modified rabies virus to selectively label cells joined by synapses with a fluorescent protein cell fill (Reardon et al., 2016). By combining this rabies virus with a membrane-bound miniSOG gene, RASCL

could be utilized to look at endogenous protein localization pre- and post-synaptically, adding another dimension to these connective studies. Ultimately the versatility of the RASCL technique means its applications towards the advancement of cell biology are limitless.

### 3.9. Figures:

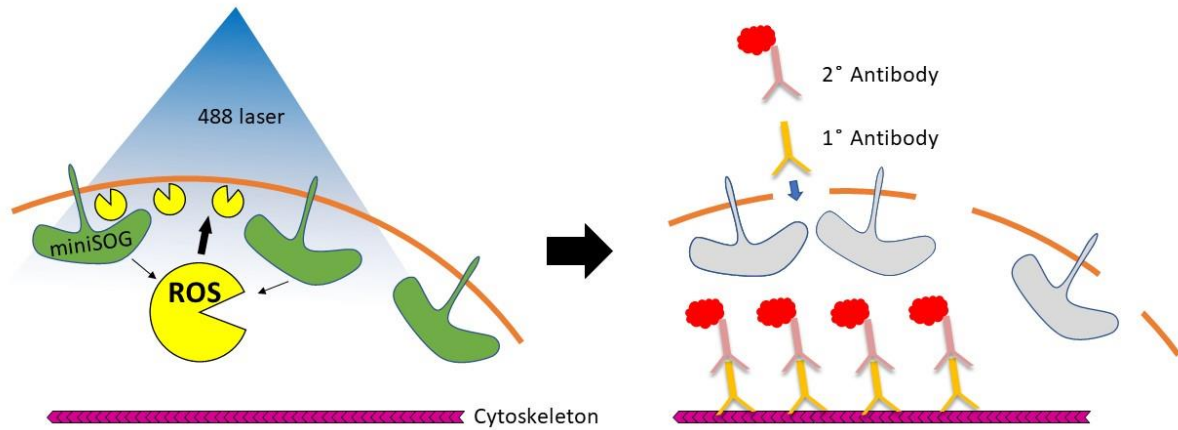


**Figure 3-1:** Diagram of RASCL mechanism of labeling. Left: Cells transfected with miniSOG bound to the membrane are bleached with a 488 laser, causing localized production of reactive oxygen singlets (ROS). These singlets travel a short distance to the cell membrane, where they react with the phospholipids and disrupt the integrity of the bilayer. Right: Disruptions in the bilayer permit antibodies or probes to enter the cell, labeling endogenous intercellular components such as the cytoskeleton.

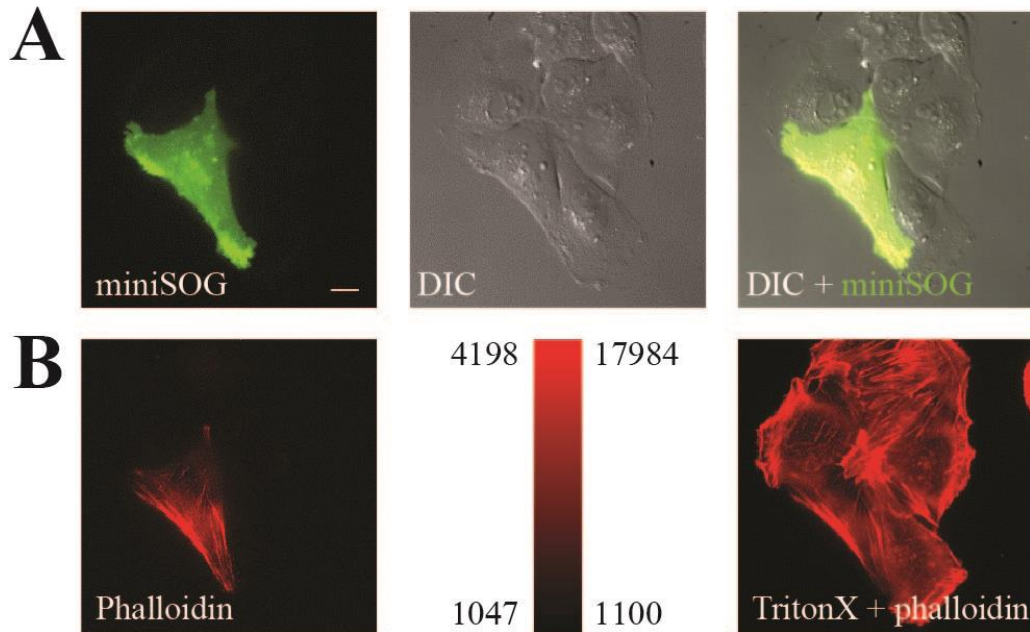


**Figure 3-2:** RASCL Labeling of F-actin with small probe phalloidin. (A) Images of MCF7 cells prior to photobleaching, with miniSOG fluorescence (green, left) and Direct Interference Contrast (DIC, middle). Merged (right), you can see that only one of the five cells in the image is expressing miniSOG. (B) F-actin labeling with phalloidin (red) after photobleaching (left) and after subsequent TritonX treatment (right), with fluorescence intensity scale (middle). Initial labeling after photobleaching shows fluorescent signals that are restricted to the cell expressing miniSOG, indicating high specificity. However, this initial staining is dimmer (scale 1047-4198 arbitrary units) than the TritonX treatment (scale 1100 – 17984 arbitrary units), indicating that RASCL-induced permeabilization is not as strong as the detergent treatment.

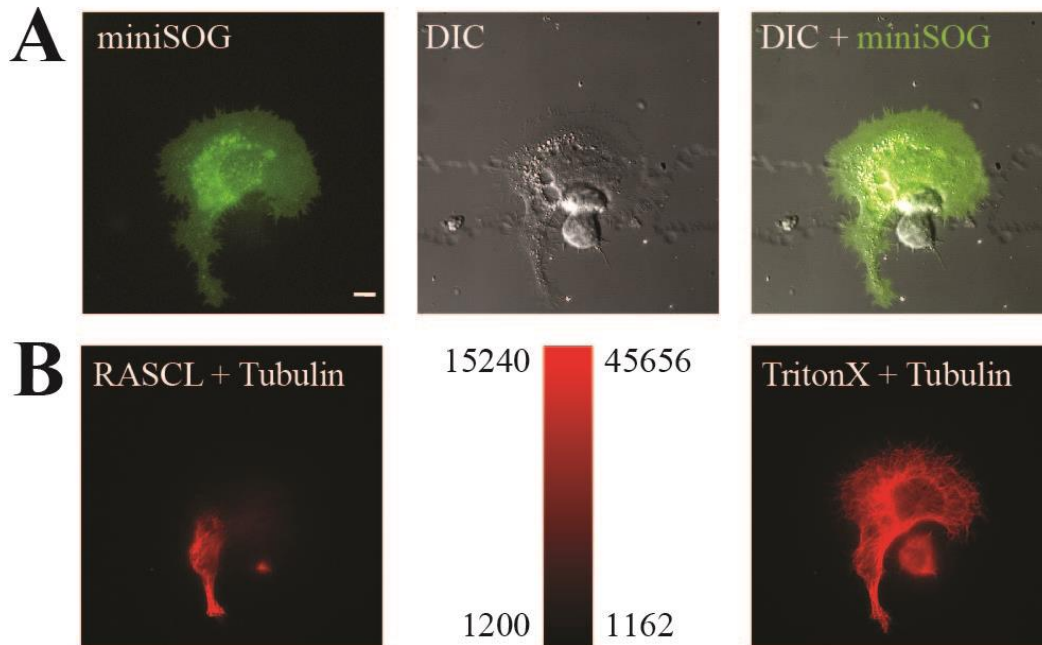


**Figure 3-3: RASCL Antibody Labeling of Microtubules.** (A) Images of CAD cells prior to photobleaching, with miniSOG fluorescence (green, left) and Direct Interference Contrast (DIC, middle). Merged (right). (B) Microtubule labeling with antibodies (red) after photobleaching (left) and after subsequent TritonX treatment (right), with fluorescence intensity scale (middle). Initial labeling after photobleaching shows fluorescent signals that resemble the microtubule staining on the right, but do not cover the entirety of the cell. This is likely due to the size of the probe, as antibodies are much larger than the phalloidin probe. Like the phalloidin labeling in **Figure 3-2B**, the patch of RASCL-induced staining is dimmer than the TritonX treatment.

# **Chapter 4:**

## **Discussion and Future Directions**

## 4.1. Summary and Discussion

The purpose of this dissertation was to answer two experimental questions: how does LASP1 promote actin-based motility, and what is the function of LASP1 in the axon growth cone. Here I demonstrated that LASP1 localizes to the edges of lamellipodial and filopodial actin structures in axon growth cones and neuroblastoma (CAD) cells. This localization depends on the protrusive activity of the lamellipodia, as LASP1 is absent from retracting membranes. Of the LASP1 subdomains, the LIM and nebulin regions regulate the localization of LASP1 to the leading edge of the cell. Furthermore, LASP1 appears to co-localize with the plus ends of actin filaments, and depends on available actin plus ends for its localization. These findings strongly indicate that LASP1 may act on actin plus ends, directly or indirectly, to achieve actin-based cellular protrusion.

In developing neurons, I have shown that LASP1 is essential for normal axon elongation and branching. Loss of LASP1 results in reduced growth cone speed and protrusion, as well as a reduction in branch initiation rates. *In vivo*, *Drosophila* Lasp promotes the elongation and fasciculation of commissural axons, which reinforces the *in vitro* phenotype while introducing a potential function for LASP1 in axon guidance. Taken together, these data suggest that LASP1 promotes axon elongation and arborization, as well as a possible role for LASP1 in regulating actin plus ends at the leading edge of the cell.

### 4.1.1. Evidence for LASP1 as a Possible Regulator of Actin Polymerization or Anti-Capping

Many studies of LASP1 have concluded that it promotes cellular motility, though the proposed mechanisms behind these findings have varied widely. Furthermore, the function of

LASP1 as an actin-binding protein is unclear, due to many contradictory studies. The clearest model for the role of LASP1 in actin dynamics was published by Nakagawa et al., which utilized overexpressed LASP1 protein in neuroblastoma cells for Fluorescence Recovery After Photobleaching (FRAP) experiments (Nakagawa et al., 2006). Photobleaching of actin filaments reveals recovery from the edge of the cell inwards, demonstrating that F-actin polymerizes at the edge of the cell. By contrast, Nakagawa et al. reported that photobleaching of LASP1 resulted in recovery from the center of the cell outwards, from which they formed a model depicting LASP1 as a stabilizer or cross-linker along actin bundles like its Nebulin family members.

Unfortunately, this paper only utilizes overexpressed LASP1, which does not resemble the endogenous staining in neuroblastoma cells (**Figure 2-2**). Based on this dramatic difference in localization, it is likely that vastly overexpressed LASP1 may not be representative of the *in vivo* function of the protein. It is therefore difficult to draw any definitive conclusions from their data.

By contrast, my data show that at endogenous levels, LASP1 localizes to the tips of actin filaments found at the edges of protruding lamellipodia. This localization depends on its LIM and nebulin regions, which in its highly similar sister protein LASP2 are both essential for binding to actin filaments (Nakagawa et al., 2009). While this evidence alone does not prove that LASP1 binds to actin plus ends directly, no other LASP1 binding partner has been shown to require both of these domains. While it is possible that LASP1 is binding to the newly polymerized filaments just behind the barbed end, the fact that LASP1 is dislodged by CytoD, a very small molecule that fits within the cleft of the barbed end, makes it unlikely to dislodge proteins further back on the filament (Nair et al., 2008). This line of logic brings us to the hypothesis that LASP1 is binding directly to the plus ends of actin filaments.

The role of LASP1 at actin plus ends is difficult to decipher from the presented data alone, and there are several candidate possibilities. Firstly, it is possible that LASP1 is promoting actin polymerization. This would fit with previous findings that show LASP1 to promote actin-based cellular motility, which is driven by active polymerization at the leading edge (Pollard and Borisy, 2003). However, one previous study of the effect of adding LASP1 to purified actin *in vitro* suggests that LASP1 may not have any effect on actin polymerization (Chew et al., 2002). However, this study was not replicated, and utilizes a cocktail of strong actin polymerizing proteins as a “control” to normalize the LASP1 results, potentially washing out any effect of LASP1 on actin polymerization. While this study needs to be replicated with more refined techniques, at present it seems unlikely that LASP1 is directly responsible for actin polymerization.

Another possibility is that LASP1 could be cooperating with its binding partner, VASP, to prevent actin plus end capping (Keicher et al., 2004). Previous studies of VASP have demonstrated that it localizes to actin plus ends, where it promotes actin polymerization by antagonizing Capping Protein activity, thus increasing cellular protrusion and motility (Laurent et al., 1999). LASP1 binds to VASP through its SH3 domain, which based on the domain deletion data make VASP an unlikely mechanism for anchoring or recruiting LASP1 to the plus ends of actin filaments (**Figure 2-3**). However, it is possible that LASP1 is anchored to plus ends by its LIM and nebulin regions, while interacting with VASP via its SH3 domain. Based on these findings and the similar functions of LASP1 and VASP in cellular motility, it is possible they could be working in concert to prevent actin plus end capping and promote cellular protrusion.

#### **4.1.2. RASCL: A New Method for Labeling Endogenous Proteins in Genetically-Targeted Cells**

Our current methods for understanding endogenous protein localization and function require immunolabeling of dissociated cell cultures or overexpression of tagged proteins *in vivo*. Both of these methods have significant drawbacks, as dissociation of cells can alter cellular morphology and function, and overexpression of proteins like LASP1 can change its localization (**Figure 2-2**). Therefore, innovation in labeling techniques is long overdue.

RASCL (ROS-Assisted Single Cell Labeling) is a method that utilizes a fluorescent membrane-bound protein called miniSOG to create reactive oxygen singlets in genetically- and optically-selected cells. These singlets oxidize nearby lipids to destabilize the plasma membrane, creating pores through which probes and antibodies can diffuse. Preliminary evidence suggests that this technique works well for small probes, such as phalloidin. However, further work is necessary to improve the efficiency of oxygen singlet production so that antibody labeling is as effective as the small probe.

#### **4.2. Future Directions**

##### *The Duality of LASP1 and LASP2*

LASP1 and LASP2 are highly sequentially similar, and are both highly expressed in the brain. However, previous evidence suggests they have different binding partners and unique roles in cellular motility, with LASP2 playing a stronger role in adhesions (Grunewald and Butt, 2008). In older developing neurons, LASP2 appears to play a stronger role in dendrite development than LASP1, whose role in dendrites is largely restricted to spine development and

synapse formation (Myers et al., 2020). Furthermore, my preliminary live cell imaging shows that LASP2 does not localize to the edges of CAD cells like LASP1, and that protruding regions of the cell appear to have less LASP2 signal than neighboring static regions. This would indicate that LASP1 and LASP2 may have dramatic differences in their roles in axon growth cones. However, the lack of a reliable LASP2 antibody has significantly hindered research on this fascinating proteins. Future studies utilizing more sophisticated methods such as speckle microscopy would be necessary to determine how LASP2 functions in the context of the growth cone and actin cytoskeleton. Furthermore, selective mutation studies that exchange selected regions of the LASP1 and LASP2 proteins could help us to understand how LASP1 and LASP2 can function so differently with such highly similar structures.

#### *LASP1 and Actin Dynamics*

Previous studies of LASP1 do not seem able to agree on the role of LASP1 in actin structure and dynamics. While a first glance at LASP1 in the context of the Nebulin family might assume it to be a smaller version of the actin stabilizing protein Nebulin, the past two decades of LASP1 research have found roles for the protein in such far-flung processes as mRNA localization, immune cell chemotaxis, and nuclear transport (Suyama et al., 2009; Orth et al., 2015). Still, very little is understood about how LASP1 functions as an actual actin-binding protein. Therefore, a critical next step in understanding how LASP1 promotes actin-based motility is to perform *in vitro* assays with LASP1 and purified actin monomers. The effect of various concentrations of LASP1 on actin polymerization, depolymerization, and stability would go far in explaining how this one protein functions in actin dynamics. Furthermore, the introduction of some of its key binding partners (such as VASP) would illuminate how these proteins function together in promoting actin-based motility. Our current understanding of

LASP1's binding partners is limited to GST pulldowns, with few to no known functional interactions. By observing how LASP1 interacts with its partners in the presence of actin, followed by speckle microscopy studies of these proteins in a living cell, it will be possible to build a model for how LASP1 promotes cellular motility.

### *LASP1 and Axon Guidance*

Data presented in this work establish LASP1 as a novel regulator of axon growth and development. However, while the *in vivo* defasciculation phenotype resulting from loss of LASP1 suggest there may be a guidance role for this protein, no studies have yet examined LASP1 in the context of axon guidance. Therefore, future studies will be necessary to elucidate how LASP1 promotes growth in the context of guidance-related signaling. This can be achieved through two experimental paradigms. Firstly, dual knockdowns of LASP1 and its binding partners, whose roles in axon guidance are more clearly established, could be used to explore how these proteins work in concert to promote axonal growth and development. Secondly, exposing cultured neurons depleted of LASP1 to various axon guidance cues and measuring the changes in growth cone motility and collateral formation could highlight which guidance signaling cascades converge on LASP1 to produce guided motility. These experiments would further our understanding of LASP1 regulation by signaling molecules, and could potentially highlight a novel role for this unique protein.

## References

- Agnew BJ, Minamide LS, Bamburg JR (1995) Reactivation of Phosphorylated Actin Depolymerizing Factor and Identification of the Regulatory Site. *J Biol Chem* 270:17582–17587.
- Aizawa H, Wakatsuki S, Ishii A, Moriyama K, Sasaki Y, Ohashi K, Sekine-aizawa Y, Seharafujisawa A, Mizuno K, Goshima Y, Yahara I (2001) Phosphorylation of cofilin by LIM-kinase is necessary for semaphorin 3A-induced growth cone collapse. *Nat Neurosci* 4:367–373.
- Akin O, Mullins RD (2008) Capping Protein Increases the Rate of Actin-based Motility by Promoting Filament Nucleation by the Arp2/3 Complex. *Cell* 133:841–851.
- Amano M, Chihara K, Nakamura N, Fukata Y, Yano T, Shibata M, Ikebe M, Kaibuchi K (1998) Myosin II activation promotes neurite retraction during the action of Rho and Rho-kinase. *Genes to Cells* 3:177–188.
- Amidzadeh Z, Behzad Behbahani A, Erfani N, Sharifzadeh S, Ranjbaran R, Moezi L, Aboulizadeh F, Ali Okhovat M, Alavi P, Azarpira N (2014) Assessment of different permeabilization methods of minimizing damage to the adherent cells for detection of intracellular RNA by flow cytometry. *Avicenna J Med Biotechnol* 6:38–46.
- Bashaw GJ (2010) Visualizing Axons in the Drosophila Central Nervous System Using Immunohistochemistry and Immunofluorescence. *Cold Spring Harb Protoc* 10.
- Bear JE, Svitkina TM, Krause M, Schafer DA, Loureiro JJ, Strasser GA, Maly I V., Chaga OY, Cooper JA, Borisy GG, Gertler FB (2002) Antagonism between Ena/VASP proteins and

- actin filament capping regulates fibroblast motility. *Cell* 109:509–521.
- Bernstein BW, Bamburg JR (2010) ADF/Cofilin: A functional node in cell biology. *Trends Cell Biol* 20:187–195 Available at: <http://dx.doi.org/10.1016/j.tcb.2010.01.001>.
- Blanchoin L, Boujemaa-Paterski R, Sykes C, Plastino J (2014) Actin Dynamics, Architecture, and Mechanics in Cell Motility. *Physiol Rev* 94:235–263.
- Blanchoin L, Pollard TD (1999) Mechanism of interaction of *Acanthamoeba* actophorin (ADF/Cofilin) with actin filaments. *J Biol Chem* 274:15538–15546.
- Bliss KT, Chu M, Jones-Weinert CM, Gregorio CC (2013) Investigating *lasp-2* in cell adhesion: new binding partners and roles in motility. *Mol Biol Cell* 24:995–1006 Available at: <http://www.pubmedcentral.nih.gov/articlerender.fcgi?artid=3608507&tool=pmcentrez&rendertype=abstract>.
- Bonzo JR, Norris AA, Esham M, Moncman CL (2008) The nebulin repeat domain is necessary for proper maintenance of tropomyosin with the cardiac sarcomere. *Exp Cell Res* 314:3519–3530 Available at: <http://dx.doi.org/10.1016/j.yexcr.2008.09.001>.
- Boyer NP, Gupton SL (2018) Revisiting netrin-1: One who guides (Axons). *Front Cell Neurosci* 12:1–18.
- Bradke F, Dotti CG (1999) The Role of Local Actin Instability in Axon Formation Published by : American Association for the Advancement of Science Stable URL : <http://www.jstor.org/stable/2896648> Linked references are available on JSTOR for this article : The Role of Local Actin I. *Science* (80- ) 283:1931–1934.
- Brankatschk M, Dickson BJ (2006) Netrins guide *Drosophila* commissural axons at short range.

Nat Neurosci 9:188–194.

Butt E, Gambaryan S, Göttfert N, Galler A, Marcus K, Meyer HE (2003) Actin binding of human LIM and SH3 protein is regulated by cGMP- and cAMP-dependent protein kinase phosphorylation on serine 146. *J Biol Chem* 278:15601–15607.

Cajal SR y (1890) A quelle époque apparaissent les expansions des cellules nerveuses de la moelle épinière du poulet? *Anat Anz* 5:609–631.

Cajal SR y (1892) La rétine des vertébrés. *Cellule* 9:121–133.

Cajal SR y, Swanson N, Swanson LW (1904) *Histology of the nervous system of man and vertebrates.*

Case LB, Waterman CM (2015) Integration of actin dynamics and cell adhesion by a three-dimensional, mechanosensitive molecular clutch. *Nat Cell Biol* 17:955–963 Available at: <http://dx.doi.org/10.1038/ncb3191>.

Chan SSY, Zheng H, Su MW, Wilk R, Killeen MT, Hedgecock EM, Culotti JG (1996) UNC-40, a *C. elegans* homolog of DCC (Deleted in Colorectal Cancer), is required in motile cells responding to UNC-6 netrin cues. *Cell* 87:187–195.

Chew C, Chen X, Qin H, Stoming T (2002) New insights into second messenger regulation of parietal cell function by novel downstream signaling proteins. In: *Mechanisms and consequences of proton transport* (Urushidani T, Forte J, Sachs G, eds), pp 185–195. Boston: Springer.

Chilton JK, Guthrie S (2016) Axons get ahead : Insights into axon guidance and Congenital Cranial Dysinnervation Disorders. *Developmental Neurobiol.*

- Colavita A, Culotti JG (1998) Suppressors of ectopic UNC-5 growth cone steering identify eight genes involved in axon guidance in *Caenorhabditis elegans*. *Dev Biol* 194:72–85.
- Crain B, Cotman C, Taylor D, Lynch G (1973) A quantitative electron microscopic study of synaptogenesis in the dentate gyrus of the rat. *Brain Res* 63:195–204.
- De La Cruz EM (2005) Cofilin binding to muscle and non-muscle actin filaments: Isoform-dependent cooperative interactions. *J Mol Biol* 346:557–564.
- Debant A, Serra-Pagès C, Seipel K, O'Brien S, Tang M, Park SH, Streuli M (1996) The multidomain protein Trio binds the LAR transmembrane tyrosine phosphatase, contains a protein kinase domain, and has separate rac-specific and rho-specific guanine nucleotide exchange factor domains. *Proc Natl Acad Sci U S A* 93:5466–5471.
- DeBello WM, Feldman DE, Knudsen EI (2001) Adaptive axonal remodeling in the midbrain auditory space map. *J Neurosci* 21:3161–3174.
- DeGeer J, Boudeau J, Schmidt S, Bedford F, Lamarche-Vane N, Debant A (2013) Tyrosine phosphorylation of the Rho guanine nucleotide exchange factor Trio regulates netrin-1/DCC-mediated cortical axon outgrowth. *Mol Cell Biol* 33:739–751 Available at: <http://www.pubmedcentral.nih.gov/articlerender.fcgi?artid=3571336&tool=pmcentrez&rendertype=abstract>.
- Deiner MS, Kennedy TE, Fazeli A, Serafini T, Tessier-Lavigne M, Sretavan DW (1997) Netrin-1 and DCC mediate axon guidance locally at the optic disc: Loss of function leads to optic nerve hypoplasia. *Neuron* 19:575–589.
- Demarco RS, Struckhoff EC, Lundquist EA (2012) The Rac GTP exchange factor TIAM-1 acts

with CDC-42 and the guidance receptor UNC-40/DCC in neuronal protrusion and axon guidance. *PLoS Genet* 8.

Dent EW, Barnes AM, Tang F, Kalil K (2004) Netrin-1 and Semaphorin 3A Promote or Inhibit Cortical Axon Branching, Respectively, by Reorganization of the Cytoskeleton. *J Neurosci* 24:3002–3012.

Dent EW, Gupton SL, Gertler FB (2011) The Growth Cone Cytoskeleton in Axon Outgrowth and Guidance. *Cold Spring Harb Perspect Biol* 3.

Desmarais V, Ghosh M, Eddy R, Condeelis J (2005) Cofilin takes the lead. *J Cell Sci* 118:19–26.

Dotti CG, Sullivan CA, Banker GA (1988) The Establishment of Polarity by Hippocampal Neurons in Culture. *J Neurosci* 8:1454–1468.

Engle EC (2010) Human disorders of axon guidance. *Cold Spring Harb Perspect Biol* 2.

Evans TA, Bashaw GJ (2010) Axon guidance at the midline: of mice and flies. *Curr Opin Neurobiol* 20:79–85 Available at:

<http://www.pubmedcentral.nih.gov/articlerender.fcgi?artid=4128228&tool=pmcentrez&rendertype=abstract>.

Evans TA, Bashaw GJ (2012) Slit/Robo-mediated axon guidance in *Tribolium* and *Drosophila*: divergent genetic programs build insect nervous systems. *Dev Biol* 363:266–278.

Fiala JC, Feinberg M, Popov V, Harris KM (1998) Synaptogenesis Via Dendritic Filopodia in Developing Hippocampal Area CA1. *J Neurosci* 18:8900–8911.

Finci LI, Krüger N, Sun X, Zhang J, Chegkazi M, Wu Y, Schenk G, Mertens HDT, Svergun DI, Zhang Y, Wang J huai, Meijers R (2014) The Crystal Structure of Netrin-1 in Complex with

- DCC Reveals the Bifunctionality of Netrin-1 As a Guidance Cue. *Neuron* 83:839–849.
- Fujita Y, Yamashita T (2014) Axon growth inhibition by RhoA/ROCK in the central nervous system. *Front Neurosci* 8:1–12.
- Gallo G, Letourneau PC (1998) Localized sources of neurotrophins initiate axon collateral sprouting. *J Neurosci* 18:5403–5414.
- Garbe DS, O'Donnell M, Bashaw GJ (2007) Cytoplasmic domain requirements for Frazzled-mediated attractive axon turning at the *Drosophila* midline. *Development* 134:4325–4334.
- Geschwind DH, Rakic P (2013) Cortical Evolution: Judge the Brain by its Cover. *Neuron* 80:633–647.
- Ghosh M, Song X, Mouneimne G, Sidani M, Lawrence DS, Condeelis JS (2004) Cofilin promotes actin polymerization and defines the direction of cell motility. *Science* 304:743–746.
- Goddette DW, Frieden C (1986) Actin Polymerization The Mechanism of Action of Cytochalasin D. *J Biol Chem* 261:15974–15980.
- Gohla A, Birkenfeld J, Bokoch GM (2005) Chronophin, a novel HAD-type serine protein phosphatase, regulates cofilin-dependent actin dynamics. *Nat Cell Biol* 7:21–29.
- Gomez TM, Letourneau PC (2014) Actin dynamics in growth cone motility and navigation. *J Neurochem* 129:221–234.
- Gonçalves JT, Schafer ST, Gage FH (2016) Adult Neurogenesis in the Hippocampus: From Stem Cells to Behavior. *Cell* 167:897–914.
- Grintsevich EE, Yesilyurt HG, Rich SK, Hung R-J, Terman JR, Reisler E (2016) F-actin

dismantling through a redox-driven synergy between Mical and cofilin. *Nat Cell Biol* 18:876–885 Available at: <http://dx.doi.org/10.1038/ncb3390>.

Grunewald TGP, Butt E (2008) The LIM and SH3 domain protein family: structural proteins or signal transducers or both? *Mol Cancer* 7:31.

Grunewald TGP, Kammerer U, Schulze E, Schindler D, Honig A, Zimmer M, Butt E (2006) Silencing of LASP-1 influences zyxin localization, inhibits proliferation and reduces migration in breast cancer cells. *Exp Cell Res* 312:974–982.

Grunewald TGP, Kammerer U, Winkler C, Schindler D, Sickmann A, Honig A, Butt E (2007) Overexpression of LASP-1 mediates migration and proliferation of human ovarian cancer cells and influences zyxin localisation. *Br J Cancer* 96:296–305 Available at: <http://dx.doi.org/10.1038/sj.bjc.6603545>.

Gu J, Lee CW, Fan Y, Komlos D, Tang X, Sun C, Hartzell HC, Chen G, Bamberg JR, Zheng JQ (2010) ADF/Cofilin-Mediated Actin Dynamics Regulate AMPA Receptor Trafficking during Synaptic Plasticity. *Nat Neurosci* 13:1208–1215.

Hailer A, Grunewald TGP, Orth M, Reiss C, Kneitz B, Spahn M, Butt E (2014) Loss of tumor suppressor mir-203 mediates overexpression of LIM and SH3 Protein 1 (LASP1) in high-risk prostate cancer thereby increasing cell proliferation and migration. *Oncotarget* 5:4144–4153 Available at: <http://www.pubmedcentral.nih.gov/articlerender.fcgi?artid=4147312&tool=pmcentrez&rendertype=abstract>.

Hall A (1998) Rho GTPases and the Actin Cytoskeleton. *Science* (80- ) 279:509–514.

- Hall A, Lalli G (2010) Rho and Ras GTPases in Axon Growth, Guidance, and Branching. *Cold Spring Harb Perspect Biol* 2.
- Hamelin M, Zhou Y, Su M-W, Scott I, Culotti J (1993) Ectopic expression of the unc-5 guidance receptor in the touch neurons steers their axons dorsally on the epidermis. *Nature* 364:327–331.
- Han L, Wen Z, Lynn RC, Baudet M-L, Holt CE, Sasaki Y, Bassell GJ, Zheng JQ (2011) Regulation of chemotropic guidance of nerve growth cones by microRNA. *Mol Brain* 4:40 Available at: <http://dx.doi.org/10.1186/1756-6606-4-40>.
- Hao YK, Briehner WM, Mitchison TJ (2008) Dynamic stabilization of actin filaments. *Proc Natl Acad Sci U S A* 105:16531–16536.
- Harrelson AL, Goodman CS (1988) Growth cone guidance in insects: Fasciclin II is a member of the immunoglobulin superfamily. *Science* (80- ) 242:700–708.
- Harris KM, Jensen FE, Tsao B (1992) Three-dimensional structure of dendritic spines and synapses in rat hippocampus (CA1) at postnatal day 15 and adult ages: Implications for the maturation of synaptic physiology and long-term potentiation (*J Neurosci* (July 1992) 12 (2685-2705)). *J Neurosci* 12.
- Hedgecock EM, Culotti JG, Hall DH (1990) The unc-5, unc-6, and unc-40 genes guide circumferential migrations of pioneer axons and mesodermal cells on the epidermis in *C. elegans*. *Neuron* 4:61–85.
- Horowitz R (2006) Nebulin regulation of actin filament lengths: New angles. *Trends Cell Biol* 16:121–124.

- Hsieh SH, Ferraro GB, Fournier AE (2006) Myelin-Associated Inhibitors Regulate Cofilin Phosphorylation and Neuronal Inhibition through LIM Kinase and Slingshot Phosphatase. *J Neurosci* 26:1006–1015.
- Hung R-J, Pak CW, Terman JR (2011) Direct Redox Regulation of F-Actin. *Science* (80-) 832:1710–1713.
- Hung R-J, Yazdani U, Yoon J, Wu H, Yang T, Gupta N, Huang Z, van Berkel WJH, Terman JR (2010) Mical links semaphorins to F-actin disassembly. *Nature* 463:823–827.
- Hung RJ, Terman JR (2011) Extracellular inhibitors, repellents, and semaphorin/plexin/MICAL-mediated actin filament disassembly. *Cytoskeleton* 68:415–433.
- Hur EM, Yang IH, Kim DH, Byun J, Saijilafu, Xu WL, Nicovich PR, Cheong R, Levchenko A, Thakor N, Zhoua FQ (2011) Engineering neuronal growth cones to promote axon regeneration over inhibitory molecules. *Proc Natl Acad Sci U S A* 108:5057–5062.
- Ito S, Song YH, Imaizumi T (2012) LOV Domain-Containing F-Box Proteins : Light-Dependent Protein Degradation Modules in Arabidopsis. *Mol Plant* 5:573–582 Available at: <http://dx.doi.org/10.1093/mp/sss013>.
- Jamuar SS et al. (2017) Biallelic mutations in human DCC cause developmental split-brain syndrome. *Nat Genet* 49:606–612 Available at: <http://dx.doi.org/10.1038/ng.3804>.
- Jarrard LE (1993) On the role of the hippocampus in learning and memory in the rat. *Behav Neural Biol* 60:9–26.
- Joo J, Lee S, Nah SS, Kim YO, Kim DS, Shim SH, Hwangbo Y, Kim HK, Kwon JT, Kim JW, Song HY, Kim HJ (2013) Lasp1 is down-regulated in NMDA receptor antagonist-treated

mice and implicated in human schizophrenia susceptibility. *J Psychiatr Res* 47:105–112

Available at: <http://dx.doi.org/10.1016/j.jpsychires.2012.09.005>.

Kaech S, Banker G (2006) Culturing hippocampal neurons. *Nat Protoc* 1:2406–2415.

Kalil K, Dent EW (2005) Touch and go: Guidance cues signal to the growth cone cytoskeleton.

*Curr Opin Neurobiol* 15:521–526.

Kalil K, Dent EW (2014) Branch management: mechanisms of axon branching in the developing

vertebrate CNS. *Nat Rev Neurosci* 15:7–18 Available at:

[/pmc/articles/PMC4063290/?report=abstract](http://www.ncbi.nlm.nih.gov/pmc/articles/PMC4063290/?report=abstract).

Kalil K, Li L, Hutchins BI (2011) Signaling Mechanisms in Cortical Axon Growth, Guidance,

and Branching. *Front Neuroanat* 5:1–15.

Kalil K, Szebenyi G, Dent EW (2000) Common mechanisms underlying growth cone guidance

and axon branching. *J Neurobiol* 44:145–158.

Keicher C, Gambaryan S, Schulze E, Marcus K, Meyer HE, Butt E (2004) Phosphorylation of

mouse LASP-1 on threonine 156 by cAMP- and cGMP-dependent protein kinase. *Biochem*

*Biophys Res Commun* 324:308–316.

Keino-masu K, Masu M, Hinck L, Leonardo ED, Chan SS-Y, Culotti JG, Tessier-Lavigne M

(1996) Deleted in Colorectal Cancer (DCC) Encodes a Netrin Receptor. *Cell* 87:175–185.

Keleman K, Dickson BJ (2001) Short- and long-range repulsion by the *Drosophila* Unc5 Netrin

receptor. *Neuron* 32:605–617.

Kennedy TE, Serafini T, de la Torre JR, Tessier-Lavigne M (1994) Netrins are diffusible

chemotropic factors for commissural axons in the embryonic spinal cord. *Cell* 78:425–435.

- Kennedy TE, Wang H, Marshall W, Tessier-Lavigne M (2006) Axon guidance by diffusible chemoattractants: A gradient of netrin protein in the developing spinal cord. *J Neurosci* 26:8866–8874.
- Kidd T, Brose K, Mitchell KJ, Fetter RD, Tessier-Lavigne M, Goodman CS, Tear G (1998) Roundabout controls axon crossing of the CNS midline and defines a novel subfamily of evolutionarily conserved guidance receptors. *Cell* 92:205–215.
- Killeen MT, Sybingco SS (2008) Netrin, Slit and Wnt receptors allow axons to choose the axis of migration. *Dev Biol* 323:143–151 Available at: <http://dx.doi.org/10.1016/j.ydbio.2008.08.027>.
- Kolodkin AL, Tessier-Lavigne M (2011) Mechanisms and molecules of neuronal wiring: A primer. *Cold Spring Harb Perspect Biol* 3:1–14.
- Kolodziej PA, Timpe LC, Mitchell KJ, Fried SR, Goodman CS, Jan LY, Jan YN (1996) frazzled Encodes a Drosophila member of the DCC immunoglobulin subfamily and is required for CNS and motor axon guidance. *Cell* 87:197–204.
- Kubo T, Endo M, Hata K, Taniguchi J, Kitajo K, Tomura S, Yamaguchi A, Mueller BK, Yamashita T (2008) Myosin IIA is required for neurite outgrowth inhibition produced by repulsive guidance molecule. *J Neurochem* 105:113–126.
- Laloi C, Havaux M (2015) Key players of singlet oxygen-induced cell death in plants. *Front Plant Sci* 6:1–9.
- Larsson H, Lindberg U (1988) The Effect of Divalent Cations on the Interaction Between Calf Spleen Profilin and Different Actins. *Biochim Biophys Acta* 953:95–105.

- Laurent V, Loisel TP, Harbeck B, Wehman A, Gröbe L, Jockusch BM, Wehland J, Gertler FB, Carlier MF (1999) Role of proteins of the Ena/VASP family in actin-based motility of *Listeria monocytogenes*. *J Cell Biol* 144:1245–1258.
- Le Clainche C, Carlier M-F (2008) Regulation of actin assembly associated with protrusion and adhesion in cell migration. *Physiol Rev* 88:489–513.
- Lee CW, Vitriol EA, Shim S, Wise AL, Velayutham RP, And, Zheng JQ (2013) Dynamic Localization of G-actin During Membrane Protrusion in Neuronal Motility. *Curr Biol* 23:1046–1056.
- Lehtokari V-L, Pelin K, Sandbacka M, Ranta S, Donner K, Muntoni F, Sewry C, Angelini C, Bushby K, Van den Bergh P, Iannaccone S, Laing NG, Wallgren-Petersson C (2006) Identification of 45 Novel Mutations in the Nebulin Gene Associated with Autosomal Recessive Nemaline Myopathy. *Hum Mutat* 27:946–956.
- Lin CH, Espreatico EM, Mooseker MS FP (1996) Myosin drives retrograde F-actin flow in neuronal growth cones. *Neuron*:769–782.
- Lin DM, Fetter RD, Kopczynski C, Grenningloh G, Goodman CS (1994) Genetic Analysis of Fasciclin II in *Drosophila*: Defasciculation, Refasciculation, and Alterned Fasciculation. *Neuron* 13:1055–1069.
- Lin DM, Goodman CS (1994) Ectopic and increased expression of fasciclin II alters motoneuron growth cone guidance. *Neuron* 13:507–523.
- Lin YH, Park ZY, Lin D, Brahmabhatt AA, Rio MC, Yates JR, Klemke RL (2004) Regulation of cell migration and survival by focal adhesion targeting of Lasp-1. *J Cell Biol* 165:421–432.

- Linford NJ, Bilgir C, Ro J, Pletcher SD (2013) Measurement of lifespan in *Drosophila melanogaster*. *J Vis Exp* 71:1–9.
- Lodish H, Berk A, Kaiser CA, Krieger M, Bretscher A, Ploegh H, Amon A, Martin KC (2016) Chapter 17: Cell Organization and Movement I: Microfilaments. In: *Molecular Cell Biology* 8th edition, pp 713–726.
- Longair MH, Baker DA, Armstrong JD (2011) Simple neurite tracer: Open source software for reconstruction, visualization and analysis of neuronal processes. *Bioinformatics* 27:2453–2454.
- Lowery LA, Van Vactor D (2009) The trip of the tip: understanding the growth cone machinery. *Nat Rev Mol Cell Biol* 10:332–343 Available at: <http://dx.doi.org/10.1038/nrm2679>.
- Luster AD, Alon R, von Andrian UH (2005) Immune cell migration in inflammation: Present and future therapeutic targets. *Nat Immunol* 6:1182–1190.
- Lyuksyutova AI, Lu CC, Milanesio N, King LA, Guo N, Wang Y, Nathans J, Tessier-Lavigne M, Zou Y (2003) Anterior-Posterior Guidance of Commissural Axons by Wnt-Frizzled Signaling. *Science* (80- ) 302:1984–1988.
- Marsick BM, Flynn KC, Santiago-Medina M, Bamburg JR, Letourneau PC (2010) Activation of ADF/cofilin mediates attractive growth cone turning toward nerve growth factor and netrin-1. *Dev Neurobiol* 70:565–588.
- Marsick BM, Letourneau PC (2011) Labeling F-actin barbed ends with rhodamine-actin in permeabilized neuronal growth cones. *J Vis Exp*:8–12.
- Marsick BM, Roche FK, Letourneau PC (2012) Repulsive axon guidance cues ephrin-A2 and

slit3 stop protrusion of the growth cone leading margin concurrently with inhibition of ADF/cofilin and ERM proteins. *Cytoskeleton* 69:496–505.

Meberg PJ, Ono S, Minamide LS, Takahashi M, Bamburg JR (1998) Actin depolymerizing factor and cofilin phosphorylation dynamics: Response to signals that regulate neurite extension. *Cell Motil Cytoskeleton* 39:172–190.

Meng Y, Takahashi H, Meng J, Zhang Y, Lu G, Asrar S, Nakamura T, Jia Z (2004) Regulation of ADF/cofilin phosphorylation and synaptic function by LIM-kinase. *Neuropharmacology* 47:746–754.

Menzies AS, Aszodi A, Williams SE, Pfeifer A, Wehman AM, Goh KL, Mason CA, Fassler R, Gertler FB (2004) Mena and vasodilator-stimulated phosphoprotein are required for multiple actin-dependent processes that shape the vertebrate nervous system. *J Neurosci* 24:8029–8038.

Meyer RL (1998) Roger Sperry and his chemoaffinity hypothesis. *Neuropsychologia* 36:957–980.

Moncman CL, Wang K (2002) Targeted disruption of nebulin protein expression alters cardiac myofibril assembly and function. *Exp Cell Res* 273:204–218.

Morita E, Arai J, Christensen D, Votteler J, Sundquist WI (2012) Attenuated Protein Expression Vectors for Use in siRNA Rescue Experiments. *Biotechniques* 0:1–5.

Moriyama K, Iida K, Yahara I (1996) Phosphorylation of Ser-3 of cofilin regulates its essential function on actin. *Genes to Cells* 1:73–86.

Murayama T, Masuda T, Afonin S, Kawano K, Takatani-Nakase T, Ida H, Takahashi Y, Fukuma

- T, Ulrich AS, Futaki S (2017) Loosening of Lipid Packing Promotes Oligoarginine Entry into Cells. *Angew Chemie - Int Ed* 56:7644–7647.
- Myers KR, Yu K, Kremerskothen J, Butt E, Zheng JQ (2020) The Nebulin Family LIM and SH3 Proteins Regulate Postsynaptic Development and Function. *J Neurosci* 40:526–541.
- Nair UB, Joel PB, Wan Q, Lowey S, Rould MA, Trybus KM (2008) Crystal Structures of Monomeric Actin Bound to Cytochalasin D. *J Mol Biol* 384:848–864 Available at: <http://dx.doi.org/10.1016/j.jmb.2008.09.082>.
- Nakagawa H, Suzuki H, Machida S, Suzuki J, Ohashi K, Jin M, Miyamoto S, Terasaki AG (2009) Contribution of the LIM domain and nebulin-repeats to the interaction of Lasp-2 with actin filaments and focal adhesions. *PLoS One* 4:e7530.
- Nakagawa H, Terasaki AG, Suzuki H, Ohashi K, Miyamoto S (2006) Short-term retention of actin filament binding proteins on lamellipodial actin bundles. *FEBS Lett* 580:3223–3228.
- Neuhaus-Follini A, Bashaw GJ (2015) The Intracellular Domain of the Frazzled/DCC Receptor Is a Transcription Factor Required for Commissural Axon Guidance. *Neuron* 87:751–763 Available at: <http://linkinghub.elsevier.com/retrieve/pii/S0896627315006819>.
- Newman LE, Schiavon C, Kahn RA (2016) Plasmids for variable expression of proteins targeted to the mitochondrial matrix or intermembrane space. *Cell Logist* 6:1–11 Available at: <http://dx.doi.org/10.1080/21592799.2016.1247939>.
- Ng J, Luo L (2004) Rho GTPases Regulate Axon Growth through Convergent and Divergent Signaling Pathways. *Neuron* 44:779–793.
- Niwa R, Nagata-Ohashi K, Takeichi M, Mizuno K, Uemura T (2002) Control of actin

reorganization by slingshot, a family of phosphatases that dephosphorylate ADF/cofilin. *Cell* 108:233–246.

O'Donnell MP, Bashaw GJ (2013a) Src Inhibits Midline Axon Crossing Independent of Frazzled/Deleted in Colorectal Carcinoma (DCC) Receptor Tyrosine Phosphorylation. *J Neurosci* 33:305–314 Available at: <http://www.jneurosci.org/cgi/doi/10.1523/JNEUROSCI.2756-12.2013>.

O'Donnell MP, Bashaw GJ (2013b) Distinct functional domains of the Abelson tyrosine kinase control axon guidance responses to Netrin and Slit to regulate the assembly of neural circuits. *Development* 140:2724–2733 Available at: <http://www.pubmedcentral.nih.gov/articlerender.fcgi?artid=3678342&tool=pmcentrez&rendertype=abstract>.

Ohta Y, Kousaka K, Nagata-Ohashi K, Ohashi K, Muramoto A, Shima Y, Niwa R, Uemura T, Mizuno K (2003) Differential activities, subcellular distribution and tissue expression patterns of three members of Slingshot family phosphatases that dephosphorylate cofilin. *Genes to Cells* 8:811–824.

Omotade OF, Pollitt SL, Zheng JQ (2017) Actin-based growth cone motility and guidance. *Mol Cell Neurosci* Oct:4–10 Available at: <http://dx.doi.org/10.1016/j.mcn.2017.03.001>.

Omotade OF, Rui Y, Lei W, Yu K, Hartzell HC, Fowler VM, Zheng JQ (2018) Tropomodulin isoform-specific regulation of dendrite development and synapse formation. *J Neurosci* 38:10271–10285.

Orth MF, Cazes A, Butt E, Grunewald TGP (2015) An update on the LIM and SH3 domain protein 1 (LASP1): a versatile structural, signaling, and biomarker protein. *Oncotarget*

6:26–42.

Palacios-Prü E, Palacios L, Mendoza R V. (1976) In vitro vs in situ development of Purkinje cells. *J Neurosci Res* 2:357–362.

Pappas CT, Bliss KT, Zieseniss A, Gregorio CC (2011) The Nebulin family: An actin support group. *Trends Cell Biol* 21:29–37 Available at: <http://dx.doi.org/10.1016/j.tcb.2010.09.005>.

Pappas CT, Krieg PA, Gregorio CC (2010) Nebulin regulates actin filament lengths by a stabilization mechanism. *J Cell Biol* 189:859–870.

Pelin K et al. (1999) Mutations in the nebulin gene associated with autosomal recessive nemaline myopathy. *Proc Natl Acad Sci U S A* 96:2305–2310.

Perrin BJ, Ervasti JM (2010) The actin gene family: Function follows isoform. *Cytoskeleton* 67:630–634.

Phillips GR, Anderson TR, Florens L, Gudas C, Magda G, Yates JR, Colman DR (2004) Actin-binding proteins in a postsynaptic preparation: Lasp-1 is a component of central nervous system synapses and dendritic spines. *J Neurosci Res* 78:38–48.

Piper M, Anderson R, Dwivedy A, Weigl C, Van Horck F, Leung KM, Cogill E, Holt C (2006) Signaling mechanisms underlying Slit2-induced collapse of *Xenopus* retinal growth cones. *Neuron* 49:215–228.

Pollard TD, Blanchoin L, Mullins RD (2000) Molecular Mechanisms Controlling Actin Filament Dynamics in Nonmuscle Cells. *Annu Rev Biophys Biomol Struct* 29:545–576.

Pollard TD, Borisy GG (2003) Cellular Motility Driven by Assembly and Disassembly of Actin Filaments. *Cell* 112:453–465.

Pollard TD, Cooper JA (2009) Actin, a central player in cell shape and movement. *Science* (80-) 326:1208–1212.

Purevjav E, Varela J, Morgado M, Kearney DL, Li H, Taylor MD, Arimura T, Moncman CL, McKenna W, Murphy RT, Labeit S, Vatta M, Bowles NE, Kimura A, Boriek AM, Towbin JA (2010) Nebulette mutations are associated with dilated cardiomyopathy and endocardial fibroelastosis. *J Am Coll Cardiol* 56:1493–1502 Available at: <http://dx.doi.org/10.1016/j.jacc.2010.05.045>.

Purohit AA, Li W, Qu C, Dwyer T, Shao Q, Guan KL, Liu G (2012) Down syndrome cell adhesion molecule (DSCAM) associates with uncoordinated-5C (UNC5C) in netrin-1-mediated growth cone collapse. *J Biol Chem* 287:27126–27138.

Qi Y, Wang JK, McMillian M, Chikaraishi DM (1997) Characterization of a CNS cell line, CAD, in which morphological differentiation is initiated by serum deprivation. *J Neurosci* 17:1217–1225.

Raman D, Sai J, Neel NF, Chew CS, Richmond A (2010) LIM and SH3 Protein -1 Modulates CXCR2-Mediated Cell Migration. *PLoS One* 5.

Reardon TR, Murray AJ, Turi GF, Wirblich C, Croce KR, Schnell MJ, Jessell TM, Losonczy A (2016) Rabies Virus CVS-N2cδG Strain Enhances Retrograde Synaptic Transfer and Neuronal Viability. *Neuron* 89:711–724 Available at: <http://dx.doi.org/10.1016/j.neuron.2016.01.004>.

Sainath R, Gallo G (2014) Cytoskeletal and signaling mechanisms of neurite formation. *Cell Tissue Res* 359:267–278.

Sanoudou D, Beggs AH (2001) Clinical and genetic heterogeneity in nemaline myopathy - A disease of skeletal muscle thin filaments. *Trends Mol Med* 7:362–368.

Schafer DA, Korshunova YO, Schroer TA, Cooper JA (1994) Differential localization and sequence analysis of capping protein  $\beta$ - subunit isoforms of vertebrates. *J Cell Biol* 127:453–465.

Schreiber V, Moog-Lutz C, Régnier CH, Chenard MP, Boeuf H, Vonesch JL, Tomasetto C, Rio MC (1998) Lasp-1, a novel type of actin-binding protein accumulating in cell membrane extensions. *Mol Med* 4:675–687 Available at:  
<http://www.pubmedcentral.nih.gov/articlerender.fcgi?artid=2230251&tool=pmcentrez&rendertype=abstract>.

Seeger M, Tear G, Ferres-Marco D, Goodman CS (1993) Mutations affecting growth cone guidance in drosophila: Genes necessary for guidance toward or away from the midline. *Neuron* 10:409–426.

Serafini T, Kennedy TE, Gaiko MJ, Mirzayan C, Jessell TM, Tessier-Lavigne M (1994) The netrins define a family of axon outgrowth-promoting proteins homologous to *C. elegans* UNC-6. *Cell* 78:409–424.

Shu X, Lev-Ram V, Deerinck TJ, Qi Y, Ramko EB, Davidson MW, Jin Y, Ellisman MH, Tsien RY (2011) A genetically encoded tag for correlated light and electron microscopy of intact cells, tissues, and organisms. *PLoS Biol* 9.

Smirnov MS, Cabral KA, Geller HM, Urbach JS (2014) The effects of confinement on neuronal growth cone morphology and velocity. *Biomaterials* 35:6750–6757 Available at:  
<https://www.ncbi.nlm.nih.gov/pmc/articles/PMC3624763/pdf/nihms412728.pdf>.

- Smith DH (2009) Stretch growth of integrated axon tracts: Extremes and exploitations. *Prog Neurobiol* 89:231–239.
- Snow PM, Zinn K, Harrelson AL, McAllister L, Schilling J, Bastiani MJ, Makk G, Goodman CS (1988) Characterization and cloning of fasciclin I and fasciclin II glycoproteins in the grasshopper. *Proc Natl Acad Sci U S A* 85:5291–5295.
- Song JK, Giniger E (2011) Noncanonical notch function in motor axon guidance is mediated by Rac GTPase and the GEF1 domain of trio. *Dev Dyn* 240:324–332.
- Sotelo C (2002) The chemotactic hypothesis of Cajal: A century behind. *Prog Brain Res* 136:11–20.
- Sperry R (1943) Effect of 180 Degree Rotation of the Retinal Field on Visuomotor Coordination. *J Exp Zool* 92:263–279.
- Sperry R (1945) Restoration of Vision after Crossing of Optic Nerves and after Contralateral Transplantation of Eye. *J Neurophysiol* 8:15–28.
- Spillane M, Gallo G (2014) Involvement of Rho-family GTPases in axon branching. *Small GTPases* 5.
- Stölting M, Wiesner C, van Vliet V, Butt E, Pavenstaedt H, Linder S, Kremerskothen J (2012) Lasp-1 Regulates Podosome Function. *PLoS One* 7.
- Stone JL, Merriman B, Cantor RM, Geschwind DH, Nelson SF (2007) High density SNP association study of a major autism linkage region on chromosome 17. *Hum Mol Genet* 16:704–715 Available at: <http://www.ncbi.nlm.nih.gov/pubmed/17376794>.
- Sussman MA, Welch S, Cambon N, Klevitsky R, Hewett TE, Price R, Witt SA, Kimball TR

- (1998) Myofibril degeneration caused by tropomodulin overexpression leads to dilated cardiomyopathy in juvenile mice. *J Clin Invest* 101:51–61.
- Suter DM, Forscher P (2000) Substrate-cytoskeletal coupling as a mechanism for the regulation of growth cone motility and guidance. *J Neurobiol* 44:97–113.
- Suyama R, Jenny A, Curado S, Pellis-van Berkel W, Ephrussi A (2009) The actin-binding protein Lasp promotes Oskar accumulation at the posterior pole of the *Drosophila* embryo. *Development* 136:95–105.
- Szebenyi G, Callaway JL, Dent EW, Kalil K (1998) Interstitial branches develop from active regions of the axon demarcated by the primary growth cone during pausing behaviors. *J Neurosci* 18:7930–7940.
- Tang F, Kalil K (2005) Netrin-1 induces axon branching in developing cortical neurons by frequency-dependent calcium signaling pathways. *J Neurosci* 25:6702–6715.
- Terasaki AG, Suzuki H, Nishioka T, Matsuzawa E, Katsuki M, Nakagawa H, Miyamoto S, Ohashi K (2004) A novel LIM and SH3 protein (lasp-2) highly expressing in chicken brain. *Biochem Biophys Res Commun* 313:48–54.
- Tomasetto C, Moog-Lutz C, Régnier CH, Schreiber V, Basset P, Rio MC (1995a) Lasp-1 (MLN 50) defines a new LIM protein subfamily characterized by the association of LIM and SH3 domains. *FEBS Lett* 373:245–249.
- Tomasetto C, Régnier C, Moog-Lutz C, Mattei MG, Chenard MP, Lidereau R, Basset P, Rio MC (1995b) Identification of four novel human genes amplified and overexpressed in breast carcinoma and localized to the q11-q21.3 region of chromosome 17. *Genomics* 28:367–376.

- Torra J, Burgos-Caminal A, Endres S, Wingen M, Drepper T, Gensch T, Ruiz-González R, Nonell S (2015) Singlet oxygen photosensitisation by the fluorescent protein Pp2FbFP L30M, a novel derivative of *Pseudomonas putida* flavin-binding Pp2FbFP. *Photochem Photobiol Sci* 14:280–287.
- Toshima J, Toshima JY, Takeuchi K, Mori R, Mizuno K (2001) Cofilin Phosphorylation and Actin Reorganization Activities of Testicular Protein Kinase 2 and Its Predominant Expression in Testicular Sertoli Cells. *J Biol Chem* 276:31449–31458.
- Trewin AJ, Berry BJ, Wei AY, Bahr LL, Foster TH, Wojtovich AP (2018) Light-induced oxidant production by fluorescent proteins. *Free Radic Biol Med*:0–1 Available at: <http://dx.doi.org/10.1016/j.freeradbiomed.2018.02.002>.
- Trinick J (1994) Titin and nebulin: protein rulers in muscle? *Trends Biochem Sci* 19:405–409.
- Trousse F, Martí E, Gruss P, Torres M, Bovolenta P (2001) Control of retinal ganglion cell axon growth: A new role for Sonic hedgehog. *Development* 128:3927–3936.
- Tyzio R, Represa A, Jorquera I, Ben-Ari Y, Gozlan H, Aniksztejn L (1999) The establishment of GABAergic and glutamatergic synapses on CA1 pyramidal neurons is sequential and correlates with the development of the apical dendrite. *J Neurosci* 19:10372–10382.
- van Rijssel J, van Buul JD (2012) The many faces of the guanine-nucleotide exchange factor trio. *Cell Adh Migr* 6:482–487.
- Vitriol EA, Zheng JQ (2012) Growth Cone Travel in Space and Time: The Cellular Ensemble of Cytoskeleton, Adhesion, and Membrane. *Neuron* 73:1068–1081.
- Wang Q, Zheng JQ (1998) cAMP-mediated regulation of neurotrophin-induced collapse of nerve

- growth cones. *J Neurosci* 18:4973–4984.
- Wang W, Goswami S, Sahai E, Wyckoff JB, Segall JE, Condeelis JS (2005) Tumor cells caught in the act of invading: Their strategy for enhanced cell motility. *Trends Cell Biol* 15:138–145.
- Wen Z, Han L, Bamburg JR, Shim S, Ming GL, Zheng JQ (2007) BMP gradients steer nerve growth cones by a balancing act of LIM kinase and Slingshot phosphatase on ADF/cofilin. *J Cell Biol* 178:107–119.
- Westberg M, Holmegaard L, Pimenta FM, Etzerodt M, Ogilby PR (2015) Rational design of an efficient, genetically encodable, protein-encased singlet oxygen photosensitizer. *J Am Chem Soc* 137:1632–1642.
- Wingen M, Potzkei J, Endres S, Casini G, Rupprecht C, Fahlke C, Krauss U, Jaeger KE, Drepper T, Gensch T (2014) The photophysics of LOV-based fluorescent proteins-new tools for cell biology. *Photochem Photobiol Sci* 13:875–883.
- Wojtovich AP, Foster TH (2014) Optogenetic control of ROS production. *Redox Biol* 2:368–376  
Available at: <http://dx.doi.org/10.1016/j.redox.2014.01.019>.
- Wolman MA, Regnery AM, Becker T, Becker CG, Halloran MC (2007) Semaphorin3D regulates axon-axon interactions by modulating levels of L1 cell adhesion molecule. *J Neurosci* 27:9653–9663.
- Xu S, Chisholm AD (2016) Highly efficient optogenetic cell ablation in *C. elegans* using membrane-targeted miniSOG. *Sci Rep* 6:21271 Available at:  
<http://www.nature.com/articles/srep21271>.

- Yang F, Zhou X, Du S, Zhao Y, Ren W, Deng Q, Wang F, Yuan J (2014) LIM and SH3 Domain Protein 1 (LASP-1) Overexpression Was Associated with Aggressive Phenotype and Poor Prognosis in Clear Cell Renal Cell Cancer. PLoS One 9:e100557 Available at: <http://dx.plos.org/10.1371/journal.pone.0100557>.
- Yang N, Higuchi O, Ohashi K, Nagata K, Wada A, Kangawa K, Nishida E, Mizuno K (1998) Cofilin phosphorylation by LIM-kinase 1 and its role in Rac-mediated actin reorganization. Nature 393:809–812.
- Yang Q, Zhang XF, Pollard TD, Forscher P (2012) Arp2/3 complex-dependent actin networks constrain myosin II function in driving retrograde actin flow. J Cell Biol 197:939–956.
- Yang T, Terman JR (2012) 14-3-3 $\epsilon$  Couples Protein Kinase A to Semaphorin Signaling and Silences Plexin RasGAP-mediated Axonal Repulsion. Neuron 74:108–121.
- Yoshikawa S, McKinnon RD, Kokel M, Thomas JB (2003) Wnt-mediated axon guidance via the Drosophila derailed receptor. Nature 422:583–588.
- Zarin AA, Asadzadeh J, Hokamp K, McCartney D, Yang L, Bashaw GJ, Labrador J-P (2013) A Transcription Factor Network Coordinates Attraction, Repulsion, and Adhesion Combinatorially to Control Motor Axon Pathway Selection. Neuron 18:1199–1216.
- Zhao L, Wang H, Liu C, Liu Y, Wang X, Wang S, Sun X, Li J, Deng Y, Jiang Y, Ding Y (2010) Promotion of colorectal cancer growth and metastasis by the LIM and SH3 domain protein 1. Gut 59:1226–1235 Available at: <http://www.ncbi.nlm.nih.gov/pubmed/20660701>.